Science Advances
AAAS

Supplementary Materials for

A chemical biology approach reveals a dependency of glioblastoma on biotin distribution

Jeehyun Yoon, Oleg V. Grinchuk, Srinivasaraghavan Kannan, Melgious Jin Yan Ang, Zhenglin Li, Emmy Xue Yun Tay, Ker Zhing Lok, Bernice Woon Li Lee, You Heng Chuah, Kimberly Chia, Roberto Tirado Magallanes, Chenfei Liu, Haonan Zhao, Jin Hui Hor, Jhin Jieh Lim, Touati Benoukraf, Tan Boon Toh, Edward Kai-Hua Chow, Jean-Paul Kovalik, Jianhong Ching, Shi-Yan Ng, Ming Joo Koh, Xiaogang Liu, Chandra Shekhar Verma, Derrick Sek Tong Ong*

*Corresponding author. Email: phsostd@nus.edu.sg

Published 3 September 2021, *Sci. Adv.* **7**, eabf6033 (2021)
DOI: 10.1126/sciadv.abf6033

This PDF file includes:

Materials and Methods

Unsupervised clustering of glioma patients based on query gene signature

We selected two gene sets from Molecular Signatures Database (MSigDB, Broad institute, https://www.gsea-msigdb.org/gsea/msigdb/), namely, "KOBAYASHI_EGFR_SIGNALING_24HR_DN" and "VERHAAK_GLIOBLASTOMA_MESENCHYMAL", and another gene set under Gene Ontology term "GO:0048699: Generation of neurons", hereafter termed as "EGFR signaling", "Mesenchymal subtype of GBM" and "Generation of neurons", respectively. Next, we filtered genes in these gene sets through an in-house RNA-Seq dataset, which was generated from the depletion of histone variant *H2AFV* in GSCs, as this led to decreased proliferation, stemness and invasiveness of GSCs (hereafter known as query signature) (**Table S1**). We checked whether the signature could stratify glioma patients into the clinically distinct subgroups using hierarchical clustering. Glioma patient's tumor gene expression data (TCGA cohort) were obtained from GlioVis (*44*) (http://gliovis.bioinfo.cnio.es/). The resulting expression matrix was drawn in R as a heatmap (*45*), applying hierarchical clustering with Pearson correlation distance. Elbow and Gap-statistic methods were implemented to determine the optimal number of groups from the clustering, using the functions from the R library factoextra (version 1.0.5). Sample information on "co-deletion status of 1p-19q", "IDH mutation status" and "tumor grade" was extracted from the metadata files downloaded from GlioVis and annotated accordingly in the heatmap. Kaplan–Meier curves and risk tables were drawn with the function kmTCGA from the library RTCGA (version 1.14.0) using as input the survival information for the patient samples in the clinical metadata. Statistical tests for survival differences between the 3 groups were calculated in a pair-wise manner using the function coxph from the R library "survival". The resulting p-values were adjusted for multiple testing using the Benjamini-Hochberg procedure.

Lentiviral Constructs

The shRNAs against human HLCS (shHLCS#1, TRCN0000233102 and shHLCS#2, TRCN0000233105), human PC (shPC#1, TRCN0000078453 and shPC#2, TRCN0000078454), human ACC1 (shACC1#1, TRCN0000232455 and shACC#2, TRCN0000232456), human ACC2 (shACC2#1, TRCN0000003093 and shACC2#2, TRCN0000010759), human MCCC1 (shMCCC1#1, TRCN0000078413 and TRCN0000078415) and human PCCA (shPCCA#1, TRCN0000078425 and shPCCA#2, TRCN0000078427) were purchased from Sigma. GSCs were transduced with viral particles. Down-regulation of the target was evaluated by western blot at 72 hr post-infection.

RNA interference

GSCs were seeded in plates the day before transfection. RNAiMAX (Invitrogen, 13778150) was used to transfect 25 nM of human CYP51A1 siRNA (Dharmacon, L-009215-01-0005) into the cells for 72 h.

Cell Viability Assay

Cell-Titer Glow (Promega) was used to determine cell proliferation rate. Briefly, GSCs and mouse astrocytes were seeded on the 96 wells, following day cells were treated with different inhibitors. Cell viability assay was performed 3 days after with Cell-Titre Glow. Data was normalized to DMSO treatment.

Tumorsphere Formation and Extreme Limiting Dilution Assays

The tumorsphere formation assay involved seeding GSCs at a density of 1-2 cell per µl with each condition of SN, and the number of tumorspheres in each well was quantified after 5 days. Data presented are from triplicate experiments.
For the extreme limiting dilution assay, GSCs were stained with PI, and PI-negative cells (n>6) were flow-sorted with decreasing number of cells per well (1, 10, 25 and 100 for TS543, 5, 25, 100 and 200 for TS603) plated in 96-well plates. The percentage of wells with tumorspheres was quantified after 7 days under a microscope. Extreme limiting dilution analysis was performed using software available at http://bioinf.wehi.edu.au/software/elda/. The tumorsphere formation assay involved seeding GSCs at a density of 1 cell per µl, and the number of tumorspheres in each well was quantified after 7 days.

Anchorage-Independent Growth Assay

Anchorage-independent growth assays were performed in replicates of 4 in 6-well plates. Indicated cells were seeded (1×104 cells per well) in stem cell proliferation media with EGF and FGF containing 0.5% low-melting agarose on the top of bottom agar containing 1% low-melting agarose stem cell proliferation media with EGF and FGF. After 14 – 21 days, colonies were stained with iodonitrotetrazoliumchloride (Sigma) and counted.

Transwell migration and invasion assay

The invasiveness of GSCs was measured using 6.5 mm Transwell with 8.0 µm pore polycarbonate membrane insert (Corning, CLS3422). Membrane was coated with Matrigel Basement Membrane Matrix (100 µg/cm^2) (BD Biosciences). The drug-treated cells were seeded in the upper compartment with serum-free GSC medium. The wells of the lower chamber were filled with GSC medium containing 10% FBS. At the end of the invasion assay, chambers were removed, fixed, and stained with a 0.5% Crystal Violet. Cells on the upper surface of the filters were removed by wiping with a cotton swab, and invasion was determined by counting the cells that migrated to the bottom side of the filter using at least ten fields per insert at 20× magnification. Data presented are from triplicate experiments.

RNA Isolation and qRT-PCR

RNA was isolated with RNeasy® Micro Kit (Qiagen), and then used for first-strand cDNA synthesis using random primers and SuperScriptIII Reverse Transcriptase (Invitrogen). qRT– PCR was performed using PowerUp™ SYBR® Green Master Mix (Applied Biosystems). Primers are listed in **Table S4**. The relative expression of genes was normalized using the indicated housekeeping genes.

Western blot analysis and antibodies

Cell lysates were prepared in RIPA buffer (Thermo) with protease inhibitor (Roche), and phosphatase inhibitor (Roche). Protein concentration was determined by DC Protein Assay (Bio-rad), and equal amount of protein samples was used to perform SDS gel electrophoresis and transferred onto nylon membranes (Bio-rad). TBST with 5% skim milk was used for blocking. Incubation with primary antibody was performed at 4 °C for 16 hours. The following antibodies were used: SREBP2 (Abcam, ab30682), phospho-ACC (Cell Signaling, 11818), ACC (Cell Signaling, 3676), Phospho-AMPK (Cell Signaling, 2535), AMPK (Cell signaling, 2532), MCCC1 (Proteintech, 14861-1-AP), PC (Novus, NBP1-49536), PCCA (Novus, NBP2-13736), H3K27ac (Abcam, ab4729), H3 (Abcam, ab1791), Pyruvate Dehydrogenase E1-alpha subunit [p Ser293]

(Novus, NB110-93479), HLCS (Novus, NBP1-81759), Cleaved-Caspase-3 (ASP-175) (Cell Signaling, 9661), H2A (Abcam, ab18255), H4 (Abcam, ab7311), Vinculin (Sigma, V9131) and β-actin (Sigma, A5316), HRP-linked anti-rabbit IgG antibody (Cell Signaling, 7074), HRP-linked anti-mouse IgG antibody (Cell Signaling, 7076). Quantification of protein expression was performed using Image J, and either Vinculin or β-actin was used as the loading control for protein normalization.

Chemical synthesis of biotin-sulconazole (BSN)

Unless otherwise noted, transformations were performed with distilled and degassed solvents under an atmosphere of dry N2 in oven-dried (120 °C) glassware with standard dry box or vacuum line techniques. ^{1}H NMR spectra were recorded on a Bruker AV500 (500 MHz) spectrometer. Chemical shifts are reported in ppm from tetramethylsilane with the solvent resonance resulting from incomplete deuterium incorporation as the internal standard (DMSO-d6: δ 2.50 ppm). Data are reported as follows: chemical shift, integration, multiplicity (s = singlet, d = doublet, t = triplet, q = quartet, br = broad, m = multiplet), and coupling constants (Hz). ^{13}C NMR spectra were recorded on a Bruker AV500 (126 MHz) spectrometers with complete proton decoupling. Chemical shifts are reported in ppm from tetramethylsilane with the solvent resonance as the internal standard (DMSO-d6: δ 39.52 ppm). High-resolution mass spectrometry was performed on a Bruker micrOTOFQ II ESI-MS (positive mode) at the NUS Chemical, Molecular and Materials Analysis Centre.

Solvents

Solvents (tetrahydrofuran and dichloromethane) were purified under a positive pressure of dry nitrogen gas by a modified Innovative Technologies purification system. N,N-dimethylformamide (anhydrous) was used as received. All purification procedures of products were carried out with reagent grade solvents (purchased from VWR chemicals) under bench-top conditions.

Reagents

4-[(tert-Butyldimethylsilyl)oxy]benzaldehyde (1, Sigma-Aldrich), 1-(2,4-dichlorophenyl)-2-(1H-imidazol-1-yl)ethan-1-ol (4, Combi-blocks), thioacetic acid (Sigma-Aldrich), diisopropyl azodicarboxylate (Combi-blocks), triphenylphosphine (Strem), lithium aluminium hydride (Alfa Aesar), thionyl chloride (Sigma-Aldrich), sodium hydride (Strem), tetrabutylammonium fluoride (Sigma-Aldrich), D-biotin (Accela), and 1-(3-dimethylaminopropyl)-3-ethylcarbodiimide hydrochloride (Combi-blocks) were used as received.
(4-((tert-Butyldimethylsilyl)oxy)phenyl)methanethiol (3)1 and 1-(2-chloro-2-(2,4-dichlorophenyl)ethyl)-1H-imidazole (5)2 were prepared in analogy to reported procedures.

4-(((1-(2,4-Dichlorophenyl)-2-(1H-imidazol-1-yl)ethyl)thio)methyl)phenol (7): To an oven-dried flask was charged with DMF (5 mL) and NaH (88 mg, 60%, 2.2 mmol, 1.1 equiv). 3 (508 mg, 2.0 mmol, 1.0 equiv) was added dropwise to the suspension via syringe at 0 oC. After the reaction mixture was allowed to stir for 30 min, 5 (550 mg, 2.0 mmol, 1.0 equiv) was added dropwise. The reaction mixture was allowed to stir for another 12 h at ambient temperature before being quenched by saturated aqueous NH4Cl (10 mL) and Et2O (10 mL). The organic phase was then seperated, washed with brine (10 mL x 3) and then dried over anhydrous Na2SO4. After removal of solvent, residues were dissolved in THF (5 mL) and TBAF (4.0 mL, 1 M in THF, 4.0 mmol, 2.0 equiv) was added. The reaction mixture was allowed to stir for 3 h at ambient

temperature before being quenched by saturated aqueous NH4Cl (10 mL) and Et2O (10 mL). The organic phase was then seperated, washed with brine (10 mL x 3) and then dried over anhydrous Na2SO4. After removal of solvent, the residues were purified by silica gel chromatography (hexane/EtOAc 1:1 – hexane/EtOAc 1:4) to afford 7 (462 mg, 1.2 mmol, 60% yield) as pale yellow powder.

^{1}H NMR (500 MHz, DMSO-d6): δ 9.41 (s, 1H), 7.57 (d, J = 8.4 Hz, 1H), 7.52 (d, J = 2.4 Hz, 1H), 7.46 – 7.36 (m, 2H), 7.07 (d, J = 8.4 Hz, 2H), 6.95 (s, 1H), 6.78 (s, 1H), 6.69 (d, J = 8.4 Hz, 2H), 4.56 – 4.38 (m, 3H), 3.70 (d, J = 12.8 Hz, 1H), 3.57 (d, J = 12.8 Hz, 1H); **^{13}C NMR (126 MHz, DMSO-d6)**: δ 156.49, 137.42, 135.63, 133.91, 132.66, 130.31, 130.10, 128.88, 128.27, 127.64, 127.24, 119.39, 115.21, 49.12, 44.74, 34.87; **HRMS (ESI) [M+H]$^{+}$** calcd for $C18H17Cl2N2OS^{+}$: 379.0433, found: 379.0441. The NMR spectra are shown in **Data S1 and S2**.

4-(((1-(2,4-Dichlorophenyl)-2-(1H-imidazol-1-yl)ethyl)thio)methyl)phenyl 5-((3aS,4S,6aR)-2-oxohexahydro-1H-thieno[3,4-d]imidazol-4-yl)pentanoate (8): To an oven dried flask was charged with DMF (2 mL), 7 (100 mg, 0.26 mmol, 1.0 equiv), D-biotin (76 mg, 0.31 mmol, 1.2 equiv) and EDCI (60 mg, 0.31 mmol, 1.2 equiv). The reaction mixture was allowed to stir for 12 h at ambient temperature before being quenched by saturated aqueous NH4Cl (10 mL) and Et2O (10 mL). The organic phase was then seperated, washed with brine (10 mL x 3) and then dried over anhydrous Na2SO4. After removal of solvent, the residues were purified by silica gel chromatography (hexane/EtOAc 1:1 – hexane/EtOAc 1:2) to afford 8 (80 mg, 0.13 mmol, 50% yield) as pale yellow powder.

^{1}H NMR (500 MHz, DMSO-d6): δ 7.58 (d, J = 8.6 Hz, 1H), 7.51 (d, J = 2.3 Hz, 1H), 7.46 – 7.39 (m, 2H), 7.31 (d, J = 8.5 Hz, 2H), 7.05 (d, J = 8.2 Hz, 2H), 6.97 (s, 1H), 6.78 (s, 1H), 6.47 (s, 1H), 6.38 (s, 1H), 4.56 – 4.45 (m, 3H), 4.34 – 4.29 (m, 1H), 4.18 – 4.13 (m, 1H), 3.81 (d, J = 13.2 Hz, 1H), 3.69 (d, J = 13.2 Hz, 1H), 3.14 (dt, J = 8.4, 5.8 Hz, 1H), 2.83 (dd, J = 12.4, 5.2 Hz, 1H), 2.62 – 2.53 (m, 3H), 1.70 – 1.39 (m, 6H); **^{13}C NMR (126 MHz, DMSO-d6)**: δ 171.71, 162.73, 149.47, 135.41, 135.08, 133.94, 132.76, 130.29, 130.01, 128.90, 128.31, 127.66, 121.80, 119.41, 115.21, 61.04, 59.21, 55.31, 49.06, 44.71, 34.54, 33.30, 27.99, 27.93, 24.37; **HRMS (ESI) [M+H]$^{+}$** calcd for $C28H31Cl2N4O3S2^{+}$: 605.1209, found: 605.1217. The NMR spectra are shown in **Data S3 and S4**.

Model generation for Molecular Dynamics (MD) Simulation

A crystal structure of the human biotin carboxylation (BC) domain of ACCA (PDB: 2YL2, 2.3 Å) was used for the modelling studies. Missing residues were built using the crystal structure of the E. coli biotin carboxylase (complex with Benzimidazoles) (PDB: 3JZF, 2.1 Å), which shares 52% similarity within the BC domains. A molecule of ATP docked into this model of the BC domain was generated guided by a structure of the ADP-bound BC domain from E. coli (complex with ADP and Biotin) (PDB: 3G8C, 2.0 Å). There are no available crystal structures of MCC1, PC and PCCA. Homology models (*46*) of these structures were built using the crystal structure of E. coli BC used above (the 3 proteins share sequence similarities with the E. coli sequence of 67%, 64% and 67% respectively).

Ligand preparation and docking

The 3D structure of the ligand sulconazole were built using the Maestro software and minimized using the Macromodel module employing the OPLS-2005 force field in the Schrodinger 9.0 suite of programs. This ligand was then prepared with Ligprep for docking. Sulconazole was next docked into the biotin-binding pocket of the models of ACCA, MCC1, PC and PCCA constructed

above using the program Glide. The search space of the docked ligand was restricted to a cubic box with 10 Å sides centred on the selected active site residues. Default Glide settings were used to generate these grids. The docking was carried out by holding the proteins rigid while the ligand was flexible. Several docked conformations of the ligand were generated and their interactions evaluated using the Glide Extra Precision (XP) scoring function. The pose that was commonly observed in all the docking runs (i.e. docking sulconazole into the BC domains of ACCA, MCC1, PC and PCCA) was selected for further refinement using molecular dynamics (MD) simulations as detailed next.

MD simulations

MD simulations of sulconazole complexed to the BC domains of ACCA/ PC/ MCC1/ PCCA as generated above were carried out with the pemed.CUDA module of the program Amber18. All atom versions of the Amber 14SB force field (ff14SB) and the general Amber force field (GAFF) were used for the protein and for sulconazole, respectively. The Xleap module of Amber18 was used to prepare the system for the MD simulations as used earlier (*47, 48*). All the simulation systems were neutralized with appropriate numbers of counterions. Each neutralized system was solvated in an octahedral box with TIP3P water molecules, leaving at least 10 Å between the solute atoms and the borders of the box. All MD simulations were carried out in explicit solvent at 300K. During the simulations, the long-range electrostatic interactions were treated with the particle mesh Ewald method (*49*) using a real space cutoff distance of 9 Å. The Settle algorithm (*50*) was used to constrain bond vibrations involving hydrogen atoms, which allowed a time step of 2 fs during the simulations. Solvent molecules and counterions were initially relaxed using energy minimization with restraints on the protein and sulconazole atoms. This was followed by unrestrained energy minimization to remove any steric clashes. Subsequently the system was gradually heated from 0 to 300 K using MD simulations with positional restraints (force constant: 50 kcal mol-1 Å-2) on protein and sulconazole over a period of 0.25 ns allowing water molecules and ions to move freely. During an additional 0.25 ns, the positional restraints were gradually reduced followed by a 2 ns unrestrained MD simulation to equilibrate all the atoms. For each system, three independent MD simulations (assigning different initial velocities) were carried out for 250 ns with conformations saved every 10 ps. Simulation trajectories were visualized using VMD and figures were generated using Pymol.

RNA-Seq analysis

GSC TS543 were treated with either DMSO or 5µM sulconazole for 3 days, followed by RNA extraction. The total RNA samples were sent to Medgenome (Medgenome, India, Bangalore) for RNA-Seq analysis on the Illumina HiSeq platform according to the standard paired-end protocol. RNA-seq data quality was monitored via FASTQC package (https://www.bioinformatics.babraham.ac.uk/projects/fastqc/). Adapters and overrepresented sequences have been removed using cutadapt software (https://cutadapt.readthedocs.io/en/stable/). Further reads preprocessing was performed by Trimmomatic (version 0.36) with the parameters: LEADING:3 TRAILING:3 SLIDINGWINDOW:4:15 MINLEN:50. Mapping of RNA-seq reads was done using STAR_2.5.0a (https://github.com/alexdobin/STAR) with default parameters for RNA-seq data; the human ENSEMBL gene annotation model (GRCh37) and RSEM software (*44*) were used to quantify the gene-level expression. EBSeq package was utilized for differential gene expression analysis (*51*). Pathway enrichment analysis was performed using ConsensusPathDB (http://cpdb.molgen.mpg.de/). The differentially expressed genes are listed in **Table S2.**

Extraction of amino acids, acylcarnitines and organic acids and their analyses

GSC TS543 was treated with 1 mM L-carnitine for 24 hrs prior to acylcarnitine extraction. We have checked that the acylcarnitine treatment did not affect the effect of sulconazole on the GSC TS543 cell viability. Methods of extraction and metabolic profiling for amino acid, acylcarnitines and organic acids were performed as previously described (*52, 53*). For acyl carnitine and amino acid extraction, 50 ul of the cell lysate was spiked with deuterium-labeled acylcarnitine and amino acid standards, (including D3-C2, D3-C3, D3-C4, D9-C5, D3-C8, and D3-C16 carnitines (Cambridge Isotope Laboratories, Andover, MA) and Glycine-D2, Alanine-D4, Valine-D8, Proline-D7, Serine-D3, Leucine-D3, Methionine-D3, Phenylanaline-D5, Histidine-D6, Tyrosine-D4, Aspartic acid-D3, Glutamic aicd-D3, Ornithine-D2, Citrulline-D2, Arginine-D5 and Tryptophan-D5 (Sigma Alrdich,USA)). The mixture was extracted using methanol. The acyl carnitine and amino acid extracts were derivatised with 3M Hydrochloric acid in methanol or butanol (Sigma Aldrich, USA) respectively, dried and reconstituted in methanol for analysis in LC-MS.

Acylcarnitine measurements were performed without a column, using flow injection tandem mass spectrometry on the Agilent 6430 Triple Quadrupole LC/MS system (Agilent Technologies, CA, USA). The sample analysis was carried out at 0.4ml/min of 80/20 Methanol/water as mobile phase, and injection of 4µL of sample. Data acquisition and analysis were performed on Agilent MassHunter Workstation B.06.00 Software.

Amino acids were separated using a C18 column (Phenomenex, 100 x 2.1 mm, 1.6 µm, Luna® Omega) on a Agilent 1290 Infinity LC system (Agilent Technologies, CA, USA) coupled with quadrupole-ion trap mass spectrometer (QTRAP 5500, AB Sciex, DC, USA). Mobile phase A (Water) and Mobile phase B (Acetonitrile) both containing 0.1% Formic acid were used for chromatography separation. The LC run was performed at a flow rate of 0.4 mL min^{-1} with initial gradient of 2% B for 0.8 min, then increased to 15% B in 0.1 min, 20% B in 5.7 min, 50% B in 0.5 min, 70% B in 0.5 min, followed by re-equilibration of the column to the initial run condition (2% B) for 0.9 min. All compounds were ionized in positive mode using electrospray ionization. The chromatograms were integrated using MultiQuant™ 3.0.3 software (AB Sciex, DC, USA). Absolute quantitation of both amino acids and acylcarnitines were done by comparing the ratios of the metabolites to their respective internal standards, against an external calibration curve. External calibration curves consisted of C2, C3, C4, C5, C6, C8, C10, C12, C14, C16 and C18 carnitines and all reported amino acids. As no column separation was used for the acylcarnitine analysis, isomers were unable to be separated. Isomeric acylcarnitines such as valerylcarnitine and isovalerylcarnitine were reported as the sum of both the acylcarnitine species.

For organic acid analysis, 300 µL of homogenate was spiked with deuterated internal standards of each metabolite analysed, extracted with ethylacetate, dried and derivatized with N,O-Bis(trimethylsilyl)trifluoroacetamide, with protection of the alpha keto groups using ethoxyamine (Sigma Aldrich, USA). Trimethylsilyl derivatives of organic acids were separated by gas chromatography on an Agilent Technologies HP 7890A and quantified by selected ion monitoring on a 5975C mass spectrometer using stable isotope dilution. The initial GC oven temperature was set at 70 °C, and ramped to 300 °C at a rate of 40 °C/min, and held for 2 min.

We applied the following criteria for the organic acid, amino acid and acylcarnitine analyses: (i) signal/noise ratio > 3 in all measurements for a given cell line; and (ii) signal/noise ratio > 10 in at least three out of six measurements for a given cell line. Relative fold changes are shown in **Table S3**.

ChIP-Seq and superenhancer analyses

Briefly, GSC cells seventy-two hours after knockdown, cells were cross-linked with 1% formaldehyde for 10 min at room temperature. The cells were lysed using SDS Lysis buffer for ChIP (1% SDS, 10 mM EDTA, 50 mM Tris-HCl pH 8). The lysate was then sonicated for 25 cycles at 30% amplitude (15 s ON and 45 s OFF). The sonicated samples were then diluted in ChIP dilution buffer (0.01% SDS, 1% Triton-X-100, 1.2 mM EDTA, 16.7 mM Tris–HCl pH 8, 167 mM NaCl) and used for the immunoprecipitation with H3K27ac (Abcam, Ab4729) beads. After an over-night incubation with antibody, the bound DNA was washed sequentially with low salt wash buffer (0.1% SDS, 1% Triton X 100, 2 mM EDTA, 20 mM Tris–HCl pH 8, 150 mM NaCl), high salt wash buffer (0.1% SDS, 1% Triton X-100, 2 mM EDTA, 20 mM Tris–HCl pH 8, 500 mM NaCl), LiCl wash buffer (0.25 M LiCl, 1% NP40, 1%deoxycholate, 1 mM EDTA, 10 mM Tris–HCl pH 8) and TE wash buffer (10 mM Tris–HCl pH 8, 1 mM EDTA) to remove non-specific sequences and eluted in the elution buffer (84 mg NaHCO3, 1 ml 10% SDS, 9 ml H2O). Then the samples were reverse cross-linked using NaCl at 65°C overnight. The eluted DNA was purified and used for library preparation.

Library preparation was performed as previously described (*54*) with minor modifications. Briefly, end repair with NEBNext End Repair enzyme (NEB, E6050) and clean-up with 2.4x volume AMPure XP beads (Beckman Coulter, A63880). A-tailing with Klenow Fragment (3'→5' exo-, NEB, M0212) and purified with 2.4x volume AMPure XP beads. Adapter ligation reactions contained annealed universal adapter and T4 rapid ligase (NEB, B0202) and clean-up with 1.8x volume AMPure XP beads. Chromatin was amplified using KAPA Real-time Library Amplification Kit (KAPABIOSYSTEMS, KK2701) with universal primer and barcoded primer. Amplified chromatin was purified with QIAquick Gel Extraction Kit (Qiagen).
Reads processing and alignment was as follows. Reads were filtered based on quality and adapter sequences were removed from the ChIP-seq experiments using Trim_galore (https://github.com/FelixKrueger/TrimGalore) with the default options. The resulting fastq files were aligned to the human reference genome (hg19) using STAR_2.5.0a (https://github.com/alexdobin/STAR) with the following parameters: "--alignIntronMax 1", "--outFilterMismatchNoverLmax 0.09", "--alignMatesGapMax 2000", "--outFilterMultimapNmax 1", "--alignEndsType EndToEnd"; the rest of the options were set to the default. Duplicated reads were removed from the bam files using MarkDuplicates software(http://broadinstitute.github.io/picard/) A bed file with H3K27ac peaks was generated with *Macs2* using the paired-end narrowPeak mode (q-value < 0.01) . Enhancers were identified using the *ROSE* algorithm (https://bitbucket.org/young_computation/rose/src/master/). The H3K27ac bed file was converted to gff format and *ROSE* was run with the stitching distance option of 12.5 Kb and a TSS exclusion zone of 2.5 Kb. Super-enhancers were ranked by counting the H3K27ac signal in the ChIP file compared to the matched input file. The resulting super enhancers were annotated to their closest gene using the *annotatePeaks* from HOMER (http://homer.ucsd.edu/homer/).

Public datasets and statistical analysis

Preprocessed RNA-seq and microarray gene expression and corresponding clinical data for glioma patients from The Cancer Genome Atlas (TCGA) (https://www.cancer.gov/tcga), REMBRANDT (*55*) and Gravendeel et al.(*56*) glioma patients cohorts have been obtained from GlioVis portal. Gene expression and clinical data for Chinese Glioma Genome Atlas (CGGA) glioma patient cohort was downloaded from (http://www.cgga.org.cn/download.jsp, DataSet ID:mRNAseq_693) (*57*).

RNA-Seq gene expression data to compare *HLCS* expression between GSC and GBM tumors was obtained from Mack et al (*43*). For gene and protein expression correlation analyses, reverse phase protein array (RPPA) data from TCGA cohort was accessed through UCSC Xena Browser (https://xenabrowser.net/datapages/).

To produce Figure 5E, H3K27ac ChIP-sequencing data from normal brain specimens were accessed through the ENCODE and Roadmap Epigenomics projects as multiple BAM files (*58*). Downloaded BAM files from 7 different regions of normal human brain have been merged using samtools "merge" command (http://www.htslib.org/) into one BAM file. Next, the reads from the merged BAM file have been randomly subsampled using DownsampleSam function from picard tools (https://broadinstitute.github.io/picard/). The reads downsampling was necessary to scale them down to the total number of mapped reads in original ChIP-seq sample generated from TS543 cells (see ChIP-seq and analysis).

Figure 6B was generated using single cell RNA-seq GBM tumor data published in Darmanis et al., 2017 (*26*). Briefly, only single cell data obtained from tumors, but not from surrounding brain tissue was included in the analysis. We included only single cells with at least 1000 genes expressed higher than 1 count per million and genes expressed in at least 2 cells per tumor sample. R package "Seurat" (*59*) was used to normalize and visualize data. Two dimensional t-SNE plot was generated using top 30 PCA components and perplexity of 40. We assigned each cell cluster to respective cell identity by marker gene expressions described in Darmanis et al., 2017 (*26*).
To analyze the associations between known tumor genotypes (molecular subtypes, IDH mutation status etc) and HLCS gene expression, we used the publicly available genotype data for each of four GBM patients' cohorts. For tumor subtype classification, 3-way classification method available from GlioVis portal (*60*) was implemented. Gene mutation/amplification status information for TCGA GBM patients of interest was obtained from cBIOPORTAL (https://www.cbioportal.org/). GBM patients with $STAT3^{low}$ and $STAT3^{high}$ TCGA GBM patients were identified using the STAT3 functionally tuned gene signature (*61*). The computational module *NearestTamplatePrediction* from GenePattern software (https://www.genepattern.org/) was used to identify patient tumors classified with statistical significance (Benjamini-Hochberg FDR p-value < 0.05, 1000 permutation tests) into $STAT3^{low}$ and $STAT3^{high}$ subgroups.

In order to estimate whether the expression of gene of interest was significantly associated with cancer patient's survival, we used the one-dimensional data-driven grouping (1-D DDg) method. Briefly, after sorting the patients by the gene expression values, the values were fitted to survival times and events using the Cox proportional hazards model; goodness-of-fit analysis was applied to maximize the separation between the sorted patients into low- and high-risk subgroups. To

compute the differences between the Kaplan-Meier survival curves, we used the Cox hazards model and Wald test statistic.

In Student's t-test, Man-Whitney exact test were performed using either R3.4.1 or Cytel Studio (version 9.0.0). Significance was defined as $p < 0.05$. For multiple testing correction Benjamini-Hochberg statistic was applied to estimate the FDR. SigmaPlot (Version 11.0), a set of R packages (e.g., ggplot2, ggpubr) were implemented for plots generation. For all experiments with error bars, standard error mean was calculated to indicate the variation within each experiment and data, and values represent mean ± s.e.m or mean ± s.d., as indicated in the figure legends.

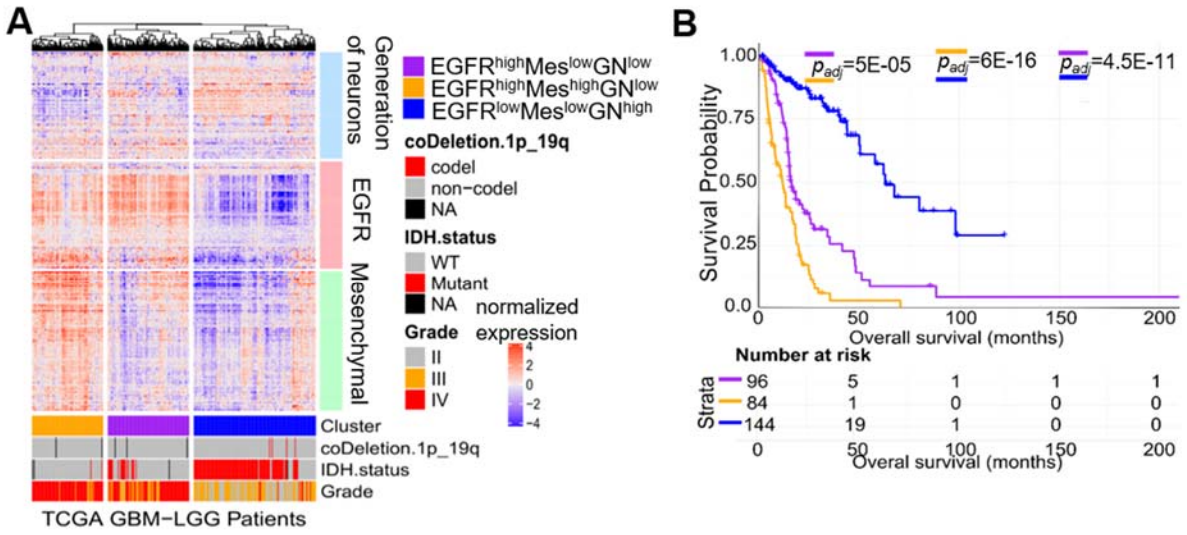

C

drug name	enrichment score	p-value	established drug targets	targeted pathway
sulconazole	0.92	4.0E-05	CYP51A1	ergosterol biosythesis
prestwick-559	0.88	3.2E-03	unknown	unknown
1,4-chrysenequinone	0.87	3.5E-02	AHR	activator of AhR
MG-262	0.87	4.6E-03	unknown	proteasome inhibitor
dexpropranolol	0.85	6.9E-03	ADRB2, ADRB3	beta-adrenergic antagonist
bromperidol	0.83	1.1E-02	DRD2	dopamine and serotonin antagonist
latamoxef	0.81	1.4E-02	pbpC, mrcA, mrcB, dacB	antibiotic and anti-inflammatory
ipratropium bromide	0.80	1.6E-02	CHRM1, CHRM2, CHRM3	muscarine receptor antagonist
chrysin	0.80	1.6E-02	ABCG2, CDK6, CYP19A1, CYP1B1	steroidogenesis inhibitor
piperidolate	0.80	1.6E-02	CHRM1	muscarine receptor antagonist

Fig. S1. Compounds identified in the Connectivity Map Analysis (CMA) using the anti-GSC signature. (A) Unsupervised clustering of all glioma patients from TCGA dataset using a customized query signature from the EGFR, Mes and GN gene sets. **(B)** Kaplan-Meier analysis of the three clusters from **(A)**. Benjamini-Hochberg adjusted Wald *p* values indicate the significance of patients' survival differences between the subgroups. **(C)** Top 10 compounds identified in CMA, along with their known targets and pathways.

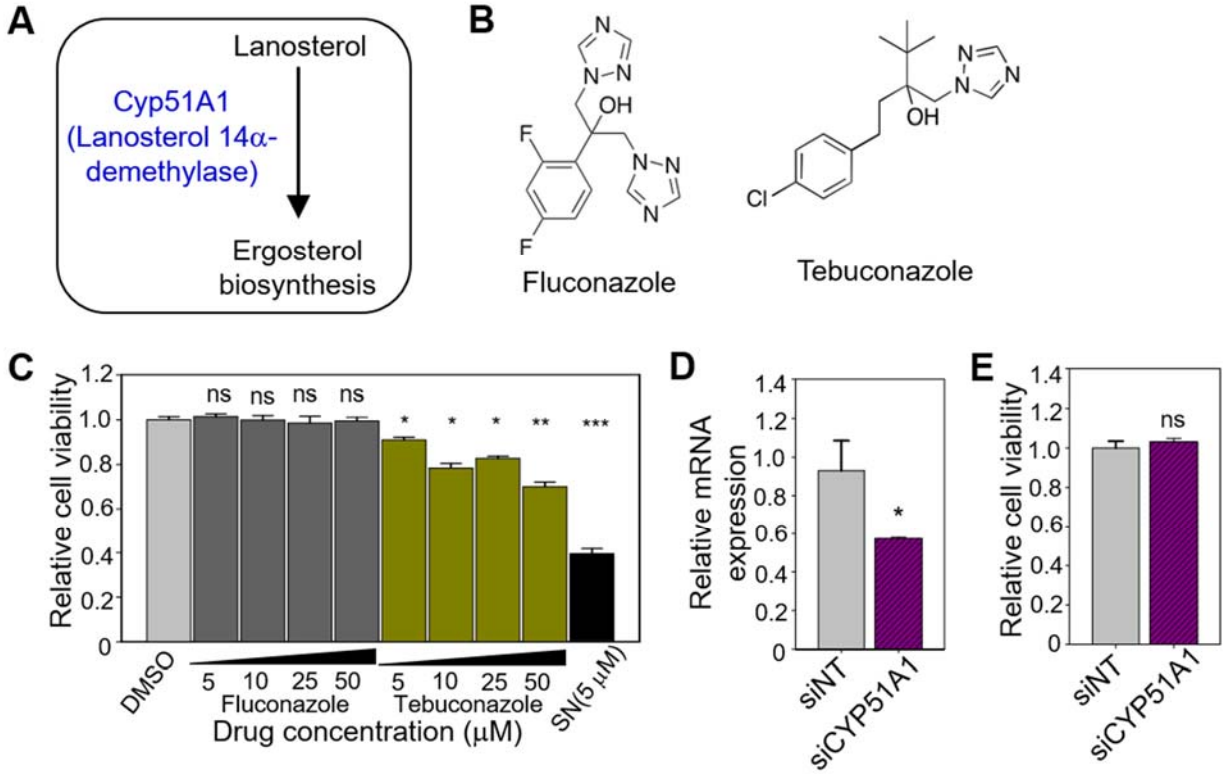

Fig. S2. SN's effect on GSC is unlikely due to the inhibition of Cyp51A1. (A) Schematic diagram of the known mechanism of SN action in fungi. **(B)** Chemical structures of fluconazole and tebuconazole. **(C)** Cell viability of GSC TS543 after three days of treatment with DMSO, fluconazole, tebuconazole or SN. SN served as a positive control (n=6). **P* < 1E-05; ***P* < 1E-07; ****P* < 1E-08. **(D)** Validation of Cyp51A1 KD by qRT-PCR analysis (n=4) (mean ± SD). *HSP70* and *TBP* serve as the housekeeping genes. **P* < 0.05. **(E)** Cell viability assay of GSCs and mouse astrocytes with SN treatment (n=6) (mean ± SD). Two-sided unpaired Student's *t*-test.

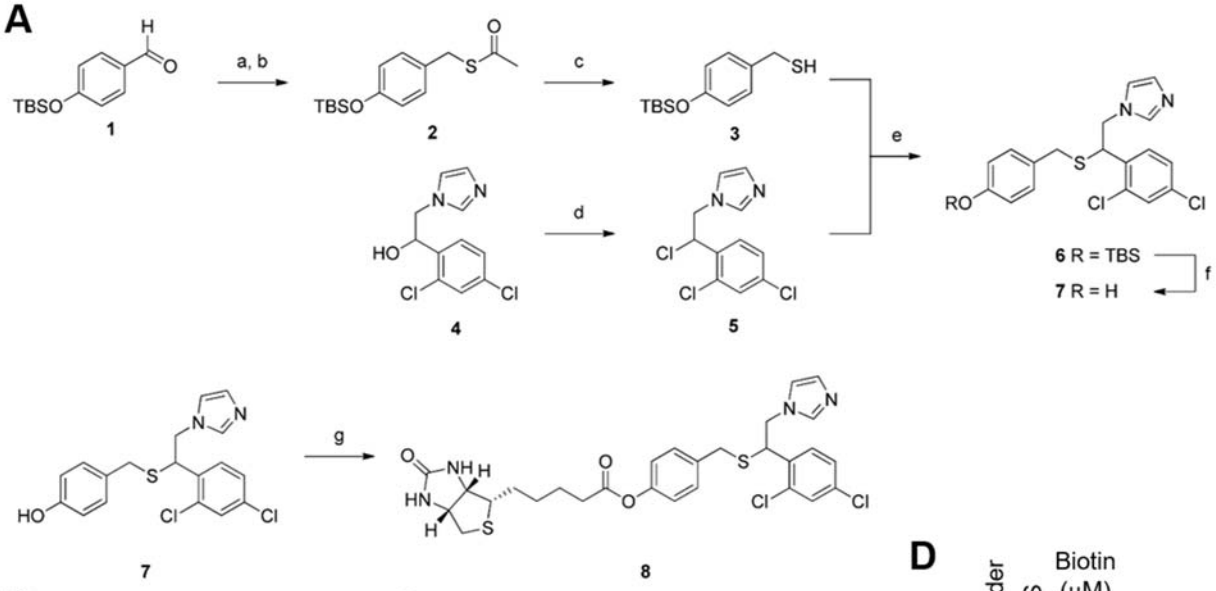
A
TBSO
1
a, b
2
c
3
d
4
5
e
RO
6 R = TBS
7 R = H
f
HO
7
g
8

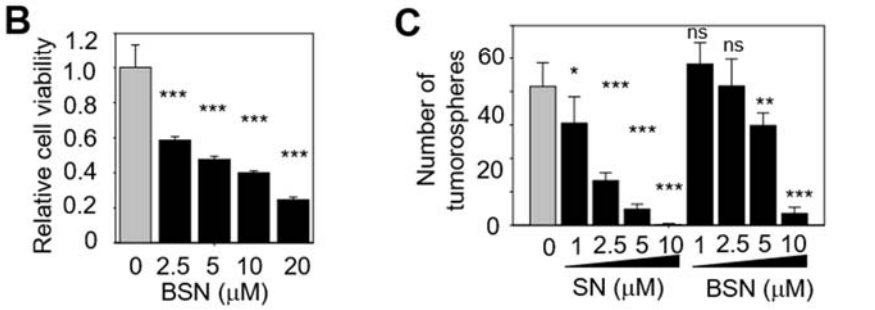
B
Relative cell viability
BSN (μM)
C
Number of tumorospheres
SN (μM)
BSN (μM)
D
kDa
Ladder
PBS
Biotin (μM)
75 50
250
150
100
75
50

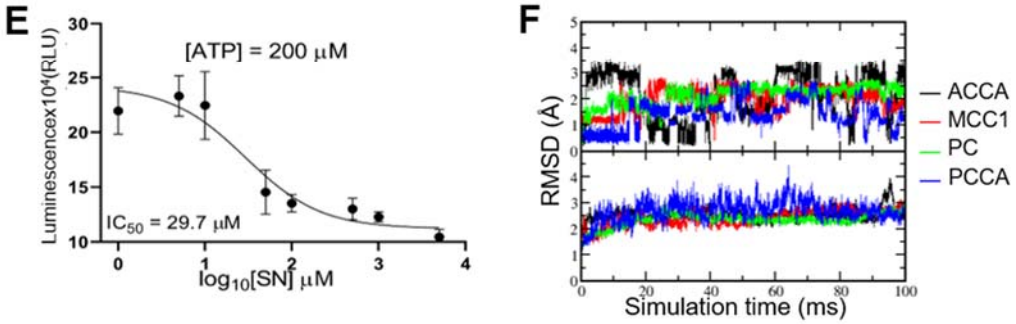
E
[ATP] = 200 μM
Luminescencex10⁴(RLU)
IC50 = 29.7 μM
log10[SN] μM
F
RMSD (Å)
Simulation time (ms)
ACCA
MCC1
PC
PCCA

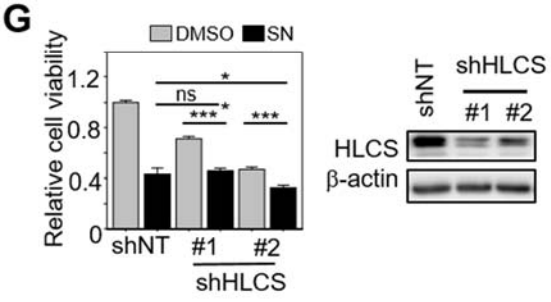
G
DMSO
SN
Relative cell viability
shNT
#1
#2
shHLCS
HLCS
β-actin

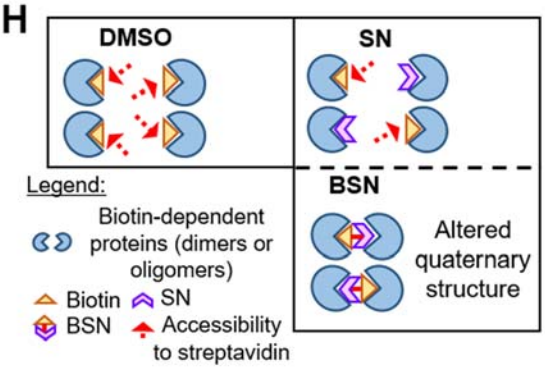
H
DMSO
SN
BSN
Legend:
Biotin-dependent proteins (dimers or oligomers)
Biotin
SN
BSN
Accessibility to streptavidin
Altered quaternary structure

Fig. S3. SN inhibits biotinylation of carboxylases by competing with biotin for the BC components of these enzymes. (A) Chemical synthesis of biotin-sulconazole (BSN). **(B)** Cell viability assay of GSC TS543 upon BSN treatment (n=6). **(C)** Tumorsphere formation of GSCs following DMSO, BSN or SN treatment (5 days) (n=6) (mean ± SD). **(D)** Silver stained SDS-PAGE gel of streptavidin pulldown lysates of 293T cells with or without 6 hr biotin treatment. **(E)** Enzymatic activity of recombinant ACC1 protein in the presence of SN, with 200 μM of ATP (n=5). **(F)** Root mean square deviation (RMSD) of SN (top) and protein conformations of ACCA, MCC1, PC, PCCA bound with SN (bottom) sampled during standard MD simulations. **(G)** Cell viability assay of shNT or shHLCS transduced GSC TS543, with or without 5 μM SN treatment (3 days) (n=6) (mean ± SD) (left). Western blot analysis of HLCS from shNT or shHLCS transduced cells (right). β-actin serves as the loading control. **(H)** Proposed model for the binding of SN and BSN to biotin-dependent carboxylases. (**B**), (**C**) and (**G**): two-sided unpaired Student's *t*-test, **P* < 0.05, ***P* <0.01, ****P* <0.001.

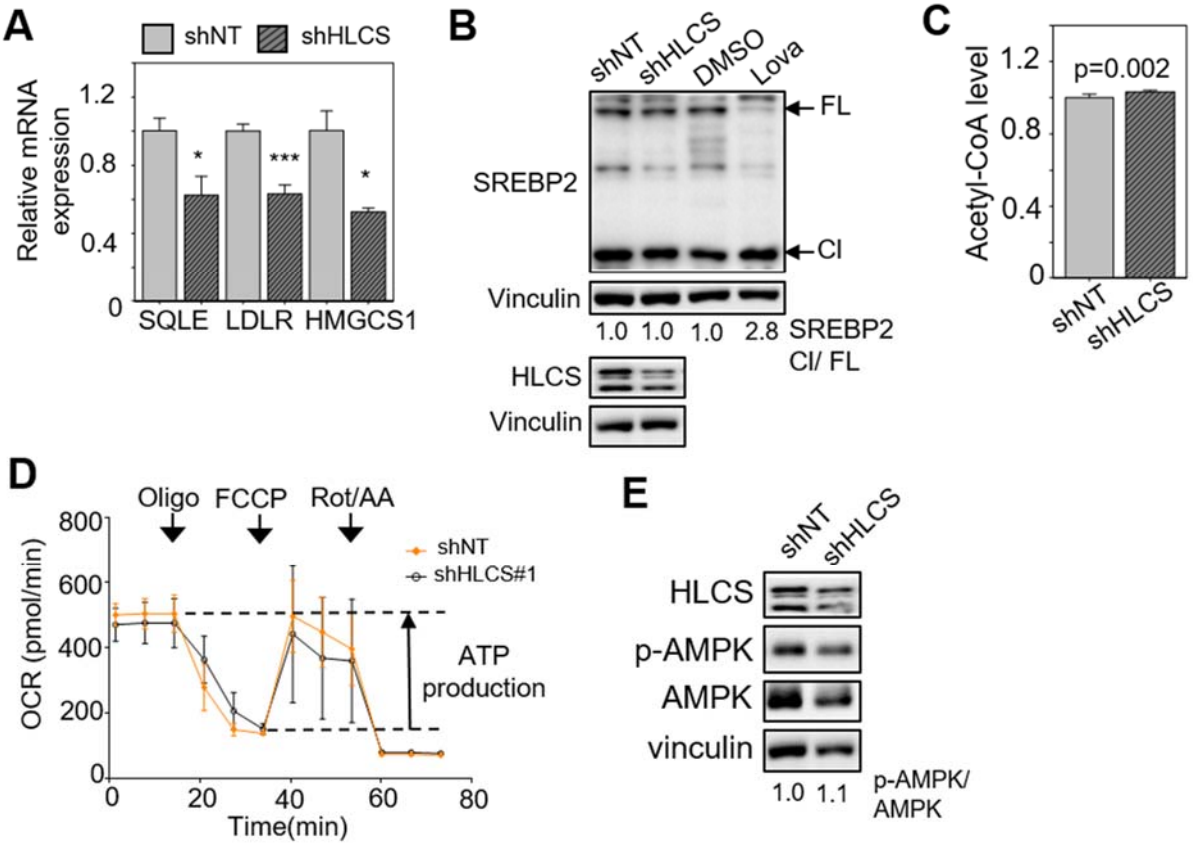

Fig. S4. *HLCS* KD does not lead to cholesterol depletion and OXPHOS impairment in 293T cells under biotin-free culturing conditions. (A) qRT-PCR analysis of representative genes in the cholesterol homeostasis pathway in *HLCS* KD 293T cells (n=4) (mean ± SD). *HSP70* and *TBP* serve as the housekeeping genes. Two-sided unpaired Student's *t*-test, $*P < 0.05$, $***P < 0.001$. **(B)** Western blot analysis of full length (FL) and cleaved (Cl) SREBP2 protein after *HLCS* KD of 293T cells. Vinculin serves as the loading control. SREBP2 Cl/FL ratios are indicated. **(C)** Relative intracellular levels of acetyl-CoA in 293T with or without *HLCS* KD (n=8) (mean ± SD). **(D)** Seahorse analysis of 293T cells with or without *HLCS* KD (n=10). **(E)** Western blot analysis of p-AMPK and AMPK levels in *HLCS* KD 293T cells. HLCS and vinculin serve as the positive and loading control, respectively. p-AMPK/AMPK ratios are indicated.

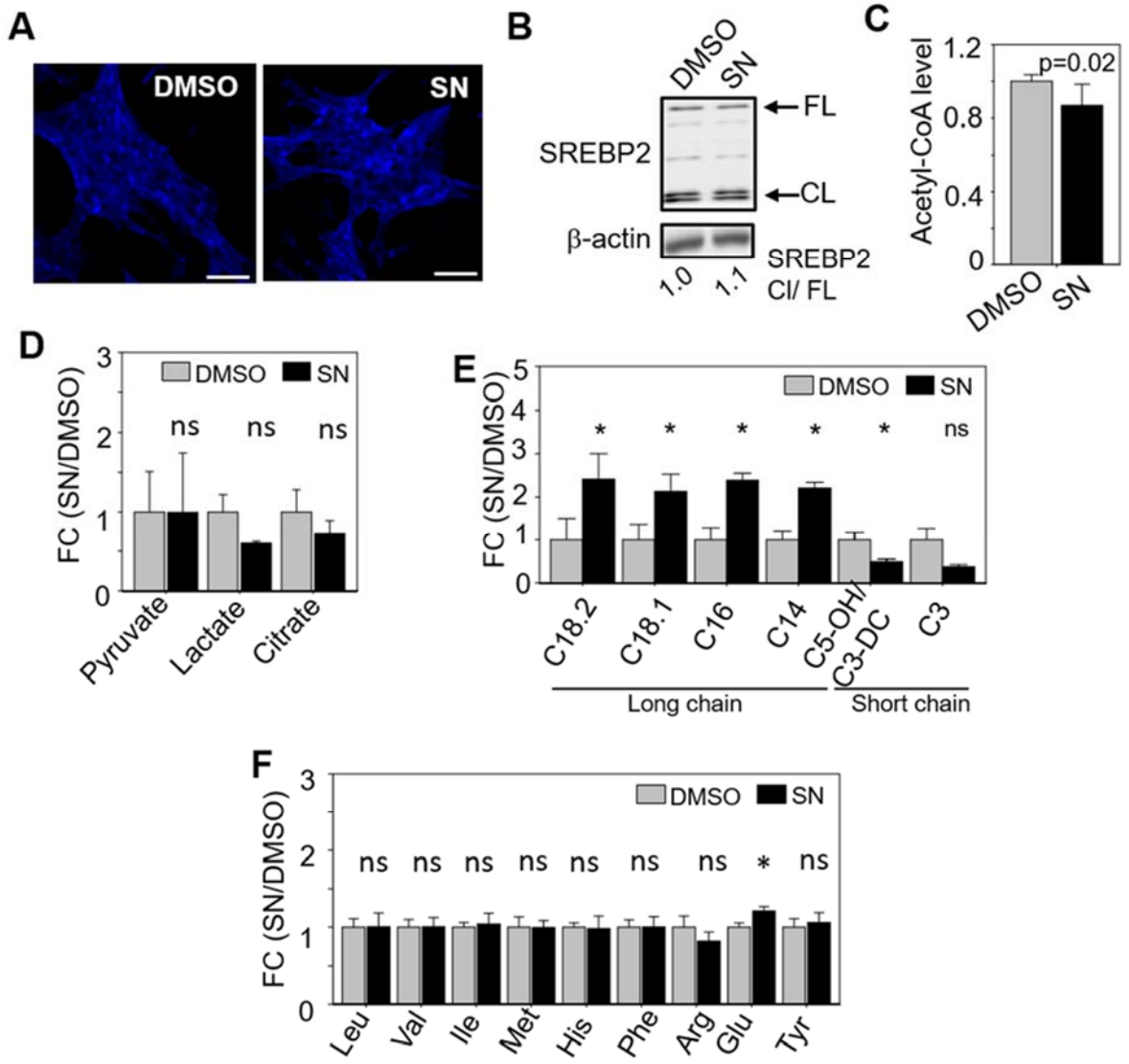

Fig. S5. Metabolite changes associated with SN treatment of mouse astrocytes. (**A**) Representative images of SN- or DMSO-treated mouse astrocytes that were stained with Filipin. **(B)** Western blot analysis of SREBP2 in SN- or DMSO-treated mouse astrocytes. β-actin serves as the loading control. SREBP2 Cl/FL ratio are indicated. (**C**-**F**) Relative intracellular levels of acetyl-CoA **(C)**, organic acids **(D)**, acylcarnitines **(E)** and amino acids **(F)** in mouse astrocytes with and without 5 μM SN treatment (3 days) (n=3). Two-sided unpaired Student's t-test, **P* < 0.05.

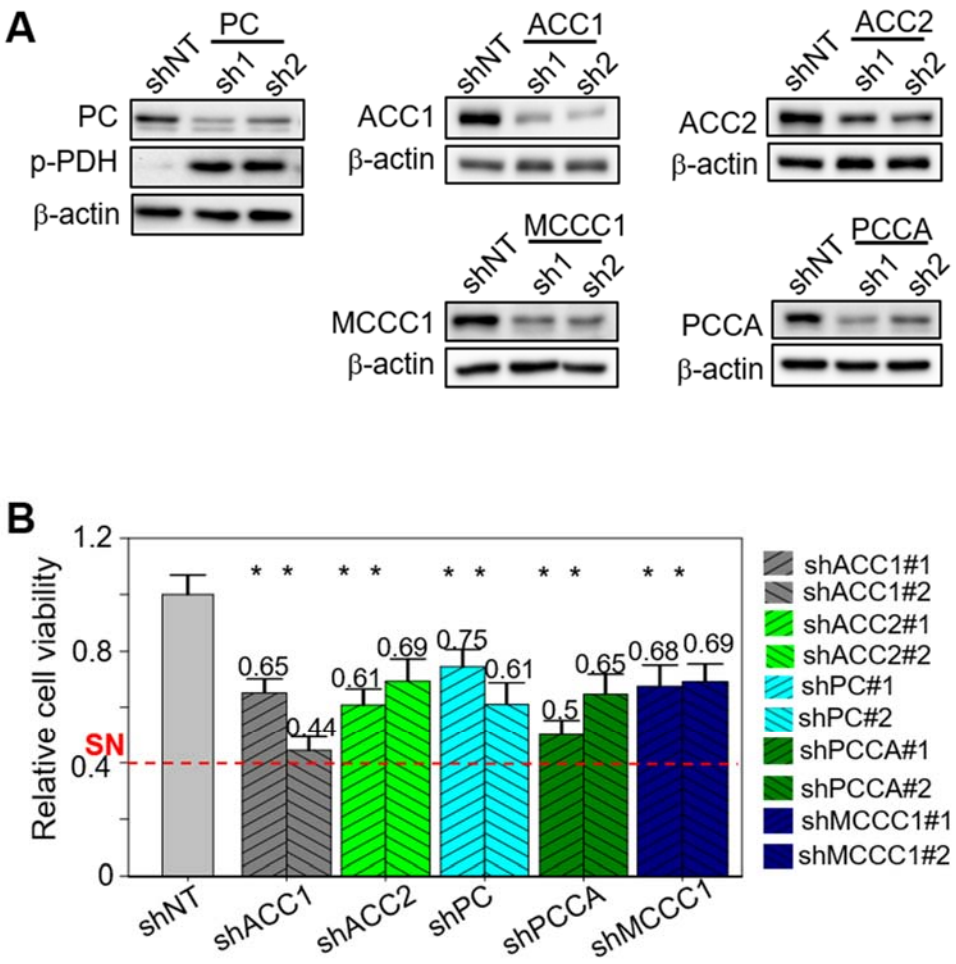

Fig. S6. SN likely inhibits multiple biotin-dependent carboxylases in GSC. (A) Western blot analysis of individual biotin-dependent carboxylases expression upon their KD. β-actin serves as the loading control. **(B)** Relative cell viability of GSC upon enzyme KD from **(A)** (n=6). Two-sided unpaired Student's t-test, **P* < 1E-05.

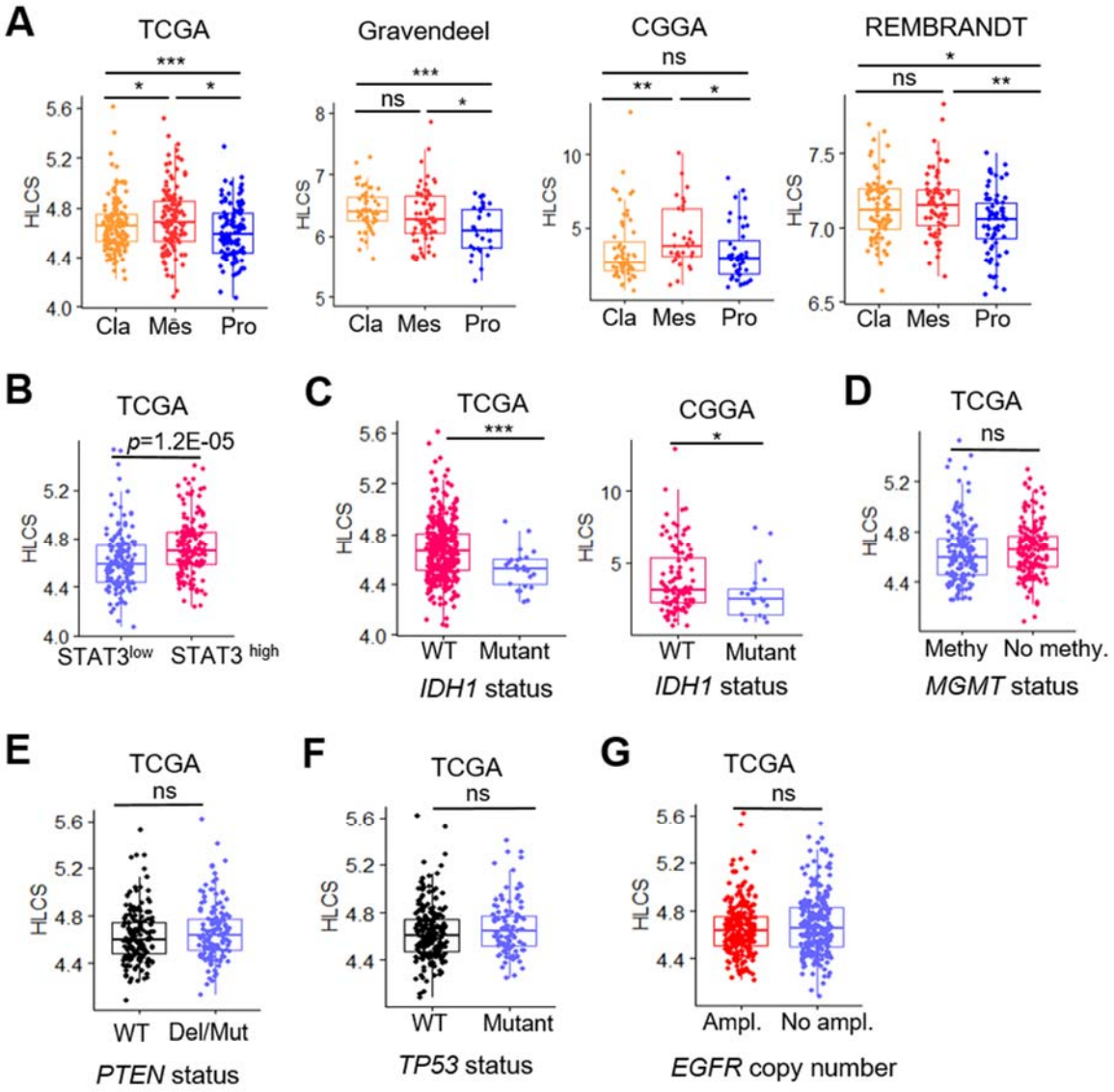

Fig S7. Correlative analyses of *HLCS* levels with various established GBM markers. (**A**) Correlative analysis of *HLCS* levels with GBM subtypes in multiple GBM patient cohorts. *Cla*, Classical; *Mes*, Mesenchymal; *Pro*, Proneural. **(B)** Correlative analysis of *HLCS* levels with GBM of STAT3-low versus -high gene signatures in the TCGA dataset. **(C)** Correlative analysis of *HLCS* levels with *IDH1* wildtype (WT) versus mutant GBM in multiple GBM cohorts. **(D)** Correlative analysis of *HLCS* levels with *MGMT* promoter methylated (Methy) versus non-methylated GBM in the TCGA dataset. **(E-G)** Correlative analysis of *HLCS* levels with GBM having alterations in *PTEN* (**E**) and *TP53* (**F**) gene status, as well as *EGFR* copy number (**G**) in the TCGA dataset. **P* < 0.05, ***P* <0.01, ****P* <0.001, Mann-Whitney exact test.

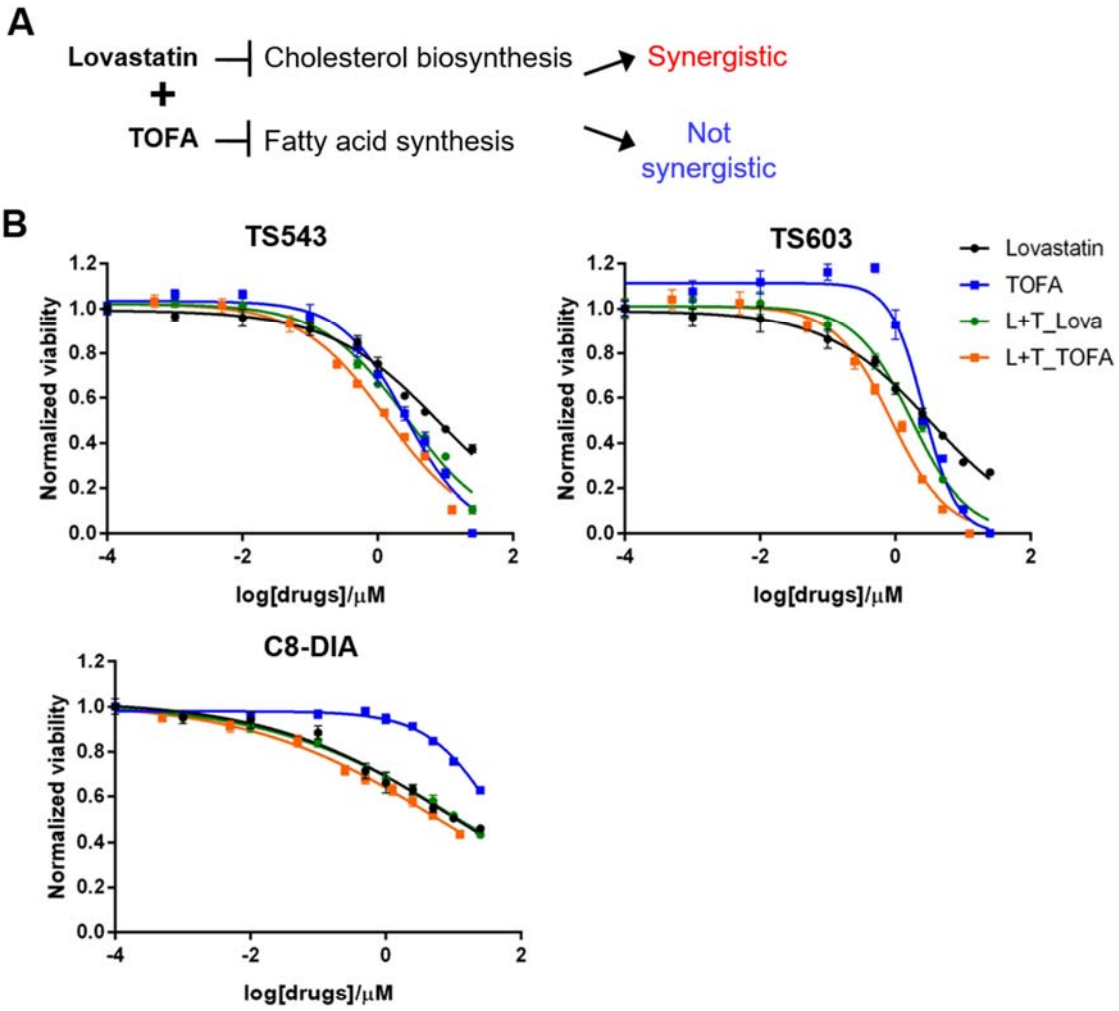

C

IC_{50} values (μM)

Cell line	Single drug		Combination		CI
	Lova	TOFA	Lova	TOFA	
C8-DIA	9.32	47.71	10.89	5.311	1.2798
TS543	7.892	2.541	2.674	1.335	0.8642
TS603	3.28	2.572	1.712	0.8559	0.8547

Fig. S8. Combined inhibition of the fatty acid and cholesterol synthesis pathways synergistically reduce cell viability of GSCs but not mouse astrocytes. (A) Diagram showing the use of TOFA and lovastatin to inhibit the fatty acid and cholesterol synthesis pathways, respectively. **(B)** Cell viability of GSCs and astrocytes after 3 days of drug treatment (n=6). **(C)** Table showing the IC_{50} values of single or combination drug treatments of the GSCs and astrocytes. A combination index (CI) of less than one indicates drug synergy.

Table S1. GSEA gene sets and the corresponding genes, along with the Affymetrix probe sets, used for Connectivity Map Analysis.

GSEA gene sets	Gene symbol	AffyProbe Set ID
KOBAYASHI_EGFR_SIGNALING_24HR_DN	ODC1	200790_at
KOBAYASHI_EGFR_SIGNALING_24HR_DN	PAICS	201013_s_at
KOBAYASHI_EGFR_SIGNALING_24HR_DN	PAICS	201014_s_at
KOBAYASHI_EGFR_SIGNALING_24HR_DN	TUBA1B	201090_x_at
KOBAYASHI_EGFR_SIGNALING_24HR_DN	ENO2	201313_at
KOBAYASHI_EGFR_SIGNALING_24HR_DN	CCND3	201700_at
KOBAYASHI_EGFR_SIGNALING_24HR_DN	TUBG1	201714_at
KOBAYASHI_EGFR_SIGNALING_24HR_DN	SLC29A1	201801_s_at
KOBAYASHI_EGFR_SIGNALING_24HR_DN	SLC29A1	201802_at
KOBAYASHI_EGFR_SIGNALING_24HR_DN	RRM2	201890_at
KOBAYASHI_EGFR_SIGNALING_24HR_DN	PSRC1	201896_s_at
KOBAYASHI_EGFR_SIGNALING_24HR_DN	CKS1B	201897_s_at
KOBAYASHI_EGFR_SIGNALING_24HR_DN	BIRC5	202094_at
KOBAYASHI_EGFR_SIGNALING_24HR_DN	BIRC5	202095_s_at
KOBAYASHI_EGFR_SIGNALING_24HR_DN	PLK1	202240_at
KOBAYASHI_EGFR_SIGNALING_24HR_DN	UNG	202330_s_at
KOBAYASHI_EGFR_SIGNALING_24HR_DN	TK1	202338_at
KOBAYASHI_EGFR_SIGNALING_24HR_DN	FABP5	202345_s_at
KOBAYASHI_EGFR_SIGNALING_24HR_DN	TYMS	202589_at
KOBAYASHI_EGFR_SIGNALING_24HR_DN	AXL	202685_s_at
KOBAYASHI_EGFR_SIGNALING_24HR_DN	AXL	202686_s_at
KOBAYASHI_EGFR_SIGNALING_24HR_DN	UBE2S	202779_s_at
KOBAYASHI_EGFR_SIGNALING_24HR_DN	CDC20	202870_s_at
KOBAYASHI_EGFR_SIGNALING_24HR_DN	RNASEH2A	203022_at
KOBAYASHI_EGFR_SIGNALING_24HR_DN	SPAG5	203145_at
KOBAYASHI_EGFR_SIGNALING_24HR_DN	UPP1	203234_at
KOBAYASHI_EGFR_SIGNALING_24HR_DN	MAD2L1	203362_s_at
KOBAYASHI_EGFR_SIGNALING_24HR_DN	BUB1B	203755_at
KOBAYASHI_EGFR_SIGNALING_24HR_DN	DLGAP5	203764_at
KOBAYASHI_EGFR_SIGNALING_24HR_DN	VRK1	203856_at
KOBAYASHI_EGFR_SIGNALING_24HR_DN	NT5E	203939_at
KOBAYASHI_EGFR_SIGNALING_24HR_DN	AURKA	204092_s_at
KOBAYASHI_EGFR_SIGNALING_24HR_DN	CKS2	204170_s_at
KOBAYASHI_EGFR_SIGNALING_24HR_DN	CDK2	204252_at
KOBAYASHI_EGFR_SIGNALING_24HR_DN	FOSL1	204420_at
KOBAYASHI_EGFR_SIGNALING_24HR_DN	CDC25A	204695_at
KOBAYASHI_EGFR_SIGNALING_24HR_DN	CDC25A	204696_s_at
KOBAYASHI_EGFR_SIGNALING_24HR_DN	PARP2	204752_x_at
KOBAYASHI_EGFR_SIGNALING_24HR_DN	MELK	204825_at
KOBAYASHI_EGFR_SIGNALING_24HR_DN	MAFF	205193_at

KOBAYASHI_EGFR_SIGNALING_24HR_DN	GPSM2	205240_at
KOBAYASHI_EGFR_SIGNALING_24HR_DN	ACOX2	205364_at
KOBAYASHI_EGFR_SIGNALING_24HR_DN	OASL	205660_at
KOBAYASHI_EGFR_SIGNALING_24HR_DN	ADORA2B	205891_at
KOBAYASHI_EGFR_SIGNALING_24HR_DN	POLE2	205909_at
KOBAYASHI_EGFR_SIGNALING_24HR_DN	PSMC3IP	205956_x_at
KOBAYASHI_EGFR_SIGNALING_24HR_DN	SNRPA1	206055_s_at
KOBAYASHI_EGFR_SIGNALING_24HR_DN	NRG1	206237_s_at
KOBAYASHI_EGFR_SIGNALING_24HR_DN	NRG1	206343_s_at
KOBAYASHI_EGFR_SIGNALING_24HR_DN	KIF14	206364_at
KOBAYASHI_EGFR_SIGNALING_24HR_DN	IL11	206924_at
KOBAYASHI_EGFR_SIGNALING_24HR_DN	IL11	206926_s_at
KOBAYASHI_EGFR_SIGNALING_24HR_DN	HAUS7	207891_s_at
KOBAYASHI_EGFR_SIGNALING_24HR_DN	AURKA	208079_s_at
KOBAYASHI_EGFR_SIGNALING_24HR_DN	AURKA	208080_at
KOBAYASHI_EGFR_SIGNALING_24HR_DN	NRG1	208230_s_at
KOBAYASHI_EGFR_SIGNALING_24HR_DN	NRG1	208231_at
KOBAYASHI_EGFR_SIGNALING_24HR_DN	NRG1	208232_x_at
KOBAYASHI_EGFR_SIGNALING_24HR_DN	NRG1	208241_at
KOBAYASHI_EGFR_SIGNALING_24HR_DN	HMGB2	208808_s_at
KOBAYASHI_EGFR_SIGNALING_24HR_DN	TUBB4B	208977_x_at
KOBAYASHI_EGFR_SIGNALING_24HR_DN	TUBB6	209191_at
KOBAYASHI_EGFR_SIGNALING_24HR_DN	TFPI2	209277_at
KOBAYASHI_EGFR_SIGNALING_24HR_DN	TFPI2	209278_s_at
KOBAYASHI_EGFR_SIGNALING_24HR_DN	KIF2C	209408_at
KOBAYASHI_EGFR_SIGNALING_24HR_DN	AURKB	209464_at
KOBAYASHI_EGFR_SIGNALING_24HR_DN	BUB1	209642_at
KOBAYASHI_EGFR_SIGNALING_24HR_DN	RRM2	209773_s_at
KOBAYASHI_EGFR_SIGNALING_24HR_DN	PHLDA2	209802_at
KOBAYASHI_EGFR_SIGNALING_24HR_DN	PHLDA2	209803_s_at
KOBAYASHI_EGFR_SIGNALING_24HR_DN	UCK2	209825_s_at
KOBAYASHI_EGFR_SIGNALING_24HR_DN	TPX2	210052_s_at
KOBAYASHI_EGFR_SIGNALING_24HR_DN	BIRC5	210334_x_at
KOBAYASHI_EGFR_SIGNALING_24HR_DN	OASL	210797_s_at
KOBAYASHI_EGFR_SIGNALING_24HR_DN	TUBA1B	211058_x_at
KOBAYASHI_EGFR_SIGNALING_24HR_DN	TUBA1B	211072_x_at
KOBAYASHI_EGFR_SIGNALING_24HR_DN	KIF2C	211519_s_at
KOBAYASHI_EGFR_SIGNALING_24HR_DN	CDK2	211803_at
KOBAYASHI_EGFR_SIGNALING_24HR_DN	CDK2	211804_s_at
KOBAYASHI_EGFR_SIGNALING_24HR_DN	MKI67	212020_s_at
KOBAYASHI_EGFR_SIGNALING_24HR_DN	MKI67	212021_s_at
KOBAYASHI_EGFR_SIGNALING_24HR_DN	MKI67	212022_s_at
KOBAYASHI_EGFR_SIGNALING_24HR_DN	MKI67	212023_s_at

KOBAYASHI_EGFR_SIGNALING_24HR_DN	MCM4	212141_at
KOBAYASHI_EGFR_SIGNALING_24HR_DN	MCM4	212142_at
KOBAYASHI_EGFR_SIGNALING_24HR_DN	TUBA1B	212639_x_at
KOBAYASHI_EGFR_SIGNALING_24HR_DN	NCAPH	212949_at
KOBAYASHI_EGFR_SIGNALING_24HR_DN	HAUS7	213334_x_at
KOBAYASHI_EGFR_SIGNALING_24HR_DN	TMEM158	213338_at
KOBAYASHI_EGFR_SIGNALING_24HR_DN	G0S2	213524_s_at
KOBAYASHI_EGFR_SIGNALING_24HR_DN	TUBA1B	213646_x_at
KOBAYASHI_EGFR_SIGNALING_24HR_DN	TUBB4B	213726_x_at
KOBAYASHI_EGFR_SIGNALING_24HR_DN	PSMC3IP	213951_s_at
KOBAYASHI_EGFR_SIGNALING_24HR_DN	PARP2	214086_s_at
KOBAYASHI_EGFR_SIGNALING_24HR_DN	ELL2	214445_at
KOBAYASHI_EGFR_SIGNALING_24HR_DN	ELL2	214446_at
KOBAYASHI_EGFR_SIGNALING_24HR_DN	PAICS	214664_at
KOBAYASHI_EGFR_SIGNALING_24HR_DN	BUB1	215508_at
KOBAYASHI_EGFR_SIGNALING_24HR_DN	BUB1	215509_s_at
KOBAYASHI_EGFR_SIGNALING_24HR_DN	SNRPA1	215722_s_at
KOBAYASHI_EGFR_SIGNALING_24HR_DN	PARP2	215773_x_at
KOBAYASHI_EGFR_SIGNALING_24HR_DN	BUB1	216275_at
KOBAYASHI_EGFR_SIGNALING_24HR_DN	BUB1	216277_at
KOBAYASHI_EGFR_SIGNALING_24HR_DN	DSCC1	216646_at
KOBAYASHI_EGFR_SIGNALING_24HR_DN	SNRPA1	216977_x_at
KOBAYASHI_EGFR_SIGNALING_24HR_DN	TYMS	217684_at
KOBAYASHI_EGFR_SIGNALING_24HR_DN	PHLDA1	217996_at
KOBAYASHI_EGFR_SIGNALING_24HR_DN	PHLDA1	217997_at
KOBAYASHI_EGFR_SIGNALING_24HR_DN	PHLDA1	217998_at
KOBAYASHI_EGFR_SIGNALING_24HR_DN	PHLDA1	217999_s_at
KOBAYASHI_EGFR_SIGNALING_24HR_DN	PHLDA1	218000_s_at
KOBAYASHI_EGFR_SIGNALING_24HR_DN	PRC1	218009_s_at
KOBAYASHI_EGFR_SIGNALING_24HR_DN	TNFRSF12A	218368_s_at
KOBAYASHI_EGFR_SIGNALING_24HR_DN	CEP55	218542_at
KOBAYASHI_EGFR_SIGNALING_24HR_DN	HJURP	218726_at
KOBAYASHI_EGFR_SIGNALING_24HR_DN	CENPM	218741_at
KOBAYASHI_EGFR_SIGNALING_24HR_DN	POLR3K	218866_s_at
KOBAYASHI_EGFR_SIGNALING_24HR_DN	DSCC1	219000_s_at
KOBAYASHI_EGFR_SIGNALING_24HR_DN	PBK	219148_at
KOBAYASHI_EGFR_SIGNALING_24HR_DN	NUDT15	219347_at
KOBAYASHI_EGFR_SIGNALING_24HR_DN	DSN1	219512_at
KOBAYASHI_EGFR_SIGNALING_24HR_DN	ECT2	219787_s_at
KOBAYASHI_EGFR_SIGNALING_24HR_DN	E2F8	219990_at
KOBAYASHI_EGFR_SIGNALING_24HR_DN	HELLS	220085_at
KOBAYASHI_EGFR_SIGNALING_24HR_DN	DEPDC1	220295_x_at
KOBAYASHI_EGFR_SIGNALING_24HR_DN	CDCA3	221436_s_at

KOBAYASHI_EGFR_SIGNALING_24HR_DN	DONSON	221677_s_at
KOBAYASHI_EGFR_SIGNALING_24HR_DN	GPSM2	221922_at
KOBAYASHI_EGFR_SIGNALING_24HR_DN	MCM4	222036_s_at
KOBAYASHI_EGFR_SIGNALING_24HR_DN	MCM4	222037_at
KOBAYASHI_EGFR_SIGNALING_24HR_DN	KIF18B	222039_at
KOBAYASHI_EGFR_SIGNALING_24HR_DN	MAFF	36711_at
VERHAAK_GLIOBLASTOMA_MESENCHYMAL	S100A11	200660_at
VERHAAK_GLIOBLASTOMA_MESENCHYMAL	NPC2	200701_at
VERHAAK_GLIOBLASTOMA_MESENCHYMAL	IQGAP1	200791_s_at
VERHAAK_GLIOBLASTOMA_MESENCHYMAL	ANXA1	201012_at
VERHAAK_GLIOBLASTOMA_MESENCHYMAL	SYNGR2	201079_at
VERHAAK_GLIOBLASTOMA_MESENCHYMAL	PLS3	201215_at
VERHAAK_GLIOBLASTOMA_MESENCHYMAL	ANXA4	201301_s_at
VERHAAK_GLIOBLASTOMA_MESENCHYMAL	ANXA4	201302_at
VERHAAK_GLIOBLASTOMA_MESENCHYMAL	SHC1	201469_s_at
VERHAAK_GLIOBLASTOMA_MESENCHYMAL	ANXA2	201590_x_at
VERHAAK_GLIOBLASTOMA_MESENCHYMAL	CNN2	201605_x_at
VERHAAK_GLIOBLASTOMA_MESENCHYMAL	TIMP1	201666_at
VERHAAK_GLIOBLASTOMA_MESENCHYMAL	LAPTM5	201720_s_at
VERHAAK_GLIOBLASTOMA_MESENCHYMAL	LAPTM5	201721_s_at
VERHAAK_GLIOBLASTOMA_MESENCHYMAL	MYOF	201798_s_at
VERHAAK_GLIOBLASTOMA_MESENCHYMAL	LRRFIP1	201861_s_at
VERHAAK_GLIOBLASTOMA_MESENCHYMAL	LRRFIP1	201862_s_at
VERHAAK_GLIOBLASTOMA_MESENCHYMAL	HEXB	201944_at
VERHAAK_GLIOBLASTOMA_MESENCHYMAL	ARPC1B	201954_at
VERHAAK_GLIOBLASTOMA_MESENCHYMAL	ACSL1	201963_at
VERHAAK_GLIOBLASTOMA_MESENCHYMAL	WWTR1	202132_at
VERHAAK_GLIOBLASTOMA_MESENCHYMAL	WWTR1	202133_at
VERHAAK_GLIOBLASTOMA_MESENCHYMAL	WWTR1	202134_s_at
VERHAAK_GLIOBLASTOMA_MESENCHYMAL	MVP	202180_s_at
VERHAAK_GLIOBLASTOMA_MESENCHYMAL	BLVRB	202201_at
VERHAAK_GLIOBLASTOMA_MESENCHYMAL	SEC24D	202375_at
VERHAAK_GLIOBLASTOMA_MESENCHYMAL	SERPINE1	202627_s_at
VERHAAK_GLIOBLASTOMA_MESENCHYMAL	SERPINE1	202628_s_at
VERHAAK_GLIOBLASTOMA_MESENCHYMAL	WIPF1	202663_at
VERHAAK_GLIOBLASTOMA_MESENCHYMAL	WIPF1	202664_at
VERHAAK_GLIOBLASTOMA_MESENCHYMAL	WIPF1	202665_s_at
VERHAAK_GLIOBLASTOMA_MESENCHYMAL	P4HA2	202733_at
VERHAAK_GLIOBLASTOMA_MESENCHYMAL	SLC16A3	202855_s_at
VERHAAK_GLIOBLASTOMA_MESENCHYMAL	SLC16A3	202856_s_at
VERHAAK_GLIOBLASTOMA_MESENCHYMAL	IL1R1	202948_at
VERHAAK_GLIOBLASTOMA_MESENCHYMAL	FHL2	202949_s_at
VERHAAK_GLIOBLASTOMA_MESENCHYMAL	PYGL	202990_at

VERHAAK_GLIOBLASTOMA_MESENCHYMAL	S100A4	203186_s_at
VERHAAK_GLIOBLASTOMA_MESENCHYMAL	IL4R	203233_at
VERHAAK_GLIOBLASTOMA_MESENCHYMAL	SH2B3	203320_at
VERHAAK_GLIOBLASTOMA_MESENCHYMAL	SAT1	203455_s_at
VERHAAK_GLIOBLASTOMA_MESENCHYMAL	ELF4	203490_at
VERHAAK_GLIOBLASTOMA_MESENCHYMAL	TNFRSF1B	203508_at
VERHAAK_GLIOBLASTOMA_MESENCHYMAL	CD4	203547_at
VERHAAK_GLIOBLASTOMA_MESENCHYMAL	FCGR2A	203561_at
VERHAAK_GLIOBLASTOMA_MESENCHYMAL	PROCR	203650_at
VERHAAK_GLIOBLASTOMA_MESENCHYMAL	EMP3	203729_at
VERHAAK_GLIOBLASTOMA_MESENCHYMAL	TGOLN2	203833_s_at
VERHAAK_GLIOBLASTOMA_MESENCHYMAL	TGOLN2	203834_s_at
VERHAAK_GLIOBLASTOMA_MESENCHYMAL	ARHGAP29	203910_at
VERHAAK_GLIOBLASTOMA_MESENCHYMAL	STAB1	204150_at
VERHAAK_GLIOBLASTOMA_MESENCHYMAL	PLA2G15	204458_at
VERHAAK_GLIOBLASTOMA_MESENCHYMAL	DSC2	204750_s_at
VERHAAK_GLIOBLASTOMA_MESENCHYMAL	DSC2	204751_x_at
VERHAAK_GLIOBLASTOMA_MESENCHYMAL	TYMP	204858_s_at
VERHAAK_GLIOBLASTOMA_MESENCHYMAL	PDPN	204879_at
VERHAAK_GLIOBLASTOMA_MESENCHYMAL	VAMP5	204929_s_at
VERHAAK_GLIOBLASTOMA_MESENCHYMAL	PLK3	204958_at
VERHAAK_GLIOBLASTOMA_MESENCHYMAL	MAN2A1	205105_at
VERHAAK_GLIOBLASTOMA_MESENCHYMAL	NCF4	205147_x_at
VERHAAK_GLIOBLASTOMA_MESENCHYMAL	RELB	205205_at
VERHAAK_GLIOBLASTOMA_MESENCHYMAL	EHD2	205341_at
VERHAAK_GLIOBLASTOMA_MESENCHYMAL	GNA15	205349_at
VERHAAK_GLIOBLASTOMA_MESENCHYMAL	FES	205418_at
VERHAAK_GLIOBLASTOMA_MESENCHYMAL	PLAU	205479_s_at
VERHAAK_GLIOBLASTOMA_MESENCHYMAL	SRPX2	205499_at
VERHAAK_GLIOBLASTOMA_MESENCHYMAL	GCNT1	205505_at
VERHAAK_GLIOBLASTOMA_MESENCHYMAL	TRPM2	205708_s_at
VERHAAK_GLIOBLASTOMA_MESENCHYMAL	ITGAM	205786_s_at
VERHAAK_GLIOBLASTOMA_MESENCHYMAL	BDKRB2	205870_at
VERHAAK_GLIOBLASTOMA_MESENCHYMAL	HK3	205936_s_at
VERHAAK_GLIOBLASTOMA_MESENCHYMAL	EFEMP2	206580_s_at
VERHAAK_GLIOBLASTOMA_MESENCHYMAL	PTPN6	206687_s_at
VERHAAK_GLIOBLASTOMA_MESENCHYMAL	ACSL1	207275_s_at
VERHAAK_GLIOBLASTOMA_MESENCHYMAL	TGFBR2	207334_s_at
VERHAAK_GLIOBLASTOMA_MESENCHYMAL	IL15RA	207375_s_at
VERHAAK_GLIOBLASTOMA_MESENCHYMAL	CAST	207467_x_at
VERHAAK_GLIOBLASTOMA_MESENCHYMAL	TNFRSF1A	207643_s_at
VERHAAK_GLIOBLASTOMA_MESENCHYMAL	NCF4	207677_s_at
VERHAAK_GLIOBLASTOMA_MESENCHYMAL	AMPD3	207992_s_at

VERHAAK_GLIOBLASTOMA_MESENCHYMAL	MAN1A1	208116_s_at
VERHAAK_GLIOBLASTOMA_MESENCHYMAL	PDPN	208233_at
VERHAAK_GLIOBLASTOMA_MESENCHYMAL	TNFAIP8	208296_x_at
VERHAAK_GLIOBLASTOMA_MESENCHYMAL	LILRB3	208594_x_at
VERHAAK_GLIOBLASTOMA_MESENCHYMAL	CLIC1	208659_at
VERHAAK_GLIOBLASTOMA_MESENCHYMAL	CAST	208908_s_at
VERHAAK_GLIOBLASTOMA_MESENCHYMAL	TGFBR2	208944_at
VERHAAK_GLIOBLASTOMA_MESENCHYMAL	LGALS3	208949_s_at
VERHAAK_GLIOBLASTOMA_MESENCHYMAL	MRC2	209280_at
VERHAAK_GLIOBLASTOMA_MESENCHYMAL	SWAP70	209306_s_at
VERHAAK_GLIOBLASTOMA_MESENCHYMAL	SWAP70	209307_at
VERHAAK_GLIOBLASTOMA_MESENCHYMAL	UAP1	209340_at
VERHAAK_GLIOBLASTOMA_MESENCHYMAL	EFEMP2	209356_x_at
VERHAAK_GLIOBLASTOMA_MESENCHYMAL	STXBP2	209367_at
VERHAAK_GLIOBLASTOMA_MESENCHYMAL	CHI3L1	209395_at
VERHAAK_GLIOBLASTOMA_MESENCHYMAL	CHI3L1	209396_s_at
VERHAAK_GLIOBLASTOMA_MESENCHYMAL	AMPD3	209491_s_at
VERHAAK_GLIOBLASTOMA_MESENCHYMAL	RAB27A	209514_s_at
VERHAAK_GLIOBLASTOMA_MESENCHYMAL	RAB27A	209515_s_at
VERHAAK_GLIOBLASTOMA_MESENCHYMAL	CLEC2B	209732_at
VERHAAK_GLIOBLASTOMA_MESENCHYMAL	NCF2	209949_at
VERHAAK_GLIOBLASTOMA_MESENCHYMAL	CTSZ	210042_s_at
VERHAAK_GLIOBLASTOMA_MESENCHYMAL	LILRB3	210225_x_at
VERHAAK_GLIOBLASTOMA_MESENCHYMAL	TNFAIP8	210260_s_at
VERHAAK_GLIOBLASTOMA_MESENCHYMAL	SWAP70	210369_at
VERHAAK_GLIOBLASTOMA_MESENCHYMAL	SLC11A1	210422_x_at
VERHAAK_GLIOBLASTOMA_MESENCHYMAL	SLC11A1	210423_s_at
VERHAAK_GLIOBLASTOMA_MESENCHYMAL	ANXA2	210427_x_at
VERHAAK_GLIOBLASTOMA_MESENCHYMAL	SAT1	210592_s_at
VERHAAK_GLIOBLASTOMA_MESENCHYMAL	SAT1	210593_at
VERHAAK_GLIOBLASTOMA_MESENCHYMAL	LILRB3	210784_x_at
VERHAAK_GLIOBLASTOMA_MESENCHYMAL	IQGAP1	210840_s_at
VERHAAK_GLIOBLASTOMA_MESENCHYMAL	PLAUR	210845_s_at
VERHAAK_GLIOBLASTOMA_MESENCHYMAL	FCGR2B	210889_s_at
VERHAAK_GLIOBLASTOMA_MESENCHYMAL	RAB27A	210951_x_at
VERHAAK_GLIOBLASTOMA_MESENCHYMAL	LILRB3	211133_x_at
VERHAAK_GLIOBLASTOMA_MESENCHYMAL	LILRB3	211135_x_at
VERHAAK_GLIOBLASTOMA_MESENCHYMAL	LRRFIP1	211452_x_at
VERHAAK_GLIOBLASTOMA_MESENCHYMAL	PLAU	211668_s_at
VERHAAK_GLIOBLASTOMA_MESENCHYMAL	MYOF	211864_s_at
VERHAAK_GLIOBLASTOMA_MESENCHYMAL	PLAUR	211924_s_at
VERHAAK_GLIOBLASTOMA_MESENCHYMAL	TGOLN2	212040_at
VERHAAK_GLIOBLASTOMA_MESENCHYMAL	TGOLN2	212043_at

VERHAAK_GLIOBLASTOMA_MESENCHYMAL	CTSZ	212562_s_at
VERHAAK_GLIOBLASTOMA_MESENCHYMAL	CAST	212580_at
VERHAAK_GLIOBLASTOMA_MESENCHYMAL	CAST	212586_at
VERHAAK_GLIOBLASTOMA_MESENCHYMAL	LHFPL2	212658_at
VERHAAK_GLIOBLASTOMA_MESENCHYMAL	IQGAP1	213446_s_at
VERHAAK_GLIOBLASTOMA_MESENCHYMAL	ANXA2	213503_x_at
VERHAAK_GLIOBLASTOMA_MESENCHYMAL	SAT1	213988_s_at
VERHAAK_GLIOBLASTOMA_MESENCHYMAL	VAMP5	214115_at
VERHAAK_GLIOBLASTOMA_MESENCHYMAL	FPR3	214560_at
VERHAAK_GLIOBLASTOMA_MESENCHYMAL	SFT2D2	214838_at
VERHAAK_GLIOBLASTOMA_MESENCHYMAL	SHC1	214853_s_at
VERHAAK_GLIOBLASTOMA_MESENCHYMAL	PLAUR	214866_at
VERHAAK_GLIOBLASTOMA_MESENCHYMAL	SEC24D	215209_at
VERHAAK_GLIOBLASTOMA_MESENCHYMAL	LRRFIP1	215375_x_at
VERHAAK_GLIOBLASTOMA_MESENCHYMAL	PLK3	215462_at
VERHAAK_GLIOBLASTOMA_MESENCHYMAL	IL1R1	215561_s_at
VERHAAK_GLIOBLASTOMA_MESENCHYMAL	SEC24D	215641_at
VERHAAK_GLIOBLASTOMA_MESENCHYMAL	CD4	216424_at
VERHAAK_GLIOBLASTOMA_MESENCHYMAL	CHI3L1	216546_s_at
VERHAAK_GLIOBLASTOMA_MESENCHYMAL	SRPX2	216639_at
VERHAAK_GLIOBLASTOMA_MESENCHYMAL	RUNX2	216994_s_at
VERHAAK_GLIOBLASTOMA_MESENCHYMAL	SLC11A1	217473_x_at
VERHAAK_GLIOBLASTOMA_MESENCHYMAL	TYMP	217497_at
VERHAAK_GLIOBLASTOMA_MESENCHYMAL	SLC11A1	217507_at
VERHAAK_GLIOBLASTOMA_MESENCHYMAL	MYOF	217518_at
VERHAAK_GLIOBLASTOMA_MESENCHYMAL	FXYD5	217655_at
VERHAAK_GLIOBLASTOMA_MESENCHYMAL	SLC16A3	217691_x_at
VERHAAK_GLIOBLASTOMA_MESENCHYMAL	TMBIM1	217730_at
VERHAAK_GLIOBLASTOMA_MESENCHYMAL	RBM47	218035_s_at
VERHAAK_GLIOBLASTOMA_MESENCHYMAL	FXYD5	218084_x_at
VERHAAK_GLIOBLASTOMA_MESENCHYMAL	CDCP1	218451_at
VERHAAK_GLIOBLASTOMA_MESENCHYMAL	PLBD1	218454_at
VERHAAK_GLIOBLASTOMA_MESENCHYMAL	FHOD1	218530_at
VERHAAK_GLIOBLASTOMA_MESENCHYMAL	CLCF1	219500_at
VERHAAK_GLIOBLASTOMA_MESENCHYMAL	COPZ2	219561_at
VERHAAK_GLIOBLASTOMA_MESENCHYMAL	RAB11FIP1	219681_s_at
VERHAAK_GLIOBLASTOMA_MESENCHYMAL	ARSJ	219973_at
VERHAAK_GLIOBLASTOMA_MESENCHYMAL	NOD2	220066_at
VERHAAK_GLIOBLASTOMA_MESENCHYMAL	C5AR1	220088_at
VERHAAK_GLIOBLASTOMA_MESENCHYMAL	BNC2	220272_at
VERHAAK_GLIOBLASTOMA_MESENCHYMAL	RUNX2	221282_x_at
VERHAAK_GLIOBLASTOMA_MESENCHYMAL	RUNX2	221283_at
VERHAAK_GLIOBLASTOMA_MESENCHYMAL	MAN1A1	221760_at

VERHAAK_GLIOBLASTOMA_MESENCHYMAL	PHF11	221816_s_at
VERHAAK_GLIOBLASTOMA_MESENCHYMAL	EHD2	221870_at
VERHAAK_GLIOBLASTOMA_MESENCHYMAL	PDPN	221898_at
VERHAAK_GLIOBLASTOMA_MESENCHYMAL	COL8A2	221900_at
VERHAAK_GLIOBLASTOMA_MESENCHYMAL	RAB27A	222294_s_at
VERHAAK_GLIOBLASTOMA_MESENCHYMAL	ELF4	31845_at
VERHAAK_GLIOBLASTOMA_MESENCHYMAL	MRC2	37408_at
VERHAAK_GLIOBLASTOMA_MESENCHYMAL	STAB1	38487_at
VERHAAK_GLIOBLASTOMA_MESENCHYMAL	EHD2	45297_at
VERHAAK_GLIOBLASTOMA_MESENCHYMAL	COL8A2	52651_at
GO: 0048699: generation of neurons	HDAC1	201209_at
GO: 0048699: generation of neurons	ID2	201565_s_at
GO: 0048699: generation of neurons	ID2	201566_x_at
GO: 0048699: generation of neurons	PLK2	201939_at
GO: 0048699: generation of neurons	ARHGAP35	202044_at
GO: 0048699: generation of neurons	ARHGAP35	202045_s_at
GO: 0048699: generation of neurons	ARHGAP35	202046_s_at
GO: 0048699: generation of neurons	SPOCK1	202363_at
GO: 0048699: generation of neurons	PPP3CB	202432_at
GO: 0048699: generation of neurons	HDAC5	202455_at
GO: 0048699: generation of neurons	TRIOBP	202795_x_at
GO: 0048699: generation of neurons	AGT	202834_at
GO: 0048699: generation of neurons	DDIT4	202887_s_at
GO: 0048699: generation of neurons	BIN1	202931_x_at
GO: 0048699: generation of neurons	SEMA3B	203070_at
GO: 0048699: generation of neurons	SEMA3B	203071_at
GO: 0048699: generation of neurons	PTK2B	203110_at
GO: 0048699: generation of neurons	PTK2B	203111_s_at
GO: 0048699: generation of neurons	HES1	203393_at
GO: 0048699: generation of neurons	HES1	203394_s_at
GO: 0048699: generation of neurons	HES1	203395_s_at
GO: 0048699: generation of neurons	LDB1	203451_at
GO: 0048699: generation of neurons	SEMA4D	203528_at
GO: 0048699: generation of neurons	RAP1GAP	203911_at
GO: 0048699: generation of neurons	PBX3	204082_at
GO: 0048699: generation of neurons	CDK5	204247_s_at
GO: 0048699: generation of neurons	EDNRB	204271_s_at
GO: 0048699: generation of neurons	EDNRB	204273_at
GO: 0048699: generation of neurons	NEO1	204321_at
GO: 0048699: generation of neurons	ARHGAP4	204425_at
GO: 0048699: generation of neurons	GNAO1	204762_s_at
GO: 0048699: generation of neurons	GNAO1	204763_s_at
GO: 0048699: generation of neurons	DCX	204850_s_at

GO: 0048699: generation of neurons	DCX	204851_s_at
GO: 0048699: generation of neurons	IL6ST	204863_s_at
GO: 0048699: generation of neurons	IL6ST	204864_s_at
GO: 0048699: generation of neurons	ATF5	204998_s_at
GO: 0048699: generation of neurons	ATF5	204999_s_at
GO: 0048699: generation of neurons	DCT	205337_at
GO: 0048699: generation of neurons	DCT	205338_s_at
GO: 0048699: generation of neurons	DPYSL4	205492_s_at
GO: 0048699: generation of neurons	DPYSL4	205493_s_at
GO: 0048699: generation of neurons	AVIL	205539_at
GO: 0048699: generation of neurons	NCAM2	205669_at
GO: 0048699: generation of neurons	TULP3	205854_at
GO: 0048699: generation of neurons	NGFR	205858_at
GO: 0048699: generation of neurons	GRIN1	205914_s_at
GO: 0048699: generation of neurons	GRIN1	205915_x_at
GO: 0048699: generation of neurons	PLXNB3	205957_at
GO: 0048699: generation of neurons	BRAF	206044_s_at
GO: 0048699: generation of neurons	LLGL1	206123_at
GO: 0048699: generation of neurons	LLGL1	206124_s_at
GO: 0048699: generation of neurons	NEUROD1	206282_at
GO: 0048699: generation of neurons	ANK3	206385_s_at
GO: 0048699: generation of neurons	INSM1	206502_s_at
GO: 0048699: generation of neurons	MAP4K4	206571_s_at
GO: 0048699: generation of neurons	SKIL	206675_s_at
GO: 0048699: generation of neurons	EDNRB	206701_x_at
GO: 0048699: generation of neurons	PTK7	207011_s_at
GO: 0048699: generation of neurons	MAPK6	207121_s_at
GO: 0048699: generation of neurons	CRTC1	207159_x_at
GO: 0048699: generation of neurons	CDON	207230_at
GO: 0048699: generation of neurons	PLXNA2	207290_at
GO: 0048699: generation of neurons	MAGI2	207702_s_at
GO: 0048699: generation of neurons	ANK3	207950_s_at
GO: 0048699: generation of neurons	LBX1	208380_at
GO: 0048699: generation of neurons	LMX1B	208487_at
GO: 0048699: generation of neurons	PTCH1	208522_s_at
GO: 0048699: generation of neurons	PLXNB2	208890_s_at
GO: 0048699: generation of neurons	TCF12	208986_at
GO: 0048699: generation of neurons	NR2F2	209119_x_at
GO: 0048699: generation of neurons	NR2F2	209120_at
GO: 0048699: generation of neurons	NR2F2	209121_x_at
GO: 0048699: generation of neurons	CXCR4	209201_x_at
GO: 0048699: generation of neurons	TSC1	209390_at
GO: 0048699: generation of neurons	ANK3	209442_x_at

GO: 0048699: generation of neurons	MAGI2	209737_at
GO: 0048699: generation of neurons	PTCH1	209815_at
GO: 0048699: generation of neurons	PTCH1	209816_at
GO: 0048699: generation of neurons	PPP3CB	209817_at
GO: 0048699: generation of neurons	VLDLR	209822_s_at
GO: 0048699: generation of neurons	LRRN3	209840_s_at
GO: 0048699: generation of neurons	LRRN3	209841_s_at
GO: 0048699: generation of neurons	ADGRL3	209866_s_at
GO: 0048699: generation of neurons	ADGRL3	209867_s_at
GO: 0048699: generation of neurons	MAP2	210015_s_at
GO: 0048699: generation of neurons	RND1	210056_at
GO: 0048699: generation of neurons	BIN1	210201_x_at
GO: 0048699: generation of neurons	BIN1	210202_s_at
GO: 0048699: generation of neurons	TRIOBP	210276_s_at
GO: 0048699: generation of neurons	BCL11A	210347_s_at
GO: 0048699: generation of neurons	FLRT1	210414_at
GO: 0048699: generation of neurons	AVIL	210507_s_at
GO: 0048699: generation of neurons	RAP1GAP	210618_at
GO: 0048699: generation of neurons	GRIN1	210781_x_at
GO: 0048699: generation of neurons	GRIN1	210782_x_at
GO: 0048699: generation of neurons	IL6ST	211000_s_at
GO: 0048699: generation of neurons	GRIN1	211125_x_at
GO: 0048699: generation of neurons	PLXNB2	211472_at
GO: 0048699: generation of neurons	CXCR4	211919_s_at
GO: 0048699: generation of neurons	IL6ST	212195_at
GO: 0048699: generation of neurons	IL6ST	212196_at
GO: 0048699: generation of neurons	AGRN	212283_at
GO: 0048699: generation of neurons	AGRN	212285_s_at
GO: 0048699: generation of neurons	USP33	212513_s_at
GO: 0048699: generation of neurons	HRAS	212983_at
GO: 0048699: generation of neurons	PLXNA2	213030_s_at
GO: 0048699: generation of neurons	NPTXR	213040_s_at
GO: 0048699: generation of neurons	CRTC1	213091_at
GO: 0048699: generation of neurons	SRC	213324_at
GO: 0048699: generation of neurons	ID2	213931_at
GO: 0048699: generation of neurons	DPYSL4	214301_s_at
GO: 0048699: generation of neurons	BIN1	214439_x_at
GO: 0048699: generation of neurons	BIN1	214643_x_at
GO: 0048699: generation of neurons	MEGF8	214778_at
GO: 0048699: generation of neurons	BRINP2	214822_at
GO: 0048699: generation of neurons	USP33	214843_s_at
GO: 0048699: generation of neurons	NR2F2	215073_s_at
GO: 0048699: generation of neurons	DOCK10	215151_at

GO: 0048699: generation of neurons	TNN	215271_at
GO: 0048699: generation of neurons	TCF12	215611_at
GO: 0048699: generation of neurons	PLXNB1	215668_s_at
GO: 0048699: generation of neurons	PLXNB1	215807_s_at
GO: 0048699: generation of neurons	SKIL	215889_at
GO: 0048699: generation of neurons	GNAO1	215912_at
GO: 0048699: generation of neurons	TRIOBP	216210_x_at
GO: 0048699: generation of neurons	TGIF2	216262_s_at
GO: 0048699: generation of neurons	DCT	216512_s_at
GO: 0048699: generation of neurons	DCT	216513_at
GO: 0048699: generation of neurons	CXCR4	217028_at
GO: 0048699: generation of neurons	NPTXR	217041_at
GO: 0048699: generation of neurons	ATF5	217389_s_at
GO: 0048699: generation of neurons	AGRN	217410_at
GO: 0048699: generation of neurons	AGRN	217419_x_at
GO: 0048699: generation of neurons	USP33	217441_at
GO: 0048699: generation of neurons	SKIL	217591_at
GO: 0048699: generation of neurons	MAP4K4	218181_s_at
GO: 0048699: generation of neurons	TGIF2	218724_s_at
GO: 0048699: generation of neurons	CHD7	218829_s_at
GO: 0048699: generation of neurons	TMEM106B	218930_s_at
GO: 0048699: generation of neurons	DOCK10	219279_at
GO: 0048699: generation of neurons	BCL11A	219497_s_at
GO: 0048699: generation of neurons	BCL11A	219498_s_at
GO: 0048699: generation of neurons	DLL3	219537_x_at
GO: 0048699: generation of neurons	PCDH12	219656_at
GO: 0048699: generation of neurons	SPTBN5	220067_at
GO: 0048699: generation of neurons	MYLIP	220319_s_at
GO: 0048699: generation of neurons	CRB1	220522_at
GO: 0048699: generation of neurons	CHD7	220619_at
GO: 0048699: generation of neurons	SRC	221281_at
GO: 0048699: generation of neurons	SRC	221284_s_at
GO: 0048699: generation of neurons	PLXNA1	221537_at
GO: 0048699: generation of neurons	PLXNA1	221538_s_at
GO: 0048699: generation of neurons	TULP3	221964_at
GO: 0048699: generation of neurons	LDB1	35160_at

Table S2: List of differentially expressed genes in SN- vs DMSO-treated GSC TS543.

Gene symbol	Fold change (SN/DMSO)	Padj value
PIM1	92.120	0
PCSK9	76.844	0
FABP3	65.413	0
GADD45G	64.259	0
PHYHIP	53.775	0
IL21R	52.219	0
MAFF	50.502	0
LIPG	49.673	0
PRDX3P1	46.527	0
PHLDA2	44.343	0
HMGCS1	42.654	0
TFCP2L1	40.964	0
PIP4P1	38.582	0
PCBP2-OT1	37.025	0
RUSC1-AS1	36.720	0
TINCR	35.317	1.06E-13
GDF15	31.386	0
MYBPC2	30.926	0
TMEM191B	28.956	0
DDIT3	28.756	0
SLC7A5P2	28.026	0
ACSS2	27.827	0
INSIG1	27.365	0
FGF21	26.451	0
HIST1H1E	26.321	1.35E-12
PLA2G3	25.009	0
MICA	24.575	0
PPP1R15A	23.889	0
HSD17B7P2	23.331	0
RPL29P14	23.316	7.51E-05
NR4A3	23.233	0
MVD	22.274	0
ICAM1	21.192	0
MSMO1	20.954	0
BBC3	20.442	0
NR1D1	20.101	0
DRD4	19.818	0
HSPA1B	19.738	0.000181622
AQP3	19.554	0
PLK2	19.465	0
ATF3	19.255	0
BIRC7	19.244	1.94E-07

RTN4R	19.102	0
IGSF6	18.974	1.21E-11
DERL3	18.679	0
YOD1	18.507	0
NEU1	18.262	0
RPSAP36	17.221	4.16E-12
DUSP8	16.923	0
FUT3	16.817	2.16E-05
MXD1	16.466	0
CHST1	16.450	1.83E-07
RN7SK	16.306	8.48E-11
RN7SKP23	16.086	0
IDI1	15.960	0
GLIPR1	15.785	0
LRRC70	15.559	2.86E-07
SNORA53	15.476	0.00136322
CDHR1	15.427	0
FIBCD1	15.119	3.72E-06
PLIN4	15.118	0
USP3-AS1	14.865	8.51E-07
PLK5	14.820	0
DNAJB9	14.799	0
BGLAP	14.765	9.82E-05
EHMT2-AS1	14.746	5.96E-06
GPR182	14.635	1.31E-10
SDS	14.352	3.47E-05
EID3	14.335	2.94E-07
FA2H	14.315	0
PTHLH	14.236	0
SLC30A3	14.228	0
CABP7	13.868	0
CREBRF	13.774	0
CYR61	13.659	0
GPRC5A	13.655	0
DHCR7	13.184	0
BANCR	12.901	4.74E-10
SIX2	12.795	0
CARS-AS1	12.775	4.70E-10
ANKRD10-IT1	12.750	0
CPEB1	12.731	0
KLF11	12.685	0
LINC02019	12.651	0
ADGRF3	12.596	2.44E-08
SNORD3B-1	12.501	8.01E-10
SERINC2	12.413	0

TRIM63	12.381	0
ACAT2	12.305	0
COL8A2	12.274	0
MUC22	12.068	0.002192858
PBX4	11.998	8.09E-08
SLC26A6	11.860	0
PIK3IP1	11.844	0
SOCS1	11.842	0
OTUD1	11.678	0
ACHE	11.619	0
PER1	11.381	0
CELF2-AS1	11.281	0
MAPT-IT1	11.178	0.000357599
RBM5-AS1	11.106	0
ELAVL3	11.015	0
CHRD	11.000	1.25E-08
KLF6	10.988	0
LDLR	10.983	0
SIK1	10.877	0
MVK	10.823	0
PLXDC1	10.752	0
FAM131C	10.738	6.20E-12
USP17L11	10.699	0.000528457
SIK1B	10.697	0
CYP51A1P2	10.696	0
VASN	10.507	0
SNORD3A	10.395	6.85E-07
VPS37D	10.271	0
CRACR2B	10.236	0
MKNK2	10.194	0
PTGES	10.125	0
GADD45B	10.112	0
SAP25	9.980	4.86E-11
CILP2	9.950	0
SPDEF	9.926	0.000251904
ATP6V1C2	9.911	1.16E-08
IGFN1	9.881	0.000607022
LINC-PINT	9.779	0
CYP51A1	9.590	0
TSIX	9.540	4.57E-07
RN7SKP255	9.514	0.001520422
NKX1-2	9.513	1.20E-06
C1QTNF12	9.496	6.44E-15
STARD4	9.370	0
SEMA3F	9.273	0

TSC22D3	9.262	0
CRYAB	9.215	0
KCNJ4	9.215	0
RASD1	9.193	0.000133048
BLOC1S3	9.156	0
NRTN	9.122	0
CLDN4	9.114	0
HAP1	9.112	0
CIART	9.081	0
CYP51A1P1	9.045	0
TBC1D26	9.011	0.001824891
SCDP1	8.929	0
CDHR5	8.686	3.10E-12
SLC20A1	8.683	0
EPHA1	8.681	3.15E-06
JUND	8.668	0
EBP	8.664	0
NAT16	8.659	0
CSF1	8.576	0
SLC43A3	8.573	0
LIF	8.550	0
ARL4C	8.508	0
MAPT-AS1	8.446	0.001393231
MIR193BHG	8.427	1.59E-09
DBP	8.423	0
MRPL23-AS1	8.379	9.54E-12
TMEM97	8.360	0
SQLE	8.336	0
MICB	8.326	0
VAT1	8.320	0
ADAMTS14	8.318	0
FMNL1	8.274	0.047791301
H19	8.147	0
CAPN12	8.110	0
BEX2	8.095	0
CDKN1A	8.029	0
HMGCR	8.008	0
SCD	8.001	0
SELENOM	7.976	2.62E-06
POU5F1P3	7.895	0.000132054
TMEM151A	7.889	0.004867028
ERG28	7.721	0
CD68	7.715	8.88E-16
TEX29	7.702	4.63E-07
MAP1LC3C	7.650	0.036581403

GSDMB	7.601	0
ELF4	7.579	0
IFITM10	7.547	8.45E-08
MAG	7.505	6.72E-05
DMKN	7.501	0.001430763
NIPAL4	7.449	0
SPATA31A3	7.364	3.77E-07
CLK1	7.308	0
HIST2H2BE	7.261	0
GEM	7.200	0
VGF	7.194	0
CCT6P1	7.142	0
SHISA9	7.108	0
FDFT1	7.100	0
SDCBP2	7.079	0
SH2D3C	7.076	9.57E-07
PRRT2	7.062	0
AHNAK	7.029	0
KCNF1	6.966	0
MIAT	6.934	0
ZFP36L1	6.918	0
LINC00598	6.912	0
HES4	6.912	0
LINC01529	6.895	1.73E-13
ABHD4	6.892	0
SERPINE1	6.854	0
EFNA1	6.829	0
MALAT1	6.815	4.30E-12
GGT7	6.799	0
HSD17B7	6.777	0
ZFAND2B	6.773	0
UNC13A	6.759	0
UBALD1	6.743	0
ZNF750	6.740	0.000945603
CISH	6.717	0
SH2D5	6.702	0
NFIL3	6.696	0
FGFBP3	6.679	0
AOC2	6.556	0
TMEM262	6.553	6.83E-08
XIRP2	6.519	0.032311935
OSER1	6.498	0
RFTN1	6.498	6.10E-08
CCDC9	6.497	0
MFAP4	6.489	0

EPPK1	6.481	0.003838988
SC5D	6.476	0
TF	6.422	0
CLCN6	6.407	0
TMEM191C	6.378	5.03E-08
ALMS1-IT1	6.374	0
MUC16	6.338	0.003108876
SNHG22	6.329	1.49E-11
HSPA1A	6.319	0.008051836
RNA5-8SN1	6.316	0
RNA5-8SN2	6.316	0
RNA5-8SN4	6.316	0
PSD2	6.290	2.22E-16
TRIM22	6.284	0.031324283
CCT6P3	6.254	0
OR7D2	6.235	6.25E-10
FTL	6.219	0
NAMPTP1	6.202	0
NSDHL	6.166	0
C2CD4C	6.119	4.04E-05
RAB3IL1	6.098	0
MAFK	6.091	0
PNP	6.088	0
DNAJB1	6.056	8.51E-06
PRR5L	6.044	0
EIF2AK3	6.038	0
SALL4	6.033	2.94E-08
LPIN1	6.030	0
SPATA31D1	6.020	0.015868449
MEG3	6.019	2.79E-11
ARHGEF5	6.007	0.001484194
NUPR1	6.005	0
PATL1	5.955	0
CCDC28B	5.944	0
MIR17HG	5.936	4.15E-11
SMG1P3	5.922	0
IDI2-AS1	5.918	1.47E-09
PRELID3A	5.916	0
OVGP1	5.915	0
TMEM75	5.877	0
FTLP3	5.870	0
KPRP	5.869	0.044115603
RGS3	5.831	0
MAGEL2	5.818	0.020326532
TMEM54	5.808	5.62E-06

MIIP	5.791	0
GABARAPL1	5.784	0
TXNIP	5.782	0
PANX2	5.737	1.24E-06
FLNC	5.733	0
IER5L	5.724	0
KIF2B	5.703	0.036886947
RN7SKP203	5.700	0.003907456
TNFRSF14	5.691	0
SNCB	5.687	1.04E-13
DUSP1	5.686	0
NAMPT	5.670	0
EEF1A2	5.652	0
SLC3A1	5.620	0.036138469
ZNF518B	5.619	0.014522357
MUC12	5.610	0.00096329
RBM15	5.608	0
LINC00824	5.607	0
BAIAP2	5.599	0
PLK3	5.574	0
MEF2B	5.557	0
JSRP1	5.550	2.00E-15
TNFRSF12A	5.547	0
KCNQ1OT1	5.506	1.28E-10
TNFRSF14-AS1	5.505	0
PTPRH	5.463	0.040397652
CKS2	5.462	0
ARFGAP1	5.460	0
ZMYM5	5.446	0
CYP2D7	5.430	1.11E-16
BMS1P10	5.427	0
WNT5B	5.418	0
MAFA-AS1	5.405	0.036950265
RDH16	5.382	2.29E-06
HIST1H4E	5.376	0.001118066
BCL6	5.368	0
TEX54	5.341	0.018535949
FDPS	5.324	0
HCN3	5.300	0
RHBDF1	5.294	2.22E-16
C22ORF24	5.290	0.006885408
TRIM11	5.282	0
SS18L2	5.265	0
WFIKKN1	5.246	0
RASSF1	5.228	0

CDKN2D	5.228	0
PIM3	5.227	0
ZFP36	5.224	0
ARC	5.208	0
FAM72C	5.189	0
EVPL	5.176	0.008553536
PIM2	5.166	0
LRP5L	5.166	0
SPOCD1	5.166	0.000860432
BLVRB	5.157	0
MAP1LC3A	5.145	0
CEP295NL	5.143	1.55E-05
C4ORF54	5.122	0.007873492
C6ORF223	5.108	6.74E-11
MDK	5.094	0
LINC00957	5.088	7.44E-14
PHF1	5.078	0
GPX3	5.070	0
PNPLA3	5.068	0
ZNF296	5.043	4.16E-06
SYNGR3	5.040	0
SBSN	5.037	0.041586624
RPRM	5.022	0.000446893
PRR36	5.020	0
FERP1	5.017	0.000582669
NPPC	5.002	4.08E-08
RASA4DP	4.999	2.67E-05
RAB26	4.987	0
SNORA73B	4.987	0.004712255
ADORA2A	4.986	0
FADS3	4.986	0
PCDHA5	4.971	0
PLAU	4.967	0
CAMK2N1	4.955	0
STRC	4.942	0.004095873
MYO5B	4.938	0
MIR4435-2HG	4.918	0
UPP1	4.902	0
SH3GL1P2	4.896	0.039055307
SPATA31A6	4.891	0.049792538
CYTOR	4.884	0
SLC17A7	4.882	0
EFNA3	4.869	0
CACTIN-AS1	4.855	2.21E-13
TNFAIP2	4.846	0

KCNG2	4.824	1.79E-06
CCNL1	4.821	0
PPP1R37	4.787	0
TSHZ3	4.783	0.033330568
DNAJA4	4.754	0
STX1A	4.748	0
PTGS1	4.742	0.000131594
ZNF460	4.741	0
CR1	4.738	0.023315168
GNA13	4.735	0
PLA2G16	4.722	0
DLG4	4.718	0
DENND3	4.717	2.90E-05
CORO6	4.709	0
MTMR11	4.705	0
EBLN2	4.697	7.21E-09
MNT	4.696	0
NPIPB6	4.693	0.000262984
DUSP10	4.692	0
PGGHG	4.691	0
ZEB2-AS1	4.669	0.031917041
RPPH1	4.668	8.10E-07
PRG4	4.660	0.001043941
SPON2	4.653	1.37E-07
KREMEN2	4.647	0
CATSPERG	4.645	0.000279804
TDRKH-AS1	4.638	0
NPC2	4.623	0
PPP1R14C	4.622	0
ENTHD1	4.575	9.51E-06
PALM3	4.570	0
ANKRD1	4.566	0.046007916
PDGFRB	4.562	0.000851061
LINC00115	4.560	7.01E-09
GP6	4.559	0.018216693
SLC25A29	4.558	0
ANGPT2	4.555	0.034679191
INPP5J	4.553	0
PI4K2A	4.549	0
RSRC2	4.547	0
BCL2L1	4.540	0
HSPA6	4.537	0.010234969
SPSB1	4.531	1.47E-11
ACBD3	4.529	0
RPS26P15	4.528	0.00391404

ITGA3	4.521	0
URAHP	4.517	1.51E-07
RAB33A	4.513	0
CDKN1C	4.509	0
SQSTM1	4.500	0
U2AF1L4	4.499	0
RN7SL81P	4.490	0.045964979
KDELR3	4.486	0
AVPI1	4.479	0
KLF4	4.477	0
AOC3	4.465	1.77E-11
HSPA5	4.462	0
OPTN	4.447	0
SEC24D	4.426	0
NPIPB3	4.426	0
CYP2T1P	4.417	7.06E-06
N4BP2L1	4.412	0
HERPUD1	4.400	0
WNT9A	4.384	1.11E-16
ANKDD1A	4.384	0
DHCR24	4.383	0
ASS1	4.383	0
LUM	4.380	6.47E-09
CTAGE8	4.377	0.030209538
DDAH2	4.370	0
PCYT2	4.361	0
RBPMS	4.360	0
DLX2	4.358	0
TMEM91	4.355	0.000213076
ACSL6	4.355	1.11E-16
RASA4B	4.354	0
DSPP	4.352	0.004515965
CIITA	4.348	0
NPIPB2	4.332	5.37E-07
KRT8P46	4.319	1.88E-08
YPEL3	4.317	5.03E-10
ITGA10	4.309	0
UBC	4.296	0
DUSP5	4.292	0
SNORA71B	4.290	0.007836515
CD44	4.287	0
IRF7	4.268	0
PEA15	4.259	0
FAT3	4.257	0.019660229
PPP3CC	4.245	0

TPM2	4.242	1.44E-12
GOLGA2	4.242	0
RNF112	4.236	1.52E-14
ECEL1	4.236	1.74E-06
G6PD	4.229	0
NPIPA5	4.223	0.003152845
ICAM5	4.217	0
SNHG12	4.202	0
LGALS3	4.194	0
PHF24	4.189	2.24E-10
CNIH3	4.187	1.11E-16
POFUT2	4.183	0
GAD1	4.183	0
SCML1	4.182	0
SLC25A25	4.179	0
MSANTD3	4.175	0
TTC9B	4.170	4.10E-07
SEMA3F-AS1	4.169	0.000776526
DEPP1	4.165	1.22E-15
INAFM1	4.160	0
PTPRU	4.153	1.10E-14
ACSL1	4.147	0
CYP2E1	4.144	0.002089435
ALDOC	4.143	0
ARMCX1	4.134	0
LPCAT4	4.121	0
GRAMD1B	4.114	0.002569689
SLC7A5P1	4.113	0
PLEKHF1	4.113	0
MAGED4	4.110	0
MYO18B	4.108	0.04406542
PRF1	4.107	0.045854408
PVT1	4.103	0
KLHL21	4.083	0
KLHL24	4.081	0
DNAJC2	4.079	0
PDIA2	4.071	1.93E-07
SRRM5	4.064	2.02E-07
HDAC10	4.054	2.19E-09
PI4KAP1	4.052	8.88E-16
ATP6V1B1	4.050	0
RFPL3S	4.049	6.62E-05
EGF	4.046	1.93E-11
JAKMIP3	4.042	0.001799807
TRIP10	4.040	0

IDUA	4.031	0
RASGEF1B	4.031	4.15E-09
ZNF57	4.025	0
ITPR3	4.020	0
AEBP1	4.004	0
TMEM59L	3.996	0.000748499
CLK3	3.993	0
LRCH4	3.991	0
HIST2H2AA3	3.987	4.61E-05
WBP2	3.968	0
MEF2D	3.968	0
FOSL1	3.965	0
CYSTM1	3.952	0
SLC2A3	3.951	0
PRICKLE2	3.947	2.01E-14
FASN	3.945	0
HSPB1	3.944	0.017433057
ELOVL5	3.940	0
CDKN1B	3.939	0
CGAS	3.936	0
HNRNPL	3.927	0
TAF1D	3.926	0
KLHL15	3.926	0
CCDC116	3.908	0.041474557
CKS1B	3.900	0
RCN3	3.900	0
HSPB1P1	3.899	0.018803089
TEAD3	3.898	0
RPL22L1	3.897	0
RAD9A	3.897	0
CALML4	3.892	0
GFOD1	3.884	0
LGALS9	3.883	8.79E-09
CCNB1IP1	3.873	0
TFAP2E	3.873	0.001931927
AKAP17A	3.869	0
AKAP17A	3.869	0
FOXO3	3.865	0
KLF9	3.857	0
SPATA31C2	3.851	0.031656122
TDRP	3.848	5.21E-07
RNF168	3.846	0
SMIM29	3.844	0
DNM1	3.840	0
TMEM120A	3.839	0

ZRSR2	3.834	0
CDK20	3.832	0
OTULINL	3.820	0
LARP6	3.817	0
STAT5A	3.807	0
TBC1D17	3.803	0
TMEM231	3.802	0
DPF1	3.799	0
CLSTN3	3.798	0
DGCR6	3.797	0
ARHGAP33	3.797	0
SH3BP5	3.796	0
NFKBIB	3.795	0
EIF1P7	3.793	1.16E-06
NPC1	3.785	0
DEDD2	3.784	0
TMEM171	3.784	0.00011455
GRIN2D	3.773	0.014366756
SEMA7A	3.772	0
BCAM	3.770	1.10E-13
ACSL3	3.767	0
AATBC	3.762	0.006575107
MEX3B	3.761	0
LYPD1	3.756	3.55E-08
FTH1P4	3.756	4.17E-11
NKTR	3.755	0
UBTD1	3.754	0
TUFT1	3.744	0
FAM72D	3.737	0
NPAS2	3.736	0
ZNF622	3.735	0
NPIPA3	3.734	5.82E-11
WDR87	3.732	0.01518321
DUSP2	3.731	0.002253825
HIST1H3B	3.727	0.001736463
IFRD1	3.725	0
UHRF2	3.724	0
SRPX	3.723	0
MLXIPL	3.723	8.31E-07
SPIN2A	3.717	1.92E-05
FAM193B	3.716	0
EIF4A2	3.712	0
LTK	3.711	0.017122299
ZBTB43	3.705	0
HIST1H1C	3.702	2.17E-10

LYST	3.693	0
MTRNR2L12	3.689	0
UBALD2	3.684	0
SAT2	3.680	0
FAM189B	3.679	0
DAPK3	3.677	0
GOLGA4	3.677	0
C1S	3.672	3.62E-06
TUBB2BP1	3.669	0
TUBB2B	3.663	0
SHB	3.657	0
GPR85	3.645	0
LATS2	3.638	0
RRAGD	3.638	0
IL6R	3.629	1.11E-16
ARAP1-AS2	3.628	0.000558029
LBX1	3.627	0.010019988
LRRC17	3.623	1.31E-08
RAB3A	3.622	0
TBC1D10A	3.616	0
CCDC168	3.609	0.00394883
HLA-B	3.607	0
MMP14	3.600	0
TNC	3.599	0
SVEP1	3.593	0.012638667
GCNT4	3.590	0.004118397
ATP1A3	3.587	0
PCA3	3.586	0
PHACTR2P1	3.582	0.021045662
JUN	3.572	0
SYNGAP1	3.565	0
BTG3	3.563	0
LENG8	3.552	1.16E-10
SLC4A8	3.551	1.39E-10
HVCN1	3.546	0.01304524
PCDH1	3.542	0
PLEKHA7	3.538	0
PATJ	3.536	0
ZFAND2A	3.535	0
GADD45A	3.534	0
LBHD1	3.534	1.78E-12
ZYX	3.531	0
STARD8	3.530	3.37E-09
PCDHB4	3.530	0.026332811
MAP1LC3B2	3.529	6.79E-10

IGFBP3	3.526	0
RNF169	3.525	0
C6ORF48	3.517	0
JMJD6	3.502	0
EMP3	3.496	0
ZC3H12A	3.495	0
CYP2D6	3.483	0.000649786
PCGF1	3.483	0
MED15	3.479	0
MAPK8IP1P2	3.478	0.04430847
DUSP14	3.471	0
LINC01578	3.471	0
CASQ1	3.468	0.008538327
HRK	3.467	0
CEBPB	3.462	0
RPS26P13	3.457	0.032467459
SMTN	3.457	0
SPTBN4	3.454	2.19E-09
GAS5	3.449	0
RABGGTB	3.445	0
ABHD17AP3	3.443	0.017239877
C1ORF174	3.442	0
GABBR1	3.441	0
DDN	3.439	0
CDK5RAP3	3.439	1.46E-09
NPIPB12	3.438	3.22E-09
ANKRD20A3	3.436	5.55E-16
KLHL17	3.436	0
MID1IP1	3.430	0
CLIC1	3.427	0
SERTAD1	3.426	0
BGN	3.417	0
ISYNA1	3.407	0
CDK2AP2	3.407	0
RASA4	3.407	0
RIN1	3.405	0
ZBTB10	3.398	0
E4F1	3.397	0
HABP4	3.396	0
C1ORF54	3.394	7.15E-07
SPATC1L	3.392	0
NPIPB5	3.392	0
FTH1P20	3.392	0
VASH2	3.389	0
PAMR1	3.389	0

EMD	3.381	0
NR3C2	3.378	3.56E-12
P4HA2	3.359	0
HYPK	3.358	0.000144932
GDI1	3.358	0
NEK2	3.354	0
IFI30	3.354	6.08E-09
UAP1L1	3.354	0
LSS	3.351	0
NEAT1	3.348	0.001227935
TBX2	3.346	0
CACNB1	3.345	0
LIN7B	3.336	0
NTAN1	3.335	0
BNIP1	3.332	0
SMG1P2	3.332	0
MCF2L	3.331	0
GOLT1B	3.331	0
HOXB2	3.329	0.013495855
NPIPB15	3.321	1.11E-16
FTH1P16	3.317	2.21E-13
TMUB1	3.317	0
GAB2	3.312	0
RNASE4	3.309	7.38E-13
PHF21B	3.306	0
SMG1P4	3.304	0
DBF4P1	3.301	2.88E-05
HNRNPLP2	3.300	0
PPIF	3.299	0
UNC5B	3.299	2.67E-11
RAB33B	3.298	0
PDP2	3.297	0
ZNF579	3.297	0
TIPARP	3.289	0
ANKZF1	3.285	0
CLASRP	3.285	0
KMT5C	3.284	0
TCEAL9	3.283	6.66E-16
SPSB3	3.280	0
MT-RNR2	3.280	0
FUT1	3.279	2.08E-13
NPIPB13	3.278	0.000194206
ISG20	3.277	1.61E-07
RUSC1	3.276	0
PRODH	3.275	1.98E-06

SNRPA1	3.274	0
JUNB	3.272	0
MTRNR2L8	3.268	0
PMM1	3.267	0
PITPNM2	3.264	0
TRPM4	3.263	0
DKK3	3.262	2.22E-16
ARMCX4	3.262	0
SHC2	3.258	0
ZNF841	3.255	0
TFE3	3.253	0
EIF1	3.252	0
FLVCR1	3.251	0
NRXN2	3.249	4.67E-13
SRRM3	3.248	1.54E-13
PLPP5	3.245	0
EML2	3.243	0
NEURL1B	3.242	6.94E-10
RSRP1	3.240	0
MEIOC	3.237	0.003557983
ATP6AP1	3.237	0
ANXA2	3.236	0
PIK3CD	3.235	0
BCL2	3.235	0
NPIPA2	3.233	0.042133855
TTC39B	3.223	0
GFPT1	3.217	0
FBXO31	3.216	0
SRF	3.214	0
C1ORF198	3.214	0
MTCO1P40	3.210	1.74E-09
FTH1P12	3.209	0
TIMM10B	3.208	0
CEACAM19	3.207	2.79E-11
PAX6	3.206	0
EMP1	3.201	0
ABI1	3.195	0
OSGEP	3.194	1.31E-10
FSD1L	3.194	0
DYRK3	3.188	0
CPZ	3.186	0
NPM1P26	3.186	0.001296489
ACTG1	3.176	0
KDM7A	3.174	0
AKAP8L	3.171	0

ARHGEF3	3.171	0
GLUL	3.165	0
SNHG16	3.160	0
AURKB	3.151	0
C2ORF69	3.145	0
FHL2	3.144	0
NTN5	3.142	1.51E-06
CIB2	3.142	0
CBX4	3.141	0
SV2A	3.132	0
METRNL	3.132	0
TFEB	3.129	0
SEC13	3.128	0
YPEL2	3.128	0
RELB	3.128	0
OSBP2	3.127	0.002363398
MVP	3.122	0
CRABP2	3.111	0.000691486
LSMEM1	3.111	2.45E-06
EIF4A2P4	3.110	0.045081332
SLC3A2	3.105	0
HMOX1	3.102	0
CARD19	3.099	0
BRICD5	3.097	7.77E-16
MEGF11	3.096	0
TMBIM1	3.095	0
WDSUB1	3.095	0
DDIT4	3.092	0
KLHL11	3.088	0
HAPLN3	3.087	8.01E-13
TUBB2A	3.084	0
ZFPL1	3.082	0
RAB40C	3.081	0
RILPL1	3.081	0
KCND1	3.080	7.99E-06
TFRC	3.078	0
PLA2G4B	3.072	1.09E-08
FABP5P11	3.070	5.33E-15
FNIP1	3.064	0
SNHG15	3.061	1.31E-08
EVA1B	3.058	5.84E-06
DDX39A	3.056	0
ASPSCR1	3.049	0
MPP3	3.045	3.28E-07
NPIPB4	3.043	0

YIPF2	3.030	0
SLC12A4	3.026	0
EBF4	3.025	0
NPIPA1	3.025	0
ITGAX	3.021	6.88E-05
SERTAD3	3.021	0
FTH1P7	3.020	0
MED26	3.019	0
PQBP1	3.019	0
C16ORF45	3.016	0
LPAR2	3.014	0
GJC1	3.013	0
SPATA20	3.010	3.66E-15
MARK4	3.003	0
FTH1P8	2.999	0
PKD1P6	2.992	0
RARRES2	2.990	0.009096898
HBP1	2.990	0
FTH1	2.987	0
DHRS3	2.985	0.008524203
NDEL1	2.984	0
CALU	2.984	0
FTH1P11	2.983	0
RHOU	2.983	0
BAZ2A	2.980	0
HIST1H2BJ	2.980	3.64E-08
HID1	2.976	0.000135966
ARHGAP24	2.975	0
PLXNA3	2.972	2.31E-12
SLC19A2	2.968	0
NOV	2.968	0
C1QTNF5	2.968	0
UBE2SP1	2.965	0
SNHG6	2.960	0
SLC45A3	2.958	0
PDP1	2.958	2.11E-15
MED8	2.957	0
HECA	2.957	0
POU2F1	2.956	0
WIPI1	2.953	0
FTH1P10	2.952	0
HIST1H2BH	2.950	2.34E-05
RND2	2.941	0
KAT5	2.938	0
GNRH1	2.938	0.003004341

MAP1LC3B	2.938	0
C7ORF61	2.935	2.22E-06
COMMD7	2.932	0
FTH1P2	2.930	0
FAM157C	2.925	7.89E-06
CSRNP1	2.923	0
PWWP2B	2.921	0
RGPD1	2.920	5.55E-16
SYF2	2.914	0
KRT10	2.913	0
ZFAS1	2.913	0
ARF1	2.913	0
GLIS2	2.910	0
STX3	2.907	0
NCK1	2.904	0
GTF2IRD1	2.904	0
NXT1	2.903	0
FHIT	2.902	1.24E-07
PNPLA2	2.900	0
ADAMTSL5	2.899	0
PANK3	2.898	0
ITGA2B	2.897	0.000824821
NPTN-IT1	2.895	1.41E-10
KMT2E-AS1	2.892	0.000860015
FBXO32	2.892	0
FXYD5	2.891	0
AQP4	2.889	2.51E-08
YJU2	2.888	0
MT-RNR1	2.883	0
SRRM1	2.881	0
CPEB4	2.881	0
FTH1P23	2.879	0
CDC42EP5	2.878	0
ACTBP2	2.877	0.00342129
MAFG	2.877	0
FNBP4	2.872	0
TSEN34	2.872	0
MEG8	2.872	0.000227817
ADPRM	2.869	0
CCNG1	2.867	0
CNN2	2.866	0
SLC15A2	2.864	1.41E-05
SLC30A1	2.864	0
RHBDL1	2.864	1.16E-05
TRIB3	2.863	0

CLIP2	2.861	0
COPB1	2.860	0
TMEM214	2.857	0
PI4KAP2	2.854	0
ITGA5	2.853	0
TRIM3	2.852	8.12E-13
AGAP6	2.851	3.03E-14
BRI3	2.850	0
TKT	2.847	0
TBC1D3D	2.847	5.81E-12
HNRNPDL	2.847	0
BRSK1	2.846	0
TMEM135	2.845	0
ZNF143	2.840	0
TMCC2	2.838	0
ZNF529	2.837	0
DCAF15	2.836	0
RFNG	2.831	0
ATF4	2.830	0
IRF2BP2	2.829	0
MTND4P12	2.827	4.44E-16
AMT	2.826	5.39E-10
SP1	2.824	0
PGD	2.823	0
FAM72B	2.819	0
CCDC107	2.818	0
PAK1	2.817	5.26E-06
ATF4P3	2.816	0
OSBP	2.814	0
FABP5P7	2.814	0
UBE2S	2.812	0
RAB11FIP5	2.811	0
MAP1B	2.809	0
ZBTB7B	2.805	0
MYO15B	2.803	9.63E-05
FAM131A	2.802	0
ANO10	2.800	0
MUC5B	2.799	0.016734377
C6ORF136	2.791	0
SNHG17	2.791	0
HSF1	2.789	0
CAMK2D	2.788	0
SLC27A1	2.788	0
TBC1D15	2.787	0
CCSER2	2.786	0

CFDP1	2.783	0
HIST1H2AE	2.782	0.007895175
DEXI	2.779	0
TXNDC16	2.778	0
NPIPB11	2.777	0.000259832
CRY2	2.774	0
PHF13	2.774	0
PPM1A	2.770	0
PGP	2.769	0
PQLC1	2.768	0
ATF4P4	2.767	2.22E-13
LONRF1	2.764	7.18E-14
CUTA	2.761	6.64E-09
DUSP3	2.760	0
PHF3	2.758	0
BHLHE40	2.758	0
PDXDC1	2.757	0
TPPP	2.755	0
GDPD3	2.753	1.70E-05
SLCO4A1-AS1	2.752	0
JAG2	2.750	0
CACNG1	2.749	0.003140468
ING2	2.748	0
RINT1	2.748	0
HLA-E	2.747	0
HJURP	2.746	0
UVRAG	2.744	0
CEP85	2.744	0
FAM72A	2.742	0
IRAK2	2.741	0
ROBO3	2.741	2.94E-06
NPTX1	2.738	0
ZBTB5	2.738	0
PMP22	2.738	0
SUPT5H	2.733	0
ELOVL6	2.730	0
TIMM17A	2.729	0
KLF3-AS1	2.727	1.10E-05
OSGIN1	2.725	0
SBDSP1	2.721	0
FABP5	2.720	0
FABP5P1	2.719	0
HLA-DMA	2.719	2.80E-07
PTOV1-AS2	2.718	6.40E-12
AMN	2.715	2.64E-06

H3F3C	2.713	3.85E-05
RBM14-RBM4	2.709	0
ANKRD10	2.707	0
SLC25A1	2.706	0
ANKRD13D	2.705	0
ATXN2L	2.704	0
RLIM	2.697	0
RPSAP47	2.696	0.016441332
SEC31A	2.695	0
DNAJC3	2.695	0
ANO8	2.692	0
PSAP	2.691	0
BTG1	2.690	0
ODF2	2.689	0
UBXN7	2.689	0
RRAS	2.686	0
ITGB4	2.685	0
IFITM2	2.682	0
TUBB3	2.680	0
MPC1	2.680	0
BCAS4	2.678	0
MOCOS	2.676	0.046294278
CARMIL3	2.676	1.37E-09
TESK2	2.676	0
NECTIN2	2.673	0
AGAP12P	2.672	0.005564849
RPL23AP65	2.672	7.83E-08
RNF5P1	2.670	2.88E-11
WDYHV1	2.670	0
GKAP1	2.662	0
NR1D2	2.661	1.01E-12
NPIPP1	2.657	9.77E-15
MSL2	2.657	0
EAF2	2.656	0.0339967
THBS2	2.655	0
POPDC3	2.653	0
CIR1	2.653	0
CNNM2	2.652	0
MFSD14A	2.652	0
CSPG4P10	2.651	0
KSR1	2.646	0
VEGFA	2.645	0
ERP29	2.642	0
PRSS53	2.639	0.000785946
STK17A	2.637	0

LINC00894	2.635	0.000117819
MAST1	2.632	0
FADS2	2.631	0
ANKHD1	2.629	0
CRY1	2.625	0
USP6	2.624	0.000423998
SMG1P5	2.623	0
STX4	2.621	0
RGS10	2.617	0
PLA2G15	2.617	0
SAE1	2.615	0
ST20-MTHFS	2.613	0.000948245
ARG2	2.613	0
CAMKK1	2.612	0
BCL3	2.611	0
FBXO6	2.609	1.64E-06
NRDC	2.609	0
PPP1R15B	2.608	0
ANKRD61	2.608	0.000759705
PDLIM4	2.607	0
ACSL4	2.607	0
PLAC9	2.606	0
TMEM259	2.603	0
SMPDL3A	2.601	1.11E-16
ATF7	2.599	0
SIAH1	2.598	0
RCE1	2.596	0
SNHG1	2.595	4.74E-13
ALAS1	2.595	0
USP32	2.594	0
FAM50A	2.594	0
YWHAZP3	2.593	5.32E-06
SLC29A2	2.590	0
TMEM167B	2.589	0
IFITM3	2.588	0
HOXC10	2.585	0
PROS1	2.583	0
DNHD1	2.581	9.43E-06
NPIPB14P	2.579	8.83E-10
GMPPA	2.579	0
MPV17L2	2.578	0
JMJD7-PLA2G4B	2.578	1.82E-10
PCDHGB1	2.576	0.040083111
HBEGF	2.576	0
ACTB	2.573	0

DBF4	2.573	0
NRBP1	2.571	0
SCART1	2.569	9.18E-10
CREB3L1	2.567	3.87E-09
RPL23AP43	2.565	0.000712329
NFKBIA	2.564	0
LONRF3	2.562	0
RNF19B	2.562	0
TUBG2	2.561	1.11E-11
MIR22HG	2.560	5.61E-10
TBC1D3L	2.558	0.00276982
TMSB4X	2.555	0
ONECUT2	2.555	0
BRD4	2.553	0
NAV2	2.553	0
SREBF1	2.552	0
SERPINA3	2.550	0
GNRHR2	2.548	3.88E-05
TBC1D10C	2.546	0.007566038
ZFP28	2.545	0
WEE1	2.543	0
IRS2	2.541	7.39E-06
C4B	2.541	0.01871953
SMG1P1	2.539	0
SERPINE2	2.539	0
CSTB	2.538	0
PKD1P1	2.537	0
ERF	2.537	0
UBE2C	2.537	0
RPL35P1	2.536	2.06E-05
RIOK3	2.535	0
IQGAP3	2.535	0
RPL14P3	2.535	0.036882085
MAN2C1	2.535	5.26E-11
ALKBH7	2.535	0
XAB2	2.533	0
ATP2A1	2.533	2.51E-08
HDAC6	2.532	0
ADA	2.530	0
HSD17B12	2.530	0
RRAGC	2.529	0
UCP2	2.529	0
MT-ND4	2.528	3.06E-05
LCAT	2.525	1.54E-06
GOLGA6L10	2.525	5.90E-08

MASTL	2.523	0
SIRT7	2.522	1.33E-12
MUC4	2.521	0.000716833
HLF	2.518	0
NPM1P21	2.518	0.002123328
MT2A	2.515	0
ACBD5	2.515	0
MTCO1P12	2.514	0.000164647
SRPRA	2.513	0
FEM1B	2.510	0
THRA	2.509	0
KDELR1	2.509	0
EZH1	2.508	0
RRP7BP	2.505	1.48E-07
TCTE3	2.500	1.33E-05
ZNF408	2.500	0
CRTC2	2.500	0
JAK3	2.499	0.000285529
RCOR3	2.497	0
MAP2K7	2.497	0
RNF5	2.495	0
RNF6	2.494	1.39E-12
ENTPD6	2.489	0
MICALL2	2.486	3.33E-16
UBE2SP2	2.484	0
YEATS2-AS1	2.484	0.011136004
TMSB10	2.484	0
SLC6A10P	2.482	0.001380598
PTPRG-AS1	2.478	0.043389257
LAPTM4A	2.473	0
HINFP	2.472	0
DACT3	2.470	0
MOB2	2.470	0
VCPKMT	2.469	0
NDUFS7	2.468	0
TMEM51	2.468	0
HMGB2	2.468	0
SNHG5	2.467	0
SIX4	2.467	0
ADGRB2	2.467	1.83E-11
MTMR3	2.466	0
CDK3	2.466	1.09E-05
FLII	2.463	0
TMEM39A	2.463	0
UBAP1	2.461	0

UNC119	2.459	3.01E-11
LINC01315	2.459	3.24E-12
CITED1	2.458	0
ATG14	2.458	0
RPS4XP6	2.456	1.05E-07
COL7A1	2.455	7.21E-05
STXBP1	2.455	0
RELT	2.454	0
AGAP3	2.454	0
CCDC28A	2.453	0
IPO8P1	2.449	0.008040936
SERTAD2	2.448	0
FSCN1	2.448	0
TSC22D2	2.448	0
FLG	2.448	0.041572521
TAF10	2.447	4.85E-14
LENG1	2.446	0
PRMT5-AS1	2.445	0.001288124
TTLL3	2.445	2.70E-05
DCUN1D3	2.444	0
THAP9-AS1	2.444	0
UCKL1-AS1	2.441	2.78E-08
CMC2	2.438	0
CTSD	2.438	0
SRRM2	2.436	0
HES7	2.436	0
GTPBP1	2.435	0
NFKB2	2.434	0
BAK1	2.434	0
CSAD	2.433	0.001752376
PLP2	2.432	0
NEDD4L	2.432	0
RIPK2	2.431	0
PPFIA3	2.430	0
ROS1	2.428	0.000708274
LZTS3	2.428	0
PFKFB2	2.428	0
CNTNAP1	2.428	0
NBAS	2.427	0
UAP1	2.427	0
ACTN1	2.425	0
PIR	2.424	0
USF2	2.421	0
ARHGAP45	2.421	0
ARFIP2	2.421	0

RN7SL4P	2.419	0.032360978
RBM25	2.417	0
FCHSD1	2.417	1.89E-07
SNHG7	2.415	0
LAMTOR5	2.415	0
FBXO44	2.414	0
RPS9	2.411	0
BEX4	2.411	0
DNAJC25	2.410	0
TRIM7	2.408	6.95E-09
GPR158	2.405	1.22E-12
ANKRD20A4	2.405	5.09E-13
PTS	2.402	0
BEST1	2.402	0
ZFAND5	2.402	0
MYL6	2.401	0
IGSF8	2.401	0
CCNG2	2.401	0
PSMD8	2.398	0
PPDPF	2.397	0
PELI1	2.396	0
ARL4D	2.395	0.006303947
RC3H1	2.393	0
NOS1AP	2.392	1.24E-07
SYT11	2.392	0
CAMSAP3	2.392	0.003352128
KIFC2	2.392	4.27E-09
DNAH17	2.391	0.01169705
NOVA2	2.391	0
SMG9	2.389	0
UBXN6	2.388	0
ZNF593	2.387	0
MIGA2	2.387	0
PACS1	2.386	0
LAMP2	2.385	0
NKAIN1	2.385	0
WHRN	2.384	1.47E-05
KCNJ14	2.383	4.93E-14
CHP1	2.383	0
YY1AP1	2.383	0
HSP90B1	2.382	0
TOM1	2.382	0
PARP6	2.381	0
PLEKHO2	2.381	0
UBE2E2	2.378	0

COX14	2.378	0
GP1BB	2.377	0.00016097
B3GAT2	2.376	0.000625236
ZNF121	2.375	0
C17ORF49	2.375	0
SF3A2	2.373	0
RENBP	2.373	2.66E-07
H1F0	2.371	0
CAB39L	2.370	0
SH3BGRL3	2.369	0
NPIPA8	2.369	0.000311773
PFKFB3	2.368	0
DNAJC1	2.368	0
B4GALNT4	2.367	0
DUSP4	2.366	1.11E-16
RPS27	2.366	0
NUMBL	2.366	0
RPS27P29	2.366	0.000870685
ING1	2.365	0
NTMT1	2.364	0
FZD5	2.363	0
WDFY1	2.361	0
STX5	2.358	0
TMED9	2.356	0
KCMF1	2.356	0
PRKD2	2.356	0
ATXN2	2.355	0
FOXN3	2.353	0
CEBPD	2.351	0.000740864
GOT1	2.351	0
MPC2	2.351	0
MANBA	2.350	0
RPL37AP1	2.350	1.02E-08
MSANTD3-TMEFF1	2.350	1.09E-14
LAMA1	2.349	0
ELN	2.348	1.74E-07
ILVBL	2.347	0
ECH1	2.347	0
MEX3D	2.346	0
PFDN2	2.346	0
BIN1	2.345	0
HSF4	2.345	2.98E-07
FAM219A	2.344	0
THBS3	2.342	0

ETV4	2.342	0
RPL21P39	2.341	0.019314161
MYNN	2.341	0
SLC22A18	2.340	0
SELENOS	2.338	0
RPS3P6	2.338	1.73E-12
CD46	2.336	0
PPFIA1	2.336	0
TOP3B	2.335	0.001268658
ZNF692	2.334	0
PTP4A3	2.333	0
CBX8	2.333	0
PRPF3	2.332	0
NPDC1	2.331	4.44E-16
WASF2	2.331	0
CIC	2.331	0
PYGB	2.331	0
C2CD2L	2.329	0
CCDC12	2.328	0
MSH5-SAPCD1	2.327	0.00518387
ZNF787	2.327	0
HLA-C	2.326	0
TPM4	2.325	0
SEC24A	2.324	0
ATN1	2.322	0
NOTUM	2.322	0
TIMP2	2.322	0
NDE1	2.321	0
ZNF394	2.321	0
COQ10B	2.320	3.55E-15
SLC39A7	2.320	0
RPS26P3	2.318	0.002266563
FABP7	2.318	0
AGAP7P	2.317	1.10E-06
SSC5D	2.315	0.000294693
PITHD1	2.313	0
TEAD4	2.313	0
TTC7B	2.312	0
ARHGAP19	2.311	0
ZNF25	2.311	0
EPB41L1	2.310	0
MICAL1	2.309	3.33E-16
CNKSR1	2.309	0.033678899
CDK10	2.309	1.05E-07
YPEL5	2.307	0

GUK1	2.305	0
RPS26P28	2.305	0.003448487
MT-CO1	2.303	0.017908894
C6ORF106	2.303	0
ABTB1	2.303	0
BRD2	2.303	0
TCEAL3	2.302	0
STAP2	2.301	7.03E-10
C20ORF96	2.301	4.27E-07
FAM102A	2.300	0
ST3GAL4	2.299	0
MTND4P24	2.298	0.000881256
NME1-NME2	2.298	2.65E-13
TRAF6	2.298	0
EIF1B	2.297	0
GMIP	2.296	0
GABARAPL2	2.296	0
RPS18P12	2.296	0
STXBP2	2.289	7.77E-09
TNPO1P3	2.289	0.049500461
WDR62	2.287	0
PDLIM7	2.285	5.44E-15
SMOX	2.285	0
EPB41L4A-AS1	2.284	0
TSPAN9	2.284	3.33E-16
RPL21P93	2.284	3.05E-10
RPL18	2.282	0
C15ORF61	2.281	0
MAPK8IP3	2.281	0
CD63	2.280	0
GNL2	2.280	0
RPL13AP6	2.279	3.85E-08
JMY	2.279	0
MAPKBP1	2.278	0
SRSF4	2.276	0
TMEM38B	2.275	0
DPP7	2.273	0
GGNBP2	2.272	0
ZBTB2	2.271	0
CETN2	2.271	0
KCTD7	2.271	0
SRSF2	2.269	8.76E-06
MAPK3	2.266	0
NID1	2.265	0
PPARD	2.265	0

TPT1P9	2.265	0
FBXL12	2.264	0
FLNA	2.263	0
RPL12P42	2.263	0
ARFGAP3	2.261	0
POP7	2.261	0
ZDHHC11B	2.260	6.00E-14
RANBP10	2.259	0
LRRC8A	2.259	0
TNFAIP8L1	2.258	0
GPR135	2.255	3.12E-08
KLHL26	2.253	3.46E-10
GSTM2	2.249	0.00431883
TMC8	2.249	5.49E-11
POLR3D	2.249	0
EPHX1	2.248	0
CNN3	2.247	0
NOP53	2.247	0
RNASEK	2.246	0
SCFD1	2.246	0
ECM1	2.246	2.38E-09
SNTA1	2.245	0
USP36	2.245	0
EFNA4	2.245	3.79E-09
DPM3	2.245	0
MICAL2	2.244	2.31E-14
CA5B	2.244	0
PTPN23	2.242	0
PROX1	2.242	0
LAMB1	2.241	0
OSBPL2	2.241	0
DDTL	2.241	1.17E-12
SDCBP	2.240	0
MRPS30	2.237	0
ELL	2.236	0
PTGDS	2.236	0
TMEM159	2.235	0
ZBTB21	2.234	0
INO80D	2.234	0
FXYD3	2.232	3.58E-06
TGFB1I1	2.230	0
SERPINH1	2.229	0
SBNO2	2.228	0
RNF187	2.227	0
CMYA5	2.227	0.019692967

EEF1A1P19	2.227	0
RPS12	2.226	0
ATXN7L2	2.224	7.02E-09
CYCS	2.224	0
MIB2	2.222	1.71E-08
ACVR2B	2.222	5.11E-05
RPL7AP31	2.219	2.05E-07
PNN	2.219	0
TPT1P6	2.219	2.18E-09
PRKAB2	2.217	0
RPL18AP3	2.217	0
RND1	2.217	0.020272459
PPP1R18	2.216	0
YIF1B	2.216	0
RPS26P47	2.214	3.98E-06
MAD2L2	2.213	0
PLEKHH3	2.213	1.30E-13
FN3K	2.213	0
ZNF513	2.212	0
FRY	2.211	0
RPL23P8	2.210	0.000497393
RPL10P3	2.209	3.83E-07
GPX4	2.209	0
PARP2	2.206	0
KLF5	2.206	2.22E-08
KCNQ4	2.206	0
POR	2.205	0
ATP1A1	2.204	0
RRP12	2.204	0
FXYD7	2.204	0.000355033
IER2	2.203	0
GNB2	2.200	0
TIMP1	2.200	0
RIT1	2.199	0
RBM33	2.199	0
ISCU	2.199	0
TRMT112	2.198	0
RPS16	2.197	0
BAG1	2.193	0
FAM157A	2.192	0.008864495
FLCN	2.192	0
NAB2	2.191	0
CSNK1E	2.190	0
RYBP	2.190	0
APBA3	2.190	0

SOCS3	2.190	8.86E-06
CEP70	2.190	0
SCAMP3	2.189	0
RPL31	2.188	0
RPL21	2.188	0
CAMLG	2.187	0
CLU	2.186	0
KDM6A	2.186	3.21E-10
GJA3	2.185	4.92E-12
RHPN1	2.184	0.000176727
PIP4P2	2.184	0
EEF1A1P11	2.183	0
SMNDC1	2.183	0
HK1	2.182	0
ZNF678	2.181	0
RPL21P120	2.181	0
RPL28	2.180	0
B3GNT2	2.179	3.64E-14
CHTF18	2.179	4.71E-12
RPL21P28	2.179	0
DRG1	2.179	0
RMC1	2.179	0
SERINC1	2.178	0
FAM214B	2.177	0
KIF3C	2.176	0
CERS1	2.175	0
RPL12P4	2.174	2.22E-16
AP5Z1	2.171	0
RPL21P11	2.170	2.07E-12
ITPKC	2.169	0
CSGALNACT2	2.169	0
MINK1	2.168	3.60E-05
CSNK1G2	2.168	0
RAB5B	2.168	0
CNKSR3	2.168	0
OTUD3	2.168	0
BANF1P3	2.167	0.006645682
CEBPG	2.165	0
RPS19	2.164	0
RBM22	2.163	0
ASAH1	2.161	0
KXD1	2.160	0
SYNE3	2.158	0
CCDC159	2.157	0.01188999
RPL21P75	2.157	0

TCEA1	2.157	0
TBC1D8	2.156	0
TMED3	2.156	0
RPLP1	2.156	0
TTC9C	2.156	0
SSSCA1	2.155	0
C12ORF49	2.154	0
TPT1P4	2.152	0.005605297
ARL8A	2.151	0
GPNMB	2.150	0
TUBB4A	2.150	0
MYC	2.149	0.000338613
TIMM23B	2.149	0
RPLP0P6	2.149	0
GLA	2.146	0
MRPL55	2.145	0
TLE3	2.144	4.06E-07
RPL13AP25	2.144	0
PGM2L1	2.143	1.78E-15
PCDHGA4	2.143	4.66E-06
SLC25A37	2.143	0
AARS	2.143	0
RPS3	2.143	0
HUS1	2.142	0
PGM3	2.142	0
RHEB	2.142	0
RAB4B	2.141	0
IRF9	2.141	9.49E-10
USP3	2.141	0
RPL23AP82	2.141	0
RPL24P8	2.140	2.90E-11
RNF126	2.139	0
LRRC75B	2.139	0
B2M	2.138	0
CBFA2T2	2.138	0
SLC9A3R1	2.137	0
CCND2	2.137	0
NFATC4	2.137	7.99E-15
GABARAP	2.136	0
BRAF	2.135	0
LRRC75A-AS1	2.135	0
VCPIP1	2.135	0
FAM47E-STBD1	2.135	0.001021198
RPL36A-HNRNPH2	2.134	0.001066765

SH3GL1	2.133	0
GNB5	2.132	0
MBOAT7	2.132	0
GIPR	2.130	0.01016119
NT5DC3	2.130	0
RPL36	2.130	0
S100A6	2.130	0
RPS15AP38	2.127	0.000582203
KDELR2	2.126	0
BRPF1	2.125	0
GPR137C	2.124	0.000383399
VIM	2.124	0
CDADC1	2.124	0
RPSAP54	2.123	1.90E-12
TOMM7	2.122	0
RPL21P134	2.121	1.63E-11
HSF2	2.121	0
USE1	2.120	0
NET1	2.119	0
COPS2	2.119	0
CDCA3	2.118	0
RPL14P1	2.117	0
CDC25B	2.117	0
NACA3P	2.117	1.08E-10
PRSS23	2.115	0
RPL7P32	2.115	0.006279543
ZFYVE1	2.114	0
SLC35A2	2.114	0
NELFA	2.114	0
KMT2B	2.112	0
DYNLL2	2.111	0
CXADR	2.110	0
SELENOK	2.110	0
CNTROB	2.110	7.20E-10
DPH7	2.110	0
THAP1	2.109	0
PAXX	2.109	0
PABPC1L	2.109	0.001388574
WHAMM	2.109	0
DYNC1LI1	2.108	0
RPS5	2.107	0
TFAP4	2.107	0
DSTN	2.107	0
ANKS3	2.105	0
R3HDM4	2.105	0

SIAH2	2.102	0
SND1	2.102	0
ANKRD9	2.102	0
FOXK2	2.101	0
ARNT	2.101	0
HPCAL1	2.101	0
DCAF11	2.100	0
FKBP10	2.100	3.65E-06
NCKIPSD	2.100	0
LMNTD2	2.099	0.023165015
FAM160B2	2.099	1.79E-13
PTTG1	2.099	0
DOCK6	2.099	1.44E-15
EEF1D	2.099	0
GAN	2.099	1.92E-07
STT3A	2.098	0
ISL2	2.098	0
OGA	2.097	0
FAM117A	2.097	0
DDX47	2.097	0
CADPS2	2.097	0.045455183
RPL13AP20	2.097	0
TXN	2.095	0
ULBP2	2.095	0.000905284
PAXBP1	2.095	0
CDK11A	2.095	3.07E-10
CCNI	2.094	0
KIF2C	2.093	0
C9ORF72	2.092	0
SEMA3B	2.091	3.75E-11
CDH24	2.089	0
C1ORF35	2.089	2.42E-07
RPS11	2.088	0
CDC34	2.088	0
IRX5	2.087	0
TESK1	2.087	4.00E-12
RBM6	2.086	1.41E-07
RAP2B	2.086	0
TNKS	2.085	0
FBXW5	2.085	0
RPL27A	2.084	0
RPL13AP7	2.084	2.28E-12
TPT1	2.083	0
BTAF1	2.083	0
ZNF433-AS1	2.083	0

SEC23A	2.083	0
GPCPD1	2.081	0
HMGA1P3	2.081	0.04633685
MTCO2P12	2.081	0.00028737
CHORDC1	2.080	1.15E-14
GOLGA5	2.079	0
RPS17	2.078	0
RPSAP19	2.077	0
CHIC1	2.077	0
GPR173	2.077	0
GIMAP2	2.075	0.000269474
LINC01001	2.074	0.003004113
RPS25	2.073	0
PILRB	2.073	0.025408012
COG5	2.073	0
PITPNM1	2.073	0
RPL21P16	2.072	0
TULP3	2.072	0
SPARC	2.072	3.25E-12
RPS15	2.071	0
MERTK	2.070	0
CCDC112	2.069	0
RPL37A	2.069	0
ARHGAP5	2.069	9.30E-06
RAB30	2.069	0
KCNE4	2.068	2.77E-07
TICRR	2.068	0
CPT1B	2.068	0.025189356
SH3PXD2A	2.068	0
TMEFF1	2.067	6.85E-12
EEF1A1P7	2.067	9.30E-11
TMEM147	2.066	0
SHISA4	2.065	0
PPL	2.065	0.003368119
RPL13AP5	2.065	0
ZBTB8A	2.065	3.03E-12
RPL12P12	2.063	7.52E-06
EEF1A1P6	2.063	0
PRPF38B	2.063	0
RELA	2.063	0
RPL36AP26	2.062	0.003052278
RPL36A	2.062	0
PNCK	2.061	0.000601467
IZUMO4	2.060	0.008774735
TAF13	2.059	0

IFITM1	2.059	4.77E-05
SF3B1	2.059	0
ZPR1	2.059	0
ARID3B	2.058	7.46E-09
EEF1DP1	2.057	0.042174421
RPL18A	2.056	0
ORAI1	2.055	0
GATAD2B	2.055	0
TPT1-AS1	2.055	0
EEF1A1P9	2.054	0
SLC25A27	2.054	8.93E-05
DDR2	2.054	0
ARNTL	2.052	2.18E-08
VDAC2	2.052	0
RHEBP1	2.050	9.18E-06
UFD1	2.050	5.56E-12
TAGLN2	2.050	0
WASH6P	2.049	2.74E-12
WASH6P	2.049	2.74E-12
TRIM67	2.048	6.90E-13
RPL41P2	2.047	0
TTK	2.047	0
RAB7A	2.047	0
PLXND1	2.047	0
SARS	2.046	0
PLEKHM2	2.045	0
MAPK6	2.045	1.93E-10
COLGALT1	2.044	0
WSB1	2.044	0
TCF20	2.044	0
RACGAP1	2.043	0
RPL10P16	2.043	0
HCN2	2.043	0
VGLL3	2.043	0.014356366
RPL35P2	2.042	3.44E-12
TIAL1	2.042	0
TMEM126A	2.041	0
ZNF133	2.041	0
AKAP2	2.040	4.00E-11
SMS	2.040	0
LMBR1L	2.040	0
LHFPL3	2.040	0
RPS26	2.040	0
SLC9A3R2	2.040	0
SLC25A36	2.040	0

RNF7	2.040	0
CHKA	2.040	0
RPSAP18	2.039	0.0012248
RPL12	2.038	0
DLGAP4	2.037	0
RIMKLB	2.036	0
RPL10	2.036	0
KIAA1671	2.036	5.34E-08
SF3B2	2.035	0
PLS3	2.034	0
SF3A1	2.032	0
EEF1A1P5	2.032	0
RAB5A	2.032	0
CD151	2.031	0
RPS23P8	2.031	0
EEF1B2P3	2.031	0
RPLP0	2.029	0
IFNGR1	2.029	0
HDLBP	2.029	0
ARF4	2.029	0
GAS6	2.028	0.012634524
L1CAM	2.027	0
NECAP1	2.026	1.82E-14
RPS13	2.026	0
RUNDC3A	2.025	0
LITAF	2.025	0
RPS18	2.025	0
MAP3K3	2.025	0
MTSS1L	2.025	0
COX10	2.023	1.12E-13
AIFM1	2.023	0
SOD2	2.023	0
MRC2	2.023	0
EME2	2.022	1.10E-05
ZW10	2.022	0
TUBBP1	2.021	8.84E-13
SPTY2D1	2.020	5.37E-12
TMEM11	2.020	0
KIT	2.019	0
LMAN1	2.018	0
ISY1	2.018	0
TBC1D25	2.018	0
RPL13A	2.017	0
RPL12P17	2.015	1.32E-08
RPS13P2	2.015	9.10E-11

YWHAZ	2.014	0
RPL38	2.014	0
PPIL4	2.013	0
GSTO1	2.012	0
PFDN5	2.012	0
UIMC1	2.012	0
EEF1A1P13	2.011	0
FBN1	2.011	0
QPCTL	2.009	0
MAP3K10	2.008	0
FOXD1-AS1	2.007	3.97E-08
EEF1A1P4	2.007	0
ZNF571	2.007	1.28E-14
GOLGA6L9	2.007	2.22E-16
FZR1	2.006	0
CEP57	2.006	0
SYPL1	2.005	0
RPL29P11	2.005	2.35E-11
EEF1A1	2.005	0
RPL10P9	2.003	0
TMEM189-UBE2V1	2.003	0.010611235
ISG15	2.003	4.01E-12
MRPL52	2.003	0
GNAI3	2.002	0
RPN1	2.002	0
RPL26	2.002	0
PTP4A1	2.002	0
LRRN4CL	2.001	0
FAF1	2.000	0
ITPA	0.500	0
ARL10	0.500	0
BPTF	0.500	0
CX3CL1	0.499	0
ZNF275	0.499	0
ZNF146	0.499	0
DCHS1	0.499	2.80E-07
ILDR2	0.499	0
INTS9	0.499	0
B3GAT1	0.499	0
DEPDC1	0.498	1.33E-11
PCDHB8	0.498	0.001853187
ZNF765	0.498	0
UPRT	0.498	1.11E-16
ASB7	0.498	1.11E-11

DCUN1D2	0.498	0
FGF12	0.498	0
KCTD17	0.497	2.58E-14
TNS3	0.497	0
TTF1	0.497	0
PDGFC	0.497	0
VSIG10	0.496	0
ZMPSTE24	0.496	0
TMSB15B	0.496	3.70E-05
KIAA1147	0.496	0
APAF1	0.496	0
ZNF48	0.496	0
ZNF862	0.496	0
DPY19L3	0.496	0
NBPF12	0.495	0
SSH1	0.495	0
FAHD1	0.495	0
C19ORF12	0.495	0
OGFOD2	0.495	0
EEF2KMT	0.495	0
TMEM181	0.495	0
ZNF470	0.495	6.14E-13
ZNF577	0.495	1.04E-11
TBRG1	0.495	0
SH3RF1	0.495	0
LIFR	0.494	0
ZMYND11	0.494	0
TRMT13	0.494	1.11E-16
MDGA2	0.494	6.85E-06
LIMCH1	0.494	0
AGPAT5	0.494	0
CNOT11	0.494	0
DSCC1	0.494	3.49E-08
PMPCA	0.494	0
MRPL50	0.493	0
SKA3	0.493	0
FYCO1	0.493	0
IL17RB	0.493	0.01437785
ZNF300	0.493	0
MTM1	0.493	7.77E-16
ZNF761	0.493	0
PEX6	0.493	0
NOP9	0.493	0
ARNTL2	0.492	4.58E-09
WRN	0.492	0

ADM5	0.491	0.000190251
TRIM21	0.491	0.002940368
TGS1	0.491	1.75E-13
GALNT1	0.491	0
GPR19	0.491	2.26E-08
CHM	0.490	1.90E-10
PPIL2	0.490	0
MRS2	0.490	0
CBY1	0.490	0
BRD7	0.489	0
PIGP	0.489	6.00E-15
TNRC18	0.489	0
FAM84A	0.489	0
ZNF43	0.489	0
FARP2	0.489	0
FAM57A	0.489	0
SMIM19	0.488	0
TEDC1	0.488	0
PIGN	0.488	0
TRMO	0.488	3.80E-13
PXMP4	0.488	0
USP27X	0.488	2.59E-08
SLC19A1	0.488	0
C14ORF119	0.488	4.44E-16
CARS2	0.487	0
C6ORF62	0.487	2.22E-16
MAK16	0.487	0
DIS3L	0.487	0
COBL	0.487	0
ZNF141	0.487	3.00E-07
CMTR2	0.487	0
EEF2K	0.486	0
RABIF	0.486	0
ADSL	0.486	0
TRIO	0.486	0
EDIL3	0.486	0
C3ORF62	0.486	4.60E-05
DCBLD2	0.486	0
NEDD9	0.486	3.44E-15
ARAP2	0.486	0
AIMP2	0.485	0
IGSF3	0.485	0
ARNT2	0.485	0
NXT2	0.485	0
CLHC1	0.485	6.75E-08

RAD17	0.485	0
MIDN	0.485	0
TM7SF3	0.485	0
ZIC1	0.484	1.28E-10
GLYCTK	0.484	4.56E-08
FAM220A	0.483	0
PHF6	0.483	0
HPS5	0.483	0
ZNF155	0.483	3.03E-14
ATG4C	0.483	0
SMAP2	0.483	0
LARP4	0.483	0
DHTKD1	0.482	0
ADPRHL2	0.482	0
SLC35B2	0.482	0
ZNF281	0.482	0
NFYC-AS1	0.482	0.003053723
METTL4	0.482	0
ZNF740	0.481	0
PEX7	0.481	2.92E-06
SLC35E2A	0.481	4.11E-14
ELMOD3	0.481	0
RMDN1	0.481	0
ZNF32	0.481	0
PPP6R2	0.481	0
ZDHHC21	0.481	0
TANK	0.481	0
FAR2	0.480	6.54E-11
ANKS6	0.480	0
ZADH2	0.480	0
AR	0.480	0
SLC38A1	0.480	0
MDP1	0.480	1.43E-07
PJVK	0.480	0.017836286
TSNAX	0.479	0
TATDN3	0.479	0
PPHLN1	0.479	0
SLC36A1	0.479	0
MISP3	0.479	1.32E-10
APBB2	0.479	0
UBE3C	0.479	0
RGMA	0.479	0
MAGI1	0.479	0
PDIK1L	0.479	1.89E-12
BCHE	0.479	0

MAP3K11	0.479	0
ESPL1	0.479	0
PSAT1	0.478	0
ITPR2	0.478	0
MTMR9LP	0.478	2.19E-12
LEF1	0.478	0
FAM171A1	0.478	0
HOXC6	0.478	6.50E-07
MOB1A	0.478	0
POLA2	0.477	0
USP18	0.477	0.000536615
B4GAT1	0.477	0
BAG2	0.477	0
OGFOD3	0.477	0
LINC00888	0.477	5.86E-05
LUC7L3	0.477	0
SLC25A53	0.477	0.027130186
GNPTAB	0.476	0
CCDC88A	0.476	0
KIAA1217	0.476	0
CMTM5	0.476	0
ATP13A2	0.476	0
EIF3EP1	0.475	0.011787069
ZCCHC14	0.475	0
NEMF	0.475	0
LLGL1	0.475	0
LRRN1	0.475	0
PARG	0.475	0
RNPC3	0.475	7.12E-09
ERCC6L2	0.475	0
GDF11	0.475	0
TAF2	0.474	0
FANCC	0.474	0
DDI2	0.474	9.99E-16
SMCR8	0.474	0
PUS7	0.474	0
SSC4D	0.473	0.016548762
DUS4L	0.473	0
ST3GAL6	0.473	0
MCCC1	0.473	0
STXBP5	0.473	0
ALKBH4	0.473	0
DNAAF2	0.473	0
DNAJB12	0.473	0
ACBD4	0.473	6.01E-08

SPRTN	0.473	0
KREMEN1	0.472	0
SDHAF2	0.472	1.11E-16
SYNJ2BP-COX16	0.472	0.013876558
PHF20L1	0.472	0
VPS50	0.472	2.40E-14
THSD1	0.472	5.34E-14
LRRC14	0.472	0
OSER1-DT	0.472	4.66E-08
ADO	0.472	0
CYB5R4	0.472	0
NPAT	0.471	0
SLF2	0.471	0
GTF3C2	0.471	0
C3ORF52	0.470	4.17E-09
DNASE1	0.470	0
DNAJC5	0.470	0
RPS6KB1	0.470	0
STK38L	0.470	0
ZNF485	0.470	2.41E-07
ZEB1-AS1	0.470	0.000416709
THAP11	0.469	0
ITPRIPL2	0.469	0
METTL8	0.469	0
FAM118B	0.469	0
FAM32A	0.469	0
RAB7B	0.469	0.022986981
ARID2	0.469	4.00E-15
TNFAIP8	0.469	0
LCTL	0.468	0.006315443
TBC1D16	0.468	0
ZNF638	0.468	0
ANKRD26	0.467	0
PPP3CB-AS1	0.467	0.045057433
KHK	0.467	0
CDKN2B-AS1	0.467	0.024961624
PCDH7	0.467	0
TGFA	0.467	9.84E-09
ST8SIA1	0.467	0
INIP	0.467	0
EMILIN1	0.467	0.004179109
CHD9	0.467	0
MYCBP	0.467	6.77E-15
ZNF564	0.467	9.57E-07
SLC30A9	0.467	0

EVI5	0.466	0
TGIF2	0.466	0
CASC11	0.466	0.005883679
MEPCE	0.466	0
NEURL2	0.466	1.48E-07
CEP72	0.465	0
NME6	0.465	0
RUVBL1	0.465	0
PCTP	0.465	4.59E-11
CHST10	0.465	0
MXD4	0.465	0
ZDHHC16	0.465	0
DLG1	0.465	0
ZFP14	0.465	3.89E-10
PLCL2	0.465	0.003404375
NSUN2	0.464	0
NUP35	0.464	0
DERA	0.464	0
ARFRP1	0.464	0
CNP	0.464	0
GCDH	0.464	0
CUL1	0.464	0
ZFYVE27	0.464	0
COL12A1	0.463	0
RNASEH1	0.463	0
CCDC126	0.463	8.71E-13
SETBP1	0.463	3.38E-07
CCDC102A	0.463	0
DOPEY1	0.463	0
RAD51	0.463	0
PROCA1	0.462	0.000118239
MAB21L2	0.462	0
RPP25L	0.462	0
NSD1	0.462	0
PRRT3-AS1	0.462	0.005988329
MMP15	0.462	0
RNF165	0.462	0
ANKRA2	0.462	1.01E-12
SHROOM1	0.462	1.34E-09
HIST2H4A	0.462	1.64E-05
RTKN2	0.462	1.32E-05
TKFC	0.461	0
COG8	0.461	0
HNF4G	0.461	0.007248736
FUS	0.461	0

MTCH2	0.460	0
HERC3	0.460	6.41E-12
HIP1R	0.460	0
STK38	0.460	0
GTF3C6	0.460	0
MYORG	0.460	2.88E-10
IL11RA	0.459	7.56E-06
LCLAT1	0.459	0
CBX5	0.459	0
NAGLU	0.459	0
JPH1	0.459	1.55E-13
METTL15	0.459	0
PGK1	0.459	0
COL9A3	0.458	0
TCAF1P1	0.458	0
CLCN4	0.458	0
RNFT1	0.458	0
PRTFDC1	0.458	0
LANCL1	0.457	0
TTC25	0.457	0.0006927
NIF3L1	0.457	2.22E-16
DENND6A	0.457	0
SHMT1	0.457	0
PANK1	0.457	1.08E-10
MAML2	0.457	0
MAEA	0.456	0
LACC1	0.456	2.69E-07
ZBED4	0.456	0
UBE2D4	0.456	0
UBE2J2	0.456	0
POC1B-GALNT4	0.455	1.75E-08
SNHG10	0.455	2.60E-11
MINDY3	0.455	0
FAM227B	0.455	5.15E-06
TMX3	0.455	0
CDKN2B	0.455	0
CENPB	0.455	0
SAP30L	0.454	0
CAP2	0.454	0
GTF2H5	0.454	0
IPO8	0.454	0
MOSMO	0.454	0
IGSF11	0.454	0
C14ORF93	0.454	0
ZNF362	0.453	0

PIK3R1	0.453	0
SLC9A8	0.453	0
HLTF	0.453	0
PCK2	0.453	0
GUF1	0.453	0
TIMMDC1	0.452	0
ABLIM1	0.452	0
AASDH	0.452	0
CASK	0.452	0
PMS2	0.452	0
GALNT18	0.452	0
CEP78	0.452	0
DNAJC22	0.452	1.23E-07
CTNNBIP1	0.452	0
TTI1	0.452	0
SLC35F5	0.452	0
DLC1	0.451	0
ETV1	0.451	0
UBLCP1	0.451	0
LLPH	0.451	0
ZSCAN26	0.451	0
NBPF1	0.451	0
MCCC2	0.451	0
PPM1F	0.451	0
MFSD1	0.450	0
RDH10	0.450	3.28E-13
ANKRD49	0.450	1.11E-16
SZT2	0.450	0
NCAN	0.450	0
MBTPS1	0.450	0
TMEM184C	0.449	0
ST6GAL1	0.449	0
NCBP1	0.449	0
ENDOD1	0.449	0
FBXO36	0.448	1.74E-05
SLC22A23	0.448	0
TMCO6	0.448	0
VPS4B	0.448	0
TRIM32	0.448	0
ZNF3	0.447	0
PPFIBP1	0.447	0
SNAPIN	0.447	0
AGPAT3	0.447	0
ZNF528	0.447	3.12E-11
PBX1	0.447	2.33E-09

STRADB	0.447	0
GLDCP1	0.446	0.002659547
ADAM19	0.446	0
ERGIC2	0.446	0
PPM1M	0.446	1.39E-06
C2ORF42	0.446	0
NDUFC2	0.446	0
CEP192	0.445	0
FAR2P2	0.445	2.55E-15
SPATA33	0.445	0.009263619
RCOR2	0.445	0
ISLR	0.445	0.025046908
ZNF507	0.445	0
NKD1	0.445	0
TFDP2	0.445	0
TOX	0.445	0
UGT8	0.444	0
BRMS1L	0.444	0
UBXN2B	0.444	0
UNG	0.444	0
FAM222B	0.444	0
ZNF717	0.443	6.82E-07
TLNRD1	0.443	0
VPS9D1-AS1	0.443	6.22E-15
LINC00174	0.443	5.09E-11
ZNF202	0.443	0
GFM2	0.442	0
PARP3	0.442	0
LINC00920	0.442	0.002177466
TPCN2	0.442	0
MYCN	0.441	1.58E-05
ANKRD11	0.441	0
NAA35	0.441	0
PAOX	0.441	0.001709508
PGGT1B	0.441	0
FLAD1	0.441	0
SLC7A8	0.440	0
RRP7A	0.440	0
NAE1	0.440	0
AKTIP	0.440	0
CREB3L4	0.440	9.66E-11
TFAM	0.439	0
CIP2A	0.439	0
AGO1	0.439	0
SIMC1	0.439	0

MT3	0.439	4.24E-12
C1GALT1C1	0.439	0
SEMA4D	0.438	2.72E-13
CCNF	0.438	0
SLC25A14	0.438	2.90E-05
SPRED1	0.438	0
TMEM260	0.438	0
ERBB2	0.438	0
BMPR1A	0.438	0
EPOP	0.438	0
GOPC	0.438	0
SLC25A20	0.437	0
TTLL6	0.437	0
KIF13A	0.437	0
PTK2B	0.437	1.63E-05
DNAH9	0.437	0
RFWD3	0.437	0
NFE2L3	0.437	0
CNPY2	0.437	0
C11ORF54	0.437	0
FRMD8	0.436	0
ZIC2	0.436	1.77E-14
ZNF736	0.436	0
GSKIP	0.436	0
ZNF883	0.436	0
HOXD3	0.436	3.40E-13
TRAF3	0.436	0
MDM2	0.436	0
WNT3	0.435	3.13E-05
DCLRE1C	0.435	1.11E-16
ERFE	0.435	0.00017335
SHROOM4	0.435	0
HELQ	0.435	0
PITPNA	0.435	0
CYB561A3	0.435	0
PCDHGB3	0.435	0.001313793
CDKN2AIPNL	0.435	0
TBCK	0.434	5.36E-13
EXOSC4	0.434	0
FBXL19-AS1	0.434	1.88E-09
WDR17	0.434	0
ITGB8	0.434	0
GYG2	0.434	0.002927342
ZNF713	0.434	1.11E-16
ZDHHC1	0.434	0.018651188

THAP7	0.434	0
CENPE	0.434	0
MDFI	0.433	0
FUT8	0.433	0
TMEM209	0.433	0
ALG11	0.433	0
B3GNT5	0.433	1.03E-12
MRM3	0.433	0
LIMD1	0.433	0
MYCL	0.433	0
WDR34	0.432	0
PCNX4	0.432	0
NABP1	0.432	7.63E-12
ATP10D	0.432	0
AMER1	0.432	0
TMPRSS5	0.432	3.33E-10
FOXD3-AS1	0.432	2.11E-08
ASF1A	0.432	0
SCG3	0.432	0.001713374
FAM49A	0.432	0
SCRG1	0.432	0
EFCAB7	0.432	1.66E-06
KATNAL2	0.432	4.44E-16
MFSD4B	0.431	0
DHX32	0.431	0
KLHL23	0.431	0
TMEM223	0.431	0
LMTK2	0.431	0
LGMN	0.431	0
ZNF649	0.431	0
FAM162A	0.430	0
AASDHPPT	0.430	0
GPR180	0.430	0
KRR1	0.430	0
NECTIN1	0.430	0
ZNF117	0.430	7.50E-13
UNC13D	0.430	0.005526805
PXMP2	0.429	0
GATB	0.429	0
DDX52	0.429	0
ORAOV1	0.429	0
ZMYM1	0.428	0
CRIM1	0.428	0
AP3M2	0.428	0
CD3EAP	0.428	6.66E-16

MANEAL	0.428	0
RCN2	0.428	0
RFESD	0.428	0.038212398
IREB2	0.428	0
SCRN3	0.427	0
LDAH	0.427	0
ACACB	0.427	0
ARSE	0.427	3.57E-05
CAMKK2	0.427	0
KIAA0232	0.427	6.66E-16
PRUNE1	0.427	0
FBXO9	0.427	0
ABCD2	0.426	0
NDUFA4L2	0.426	0.003206701
ZNF814	0.426	0
STAG3L3	0.426	0
RPGR	0.426	2.46E-14
ATP11C	0.426	0
TOR1B	0.426	0
FAM184B	0.426	4.54E-07
ZNF783	0.426	0
SMG1P7	0.425	1.98E-09
ZNF614	0.425	0
SESN3	0.425	0
RBM24	0.425	0
PAQR4	0.425	0
PYM1	0.425	0
ZNF597	0.424	1.41E-11
TMEM14A	0.424	7.66E-15
MYD88	0.424	0
POP4	0.424	0
EVC	0.424	0
GTF2IP12	0.423	0.000199869
HGH1	0.423	0
GNB4	0.423	0
C1ORF226	0.423	2.48E-05
NCEH1	0.422	0
USP53	0.422	5.70E-11
METTL23	0.422	0
UBR1	0.422	0
LRTOMT	0.422	1.44E-07
IQCE	0.422	0
MINPP1	0.422	4.00E-15
LINC01184	0.422	0
DDIT4L	0.422	0.003848836

TSPYL1	0.421	0
NUDT19	0.421	0
RGS19	0.421	0
CAV1	0.421	1.80E-08
ATP6V0E2	0.420	0
MOCS2	0.420	0
TMEM38A	0.420	0
WWTR1	0.420	0
POFUT1	0.420	0
EPN2	0.420	0
ZNF667	0.420	0
ZKSCAN4	0.419	3.40E-11
KIF14	0.419	0
TMOD2	0.419	0
OGFRL1	0.419	0
APPBP2	0.419	0
ODF2L	0.419	0.00239612
GFAP	0.419	0
ZNF626	0.418	3.75E-05
C9ORF3	0.418	0
EFR3B	0.418	2.08E-10
ALG10	0.418	0
ZNF204P	0.418	0.008690516
SLF1	0.418	0
RAD51AP1	0.418	0
GRIK2	0.418	0
CASP8AP2	0.418	0
SH3BP5L	0.417	0
E2F2	0.417	0
KIN	0.417	0
TRAM2	0.417	0
NAPEPLD	0.417	0
ZNF559	0.417	0
TLDC1	0.416	0
ST7L	0.416	7.77E-16
FECH	0.416	0
BRCA2	0.416	0
EED	0.416	0
ANTXR2	0.416	0
CDC45	0.416	0
SLC38A2	0.416	0
MEGF8	0.415	0
CLOCK	0.415	0
FKBP7	0.415	0
SGK3	0.415	0

ARMH4	0.415	7.89E-14
GEMIN6	0.415	0
DDIAS	0.414	0
SORBS1	0.414	0.001774047
CYB561D2	0.414	0
EOGT	0.414	1.11E-16
USF3	0.414	0
COA5	0.414	0
RNF141	0.414	0
CADM1	0.414	0
UBXN2A	0.414	0
GSAP	0.413	0
EXTL2	0.413	0
MRPS14	0.413	0
SLC30A4	0.413	3.56E-14
ANKHD1-EIF4EBP3	0.413	0
ZNF845	0.413	0
MIA-RAB4B	0.413	0.016999217
NACC2	0.413	0
SLFN5	0.412	1.08E-08
PPIP5K2	0.412	0
RANBP6	0.412	0
TAF9B	0.411	0
BORCS8	0.411	0
ZNF250	0.411	0
MCM4	0.411	0
DZIP3	0.411	0
API5	0.411	0
PRMT9	0.411	4.25E-14
PDK3	0.411	0
GINS2	0.410	0
N4BP2	0.410	0
PUS10	0.410	0
TMOD1	0.410	0
ARHGAP20	0.410	0
MANEA	0.410	0
TRIM14	0.410	0
NPB	0.410	0.003373144
KCND2	0.410	0
C5ORF15	0.410	0
GNAZ	0.410	1.55E-15
FAM185A	0.410	1.22E-13
GPALPP1	0.410	0
PHLDB1	0.409	0

OAZ2	0.409	0
DEPDC1B	0.409	0
INTS14	0.409	0
WASHC3	0.409	0
ARHGEF25	0.409	0
MAML3	0.408	0
UBTF	0.408	0
EGLN1	0.408	0
TCTN1	0.408	0
GALNT10	0.408	0
C5ORF24	0.408	0
NCBP2-AS2	0.407	0
RNASEH1-AS1	0.407	0
XXYLT1	0.407	0
TMEM267	0.407	3.90E-13
NUP50-DT	0.406	0
HMBS	0.406	0
FGD5-AS1	0.406	0
PIK3C2B	0.406	0
CENPK	0.406	0
ZNF618	0.406	0
ACOT11	0.405	0.003678687
CHCHD7	0.405	0
BLOC1S4	0.405	0
KCNIP2	0.405	0
APC	0.405	0
RCC2	0.405	0
CLUHP3	0.405	1.45E-07
TNFSF13	0.405	2.36E-06
IMP3	0.405	0
TOR2A	0.404	1.05E-11
RECQL5	0.404	0
TDRD7	0.404	0
TPM3P9	0.404	0
PANX1	0.404	0
C4ORF3	0.404	0
CYBC1	0.404	0
ZNF471	0.404	0.000405453
IRS1	0.404	0
MCM3AP-AS1	0.404	1.01E-13
TCF4	0.404	0
MCAT	0.404	0
PRKACB	0.404	0
RAMP1	0.403	0.023011134
NT5DC2	0.403	0

NIM1K	0.403	0
SLC25A16	0.403	0
VXN	0.403	0
ATRIP	0.403	0
MCM3	0.403	0
TTLL1	0.402	5.12E-06
TBP	0.402	0
C11ORF96	0.402	0.003005939
SLC2A13	0.402	0
MTR	0.402	0
SAPCD2	0.402	0
STAG3L2	0.402	2.53E-06
FASTKD3	0.401	0
FRAS1	0.401	0
EIF5	0.401	0
NAA40	0.401	0
RTKN	0.401	0
NLGN1	0.401	3.61E-13
COG2	0.401	0
GANC	0.401	0
IGFBP2	0.401	0
UTP14C	0.401	0
SNHG21	0.401	4.20E-06
EXOC7	0.401	0
RSPH3	0.400	2.43E-11
MCM6	0.400	0
RBM12B	0.400	0
PTCH1	0.400	0
MAN1B1-DT	0.399	0.003119448
HARBI1	0.399	0.000244834
SPAG16	0.399	0
WBP1L	0.399	0
ZBTB1	0.399	0
FUCA1	0.399	3.84E-12
CDPF1	0.399	0
TM2D2	0.399	0
SOS2	0.399	0
IPO9	0.398	0
ASB1	0.398	0
SUFU	0.398	0
FYN	0.398	0
NRARP	0.398	0
ZNF70	0.398	0
PELI3	0.398	8.55E-15
S1PR2	0.398	0

TRMT2B	0.397	0
WDR73	0.397	0
CCDC51	0.397	0
TAF11	0.397	0
EFR3A	0.397	0
CDC14A	0.397	0
RABL2A	0.397	8.59E-06
HIBCH	0.397	0
DSN1	0.397	0
ZNF33B	0.397	0
RNF144A	0.396	0
LRFN3	0.396	0
ANGEL2	0.396	0
SNHG20	0.396	0
ASF1B	0.396	0
C2ORF27A	0.396	1.39E-06
FBXO10	0.396	0
PHLDA1	0.396	0
NKAPD1	0.395	0
ZBED5	0.395	0
PLEKHG2	0.395	0
MTHFSD	0.395	0
JRKL	0.395	0
MAF	0.395	0
GYS1	0.395	0
SNTB1	0.395	0
TCFL5	0.395	0
THTPA	0.395	0
CDK14	0.395	0
ZNF440	0.394	4.41E-14
COMMD9	0.394	0
ZCCHC17	0.394	0
ZNF446	0.394	0
NALCN	0.394	0.015923021
GATD3A	0.394	0
DYNLL1	0.393	0
ZNF551	0.393	1.11E-16
TTC5	0.393	0
ENOX2	0.393	0
OLFML2A	0.393	1.93E-14
CECR7	0.393	0
TMEM121B	0.393	5.06E-05
NIPAL3	0.392	0
CABLES2	0.392	2.47E-12
C6ORF47	0.392	0

MCM8	0.392	0
ARHGAP42	0.392	0
FAM120AOS	0.392	0
RHOJ	0.392	0
E2F3	0.392	0
MBNL1-AS1	0.392	0.021797246
PEG3	0.392	2.57E-09
EPDR1	0.391	0
KIAA0556	0.391	0
CPT1C	0.391	5.52E-05
POLR2D	0.391	0
GPATCH4	0.390	0
THUMPD3-AS1	0.390	9.77E-15
ELP6	0.390	0
MATN1-AS1	0.390	0.000928547
CARMIL1	0.390	0
ZNF680	0.390	0
PCDHGA6	0.390	4.36E-10
ITGAV	0.390	0
DNAJC14	0.389	0
APOD	0.389	0
HYAL3	0.389	4.06E-14
RAB29	0.389	0
MAP1A	0.389	0
RGL1	0.389	0
KCNK10	0.389	0
FOXRED2	0.389	0
TSHZ1	0.389	0
KCNA2	0.389	0
PTCHD1	0.389	6.04E-06
MRPS28	0.388	1.35E-14
RDH14	0.388	0
ZNF23	0.388	0
GABPB2	0.388	0
FUZ	0.388	0
LTBP2	0.388	0.020341641
MEX3A	0.388	0
WDR4	0.388	0
KRIT1	0.388	0
ZNF827	0.387	0
ADAM22	0.387	0
METAP1D	0.387	0
PTCD2	0.387	0
GATD3B	0.387	0
LRRC20	0.387	0

UNC5C	0.386	0
SLC18B1	0.386	0
EIF4EBP2	0.385	0
HOXC13	0.385	5.43E-12
UBL7-AS1	0.385	0.004440395
STAG1	0.385	0
ARL15	0.385	0
DGCR2	0.384	0
ERCC6	0.384	5.82E-12
ZNF81	0.384	0
ZSCAN16	0.384	5.15E-13
ARL17B	0.384	0.007798561
PRR14L	0.384	0
MARS2	0.384	0
ITPRIPL1	0.383	0
STXBP4	0.383	0
ZNF853	0.383	0
TMEM250	0.383	0
ARL6IP6	0.383	0
IL16	0.383	0
RNF145	0.383	0
DPY19L2	0.383	5.32E-05
GLCE	0.383	0
ZFP30	0.382	0
ZNF337	0.382	0
ADAMTS1	0.381	0
PMS2CL	0.381	0
NDST1	0.381	0
FAM27E3	0.381	0
MARVELD1	0.381	0
CYB561D1	0.381	0
SUV39H2	0.381	0
ZNF292	0.381	0
MCC	0.381	0
FTSJ3	0.380	0
POLQ	0.380	0
ZKSCAN5	0.380	0
SMARCAD1	0.380	0
ZNF852	0.380	9.39E-05
HSPE1-MOB4	0.380	3.51E-07
NCOA7	0.380	0
GIMAP6	0.380	0.00026051
ZNF260	0.380	0
RMND5B	0.380	0

SUGT1P4-STRA6LP	0.379	0.001661478
PTPRJ	0.379	0
ARMC5	0.379	0
TRUB1	0.379	0
GSTA4	0.379	0
ZNF75D	0.378	0
LYPD6	0.378	0
TTF2	0.378	0
INHBB	0.378	2.91E-05
RWDD3	0.378	4.42E-05
CAVIN4	0.378	0.000674568
SSH2	0.378	0
VPS33A	0.378	0
PPP6R3	0.378	0
AMH	0.377	7.89E-09
GSEC	0.377	0.023469834
FBXL19	0.377	0
NEK1	0.377	0
TBC1D31	0.377	0
FZD4	0.377	0
KCNMB4	0.377	0.000891994
ZNF792	0.377	9.44E-12
MAP2K4	0.377	0
C2ORF74	0.376	9.66E-10
TMEM200C	0.376	2.33E-15
TOP2B	0.376	0
PTPRD	0.376	0
LRR1	0.376	0
C10ORF143	0.376	0.008577247
KIAA1755	0.376	0
CCDC90B	0.376	0
FRYL	0.375	0
LMLN	0.375	0
GABPB1-AS1	0.375	1.98E-09
SHQ1	0.375	0
ZNF510	0.375	0
PTPN4	0.375	0
LRRC45	0.375	0
GALNT7	0.375	0
DEPDC5	0.375	0
ZNF30	0.375	3.89E-15
RIDA	0.375	0
STRA6LP	0.375	3.03E-09
ATP6V0A4	0.375	1.61E-10

WDR81	0.374	0
TBC1D13	0.374	0
TMEM107	0.374	6.97E-07
MESD	0.374	0
ZNF283	0.374	0
TRIP13	0.373	0
ANKRD44	0.373	0
FKBP9	0.373	0
PSMG4	0.373	0
ATXN7L3B	0.373	0
CROCCP3	0.373	0.000158467
BCAP29	0.372	0
SCD5	0.372	0
ALG6	0.372	0
STIMATE	0.372	0
GHDC	0.372	0
LHX9	0.371	0.04572819
KIAA0586	0.371	0
ZNF395	0.371	0
FOXP2	0.371	1.83E-12
SNHG11	0.371	8.87E-14
DHRS13	0.371	0
ZSCAN30	0.371	0
MAGEF1	0.370	0
MVB12B	0.370	0
CACNA2D1	0.370	0
HLCS	0.370	0
XRCC4	0.369	1.27E-08
NTN1	0.369	0
CHAF1B	0.369	0
NUDT7	0.369	0.000922874
HSPA12A	0.369	0
FRG1HP	0.369	6.11E-13
ADD3	0.368	0
DBNL	0.368	0
MGLL	0.368	0
HGSNAT	0.368	0
OXSM	0.367	0
DUXAP9	0.367	0
SOS1	0.367	0
HTRA1	0.367	0
ERLIN2	0.367	0
P3H4	0.367	0
ATP1A2	0.367	0
WDR35	0.367	0

ABHD14A-ACY1	0.367	1.73E-05
STARD13	0.367	0
PYGO1	0.366	0
RALGAPA2	0.366	0
ENOSF1	0.366	0
SIPA1L2	0.366	0
POLA1	0.366	0
LRRTM2	0.365	0.007630777
LINC00294	0.365	0
MPI	0.365	0
DHRS11	0.365	0
METTL25	0.364	7.01E-08
C17ORF75	0.364	0
HOXA3	0.363	0.01039296
KIAA1143	0.363	0
PPP3CA	0.363	0
NSMCE4A	0.362	0
SNHG14	0.362	0
BPHL	0.362	0
RPUSD2	0.362	0
IFT88	0.362	0
SYT15	0.361	0.022482049
MRPL13	0.361	0
RTL6	0.361	0
DBR1	0.361	0
XPA	0.361	0
PDE4B	0.361	0
ICE2	0.361	0
ARID5B	0.360	0
TP53I3	0.360	0
FBXL14	0.360	0
C9ORF163	0.360	0.034150915
KBTBD11	0.360	4.33E-15
LANCL2	0.360	0
CRYBB2P1	0.359	0
GTF2H2C	0.359	0
CLSPN	0.359	0
MTERF4	0.359	0
RYR2	0.359	1.55E-15
ZNF418	0.358	3.56E-12
NEK4	0.358	0
ADAL	0.358	0
ASL	0.358	0
ZNF557	0.358	0
ZSCAN25	0.357	0

SCN7A	0.357	0.000117132
ZNF7	0.357	0
DPP8	0.357	0
MFN1	0.357	0
ALG1	0.357	0
ZNF544	0.357	0
GPR161	0.357	0
B9D1	0.356	0
SBF2-AS1	0.356	1.87E-12
COX18	0.356	0
AARS2	0.356	0
ZNF514	0.356	0
SRGAP3	0.356	0
UROS	0.355	0
RHOB	0.355	0
MGME1	0.355	0
METTL7B	0.355	0
ATG9B	0.355	0.030192975
CEP68	0.355	0
CCDC138	0.355	0
SELENBP1	0.355	0
DDX11-AS1	0.354	0.003118095
IRAK1BP1	0.354	0
RXRG	0.354	6.95E-05
XYLB	0.353	0.000206546
FCF1P2	0.353	0.025342378
NREP	0.353	0
SNX19	0.353	0
C11ORF95	0.353	0
HIF1AN	0.353	0
IL17D	0.352	0
RALGPS2	0.352	0.001125935
TRPM3	0.352	0
NR5A2	0.352	0
DLGAP1-AS1	0.352	2.98E-05
TMEM117	0.352	0
WRB	0.352	0
NIFK-AS1	0.352	0
HES1	0.352	0
SPPL2A	0.352	0
DCLRE1B	0.352	0
RAB43	0.352	4.87E-12
ZFP82	0.352	0
SNHG4	0.352	0
SMO	0.352	0

RAD51D	0.351	0
RNF175	0.351	0
CDKL5	0.351	0
POLR3G	0.351	0
POLR3F	0.351	0
CEP83-DT	0.351	0.000981804
HIST1H2AG	0.351	1.32E-10
UTP20	0.350	0
SARM1	0.350	0
CHMP6	0.350	0
SOX1	0.350	0
MED22	0.350	0
ZBTB38	0.349	0
ACAN	0.349	0
KIF1BP	0.349	0
ATP5MF-PTCD1	0.349	0
MRO	0.349	0
HSPA2	0.349	0
PTPN13	0.349	0
ICMT	0.348	0
DUS2	0.348	0
TMEM165	0.348	0
CCND3	0.348	0
ZNF772	0.348	0
KIAA1614	0.348	5.07E-14
CUL5	0.348	0
ST20-AS1	0.347	0
B4GALT7	0.347	0
RPTOR	0.347	0
ZNF530	0.347	0
FAM122B	0.347	0
TYSND1	0.347	0
EDEM3	0.347	0
MOB3B	0.346	0
SEMA6D	0.346	0
ZNF517	0.346	1.96E-12
ELOA-AS1	0.346	2.33E-07
IRF2BPL	0.346	0
DCP1B	0.346	0
ENPP1	0.346	0
BTBD8	0.345	1.64E-07
PRDM2	0.345	0
MIR4453HG	0.345	0.000133486
ABCD3	0.345	0
HIRA	0.345	0

SYNJ2BP	0.345	0
SALL2	0.344	0
SNX1	0.344	0
S100B	0.344	0
ATP7A	0.344	0
THAP10	0.344	3.81E-14
ZNF839	0.343	4.92E-14
MPHOSPH6	0.343	0
ADPRH	0.343	4.31E-14
SLC35D1	0.343	0
FAM114A2	0.343	0
NSL1	0.342	0
LIG4	0.342	0
SLITRK5	0.342	7.11E-15
GAS2	0.342	4.34E-10
PAPSS2	0.342	0
ZNF502	0.341	1.17E-12
ZNF12	0.341	2.00E-15
TRADD	0.341	0
ZBTB26	0.341	0
KCNJ10	0.340	0
GEMIN7	0.340	0
LYSMD4	0.340	2.44E-11
ZSCAN12P1	0.339	0.018732989
FOXD2	0.339	0
LINC00665	0.339	0
ZMYM4	0.339	0
DNAL1	0.338	0
RFX5	0.338	0
TRIM66	0.338	0
CLGN	0.338	0
TIA1	0.338	0
RNASE1	0.338	0.002432845
MFSD9	0.337	0
ADM2	0.337	1.15E-06
POP5	0.337	0
FAM81A	0.337	7.67E-08
CHRNA4	0.337	0.001838757
RAB23	0.337	0
NHSL1	0.337	0
FOXD2-AS1	0.336	0
STARD4-AS1	0.336	2.56E-07
SRD5A3	0.336	4.90E-08
GOLIM4	0.335	0
ALCAM	0.335	0

ESCO2	0.335	0
UHRF1	0.335	0
CHL1-AS2	0.335	3.26E-08
ARPIN	0.335	0
SLC25A13	0.335	0
SPDL1	0.335	0
EIF4EBP3	0.334	7.57E-07
FGF14	0.334	0.003793049
AGL	0.334	0
ZSWIM1	0.334	0
TMEM131L	0.333	0
MAPKAP1	0.333	0
SRSF8	0.333	0
SLC12A2	0.333	0
NRGN	0.333	0.005262413
HOXA13	0.333	0
TTC3P1	0.333	0
ASAH2	0.333	0.00372074
AK4	0.332	0
SLC46A1	0.332	0
VAPB	0.332	0
GDF10	0.332	0
SMAD1	0.332	0
GNG2	0.332	0
ID3	0.332	0
KCTD18	0.332	0
ZSCAN20	0.331	0
FAM198A	0.331	0
FTX	0.331	8.88E-16
SATB1	0.331	0
THAP5	0.331	0
COQ7	0.331	0
SOX10	0.330	0
TSEN2	0.330	0
PSMA3-AS1	0.330	0
RHOBTB1	0.330	0
TRDMT1	0.330	0
PTGFRN	0.330	0
ZNF468	0.330	0
HMMR	0.330	0
FBF1	0.330	0
POLR3B	0.329	0
FMO4	0.329	2.48E-05
SLC13A3	0.329	0.046366267
FAM135A	0.329	0

ZNF91	0.329	0
HMGN3	0.329	0
KCNAB1	0.329	7.58E-09
LINC02119	0.329	0.01614296
PCDH9	0.329	0
GPAA1	0.329	0
PTPRO	0.328	0
ZNF20	0.328	2.26E-10
NEMP2	0.328	0
PGBD4	0.328	0
RAPGEF2	0.328	0
RMI2	0.328	0
FBXL17	0.328	0
METTL18	0.328	3.20E-13
ZNF625	0.327	0.00064357
CPSF1P1	0.327	0.000417185
TIAM2	0.327	0
SLC38A7	0.327	0
NUDT12	0.326	0
TMEM17	0.326	0.000272498
UTP3	0.326	0
SLC16A1-AS1	0.326	0
CCDC113	0.326	0.013024062
NPHP1	0.325	2.51E-08
FER	0.325	0
CYP2J2	0.325	6.13E-10
SLC6A6	0.325	0
ZNF776	0.325	0
EFCAB11	0.324	0.001113709
ZNF730	0.324	3.85E-06
CICP14	0.324	1.69E-13
ZNF169	0.324	1.98E-10
NAP1L4	0.324	0
EML5	0.323	8.66E-05
ZNFX1	0.323	0
GSPT2	0.323	0
CEND1	0.323	0.000386401
ZNF701	0.323	0
TEX261	0.323	0
SPRN	0.323	6.72E-10
HNRNPM	0.322	0
SNHG26	0.322	1.05E-05
C12ORF66	0.322	0
ASPM	0.322	0
ING4	0.322	0

CPTP	0.322	0
NTRK2	0.322	0
IGF2BP3	0.321	0
DOCK9	0.321	0
CTRL	0.321	1.41E-05
FKRP	0.321	0
GPR157	0.321	0
USP40	0.320	0
ALG8	0.320	0
EID2B	0.320	1.65E-11
C15ORF40	0.320	0
PKDCC	0.319	0
TEFM	0.319	0
DNAJC30	0.319	0
SEMA4F	0.318	1.01E-14
NOVA1	0.318	0
TIGD1	0.318	0
PRIMPOL	0.318	0
ZKSCAN1	0.318	0
NT5E	0.318	0
MAP2	0.318	0
AMIGO1	0.318	0
COL5A2	0.318	2.19E-06
ARSJ	0.318	0
BTBD9	0.318	0
PHF7	0.317	1.98E-12
LMBRD2	0.317	0
FAM172A	0.317	0
RBM45	0.317	0
ATP5S	0.316	0
GPRASP2	0.316	1.90E-08
PNMA8A	0.316	0
PLEKHG1	0.316	0
OMA1	0.315	0
GLCCI1	0.315	0
DAGLA	0.314	0
DEGS1	0.314	0
PLOD2	0.314	0
MAPK4	0.314	0
BBS1	0.314	0
E2F8	0.313	0
FZD2	0.313	0
STS	0.313	0
SAMHD1	0.313	0
ATMIN	0.313	0

SLC10A5	0.313	0.03433602
PFAS	0.312	0
DCAF16	0.312	0
MT-ND3	0.312	0
LAG3	0.311	0.019161309
TADA2A	0.311	0
MAP3K5	0.311	0
CTSV	0.311	0.001425203
ZNF337-AS1	0.311	0.026085155
HSPA7	0.311	7.68E-05
FANCF	0.311	0
SLC7A11	0.311	0
CDK6	0.310	0
RPL7L1	0.310	0
PCNA	0.310	0
MCOLN2	0.310	0
ZNF324B	0.310	0
C12ORF43	0.310	0
EEF1AKMT1	0.310	0
GPAM	0.310	0
ACSS1	0.310	0
PALB2	0.310	0
SLC35B4	0.310	0
CCNYL1	0.310	0
RBM15B	0.310	0
MFSD6	0.309	0
SLC25A10	0.308	0
ACOX3	0.308	0
CEP295	0.308	0
HILS1	0.308	0
ASTN1	0.308	9.70E-05
DNAJC16	0.308	0
CYB5D1	0.307	0
ALKBH8	0.307	0
PCBD2	0.307	2.27E-07
RGS5	0.307	2.66E-07
UEVLD	0.307	0
HTD2	0.307	0
FREM2	0.306	0
ACAD10	0.306	0
ZNF248	0.306	0
DGKG	0.306	8.72E-11
CSGALNACT1	0.305	0
ZACN	0.305	0
WNK4	0.305	0

MFAP3L	0.305	0
WSCD1	0.305	0
UBE3B	0.305	0
IFNAR1	0.305	0
FRMD6	0.305	0
GTF2H3	0.305	0
CEP128	0.304	0
DNAAF5	0.304	0
GRK4	0.304	0
ALG10B	0.303	0
IFT80	0.303	0
RRP15	0.303	0
ZNF232	0.303	0
FAM216A	0.303	0
FZD1	0.303	0
RFT1	0.302	0
CPSF6	0.302	0
POLR1A	0.302	0
HIPK2	0.301	0
ZNF519	0.301	0
PARD6G	0.301	0
MED11	0.301	0
STX18-AS1	0.301	3.24E-05
NUDT6	0.301	0
BRI3BP	0.300	0
HS6ST1P1	0.300	0.000109957
TMX1	0.300	0
WDCP	0.300	0
COL11A1	0.300	0
AP5B1	0.300	0
C12ORF4	0.299	0
ENC1	0.299	0
ERBB3	0.299	0
TCHP	0.299	0
CTR9	0.299	0
LRRC37A17P	0.299	0
ECHDC3	0.299	0.000274335
ACADL	0.299	0.0096953
ZFP90	0.298	0
GGACT	0.298	0.000323719
MFAP3	0.298	0
SHROOM3	0.297	0
ABCA8	0.297	0.020844022
DET1	0.297	1.26E-12
PPP2R1B	0.297	0

PRKAR1B	0.296	0
MIR9-3HG	0.296	0.000731931
TRIOBP	0.295	0
FAM120B	0.295	0
ZFP69B	0.295	0
BTRC	0.295	0
NEU4	0.295	0
CHST12	0.295	0
ZBED3	0.294	0
APPL2	0.294	0
SEC14L2	0.294	0
THRB-AS1	0.294	0.036300912
SLC35A4	0.294	0
THRB	0.294	0
NETO2	0.293	0
CDO1	0.293	0
ZBED9	0.292	9.76E-10
FANCD2	0.292	0
EFS	0.292	0
LIMS2	0.292	1.64E-06
ARMC4	0.292	0.002594905
HOXA7	0.291	4.48E-12
CTDSP1	0.291	0
PNPO	0.291	0
ZNF416	0.291	0
ACY1	0.291	0
RASSF2	0.291	0
APOLD1	0.291	0
ZNF708	0.291	0
UTP23	0.291	0
ZNF174	0.291	0
AFAP1L2	0.291	0
SLC26A4-AS1	0.290	0.000313599
JPX	0.290	0
RPP14	0.290	0
LINC00667	0.290	0
CHAC2	0.290	0
TUB	0.290	0
CD83	0.290	0
RCBTB2	0.290	4.00E-15
CBX6	0.289	0
FKBP9P1	0.289	0
RNF150	0.289	0
TIGAR	0.289	0
ZNF829	0.289	0

C4ORF19	0.289	2.22E-16
HEATR3	0.288	0
TMEM187	0.288	0
FAM86DP	0.288	0
LOH12CR2	0.288	0.000517172
RASGEF1C	0.288	0
JRK	0.287	0
TTLL11	0.287	0
WASHC5	0.287	0
CNPY4	0.287	0
RASSF8-AS1	0.287	1.57E-13
PHACTR2	0.286	0
GAS1	0.286	0
ZNF480	0.286	0
H6PD	0.286	0
ACTL10	0.286	4.32E-10
BEND3	0.286	0
KCTD21	0.286	0
PAWR	0.286	0
MTND2P28	0.285	7.88E-06
ZNF542P	0.285	0
BORCS7	0.285	0
FRG1BP	0.285	3.46E-11
TECPR2	0.284	0
OPRL1	0.284	0
RMDN2	0.284	2.20E-07
OXLD1	0.284	0
C17ORF67	0.284	0.020115169
KCTD12	0.284	0
CBR4	0.284	0
STOML1	0.284	0
SLC2A12	0.283	3.15E-06
ZNF175	0.283	0
EPHA3	0.283	0
TLE6	0.283	2.21E-05
CROT	0.283	0
OIP5	0.283	0
COL24A1	0.282	6.66E-15
RIN2	0.282	0
ZNF891	0.282	0
SLC38A10	0.282	0
TXLNB	0.281	1.11E-16
TGFB3	0.281	0
PDF	0.281	0
GRAMD2B	0.281	0

SLC35A1	0.281	0
GINS3	0.280	0
KHDC1	0.279	3.74E-11
SFXN5	0.279	0
PGBD2	0.279	1.24E-12
LINC02043	0.279	0.009304243
LRRC37A4P	0.279	0
SEMA6A	0.279	0
ADAM23	0.278	0
MEF2C	0.278	0
QRICH2	0.278	0
IMPG2	0.278	0.042394781
AP5S1	0.278	0
ANKRD16	0.278	0
SKP2	0.277	0
ARSB	0.277	0
ZNF616	0.277	0
MTAP	0.276	0
BCKDHB	0.276	0
MAP3K1	0.276	0
GAL3ST4	0.276	0
PTGES3L-AARSD1	0.276	0.017910095
ZBTB42	0.276	0
LYPLAL1	0.275	0
ERI2	0.275	0
COX10-AS1	0.275	0
STAG3L1	0.275	2.22E-16
ZNF334	0.275	0
MKL2	0.275	0
PLAGL2	0.274	0
LHFPL4	0.274	7.59E-10
CDC42EP3	0.274	0
IFT81	0.274	0
LINC01011	0.274	0.016450027
NPL	0.273	1.33E-13
TRIM68	0.273	0
SGCD	0.273	0
SAMD10	0.273	2.06E-12
ZNF525	0.272	0
SPDYE3	0.272	2.07E-09
UNC50	0.272	0
GIN1	0.272	0
PDGFRA	0.272	0
CCDC8	0.271	0

LRRTM4	0.271	8.09E-05
SPOCK1	0.271	4.80E-14
ZNF345	0.271	2.57E-05
MRPS18A	0.271	0
SAMD5	0.270	7.77E-16
PIGCP1	0.270	2.78E-15
BCDIN3D-AS1	0.270	2.80E-06
KCNC3	0.270	0.000294778
CCDC125	0.270	0
ZNF691	0.269	0
BAIAP2-DT	0.269	0
CPB2-AS1	0.269	0.042199926
YY2	0.269	1.92E-13
SMUG1	0.269	0
EMILIN3	0.268	1.12E-13
GEMIN4	0.268	0
KLF15	0.268	0
IFIT3	0.268	4.82E-07
RPGRIP1L	0.268	0
SEMA3A	0.268	0
THAP6	0.268	0
MBNL3	0.268	0
SLC24A1	0.267	0
SLC31A2	0.267	1.09E-07
FAM187A	0.267	1.46E-08
N6AMT1	0.267	0
ENPP4	0.267	0
RBBP9	0.267	0
TTC31	0.266	0
SLC43A2	0.266	0
GTF2IRD2B	0.266	0
ELMOD2	0.266	0
HS6ST1	0.266	0
CRB1	0.266	0
MRM2	0.265	0
ZBTB8OS	0.265	0
ADGRL3	0.265	0
FZD8	0.265	0
APC2	0.265	0
FLVCR2	0.265	0
MANSC1	0.264	0
UBAP1L	0.264	3.27E-05
NAIP	0.264	0
SPRYD4	0.264	0
KLHL32	0.264	0.01095831

FAM155B	0.264	0
FEN1	0.263	0
HFM1	0.263	0.000324908
FRMD4B	0.263	0
MT-ND2	0.263	0.007563298
SEPHS2	0.263	0
POLE2	0.263	0
NNT-AS1	0.263	0
GDAP1	0.262	0
ZNF646	0.262	0
AP4E1	0.262	0
ARSD	0.262	0
TUBGCP5	0.262	0
C18ORF54	0.261	0
BHLHB9	0.261	2.68E-12
CSRNP3	0.261	0
UCN2	0.261	0.021723855
TMTC4	0.261	0
RBMS3	0.261	0
TNFSF4	0.261	0.007166794
PKD2	0.261	0
TSPYL4	0.260	0
SSPN	0.260	9.14E-06
SRP14-AS1	0.260	0
CPM	0.260	0
GTF2IP13	0.260	0
C19ORF57	0.260	0
NDUFAF1	0.260	0
FKTN	0.259	0
PEX12	0.259	0
DNAAF4	0.257	8.18E-05
ZNF425	0.257	1.40E-11
C1ORF61	0.257	0
ZNF613	0.257	0
GCA	0.257	0
VASH1-AS1	0.257	0
PPP1R3D	0.257	0
WDR53	0.257	1.90E-13
NBR2	0.257	2.01E-06
CHAMP1	0.256	0
ACADSB	0.256	0
ERBB4	0.256	0
DAB1	0.256	2.78E-07
P2RX6	0.256	0
SIRT4	0.256	1.90E-11

HILPDA	0.256	0
TIMP4	0.256	0
PTGR2	0.256	0
GPR155	0.256	0
ELOVL2	0.255	0
EHD3	0.255	0
GVQW2	0.255	0.031055435
CYP7B1	0.255	4.92E-05
LRRCC1	0.254	1.39E-12
PRRX1	0.254	0
MBTD1	0.254	0
GON7	0.254	0
ARV1	0.254	0
SRCIN1	0.254	1.23E-07
FGF11	0.254	1.23E-06
ADORA2B	0.254	3.86E-10
MKKS	0.254	0
ZNF688	0.253	0
DTWD2	0.253	0
CCT6B	0.253	3.27E-05
DIDO1	0.253	0
ZSCAN22	0.253	0
CNTN1	0.253	0
LYRM2	0.253	0
UFSP1	0.253	1.10E-05
CETN3	0.253	0
SRR	0.253	1.66E-08
SLC35A5	0.252	0
REEP1	0.252	2.24E-08
CEP41	0.252	0
BRCA1	0.252	0
TIGD3	0.252	0.000272968
C5ORF63	0.251	0
MDFIC	0.250	6.04E-07
DENND2A	0.250	0
ETAA1	0.250	0
ENTPD1-AS1	0.249	0
MAST4	0.249	8.16E-05
LRRC26	0.249	1.51E-14
SLX4IP	0.249	0
NRAV	0.249	7.22E-15
SPATA25	0.249	0.010913788
GRIA2	0.248	0.000603065
ALDH5A1	0.248	0
CHKB-DT	0.248	0.032355462

TTN-AS1	0.247	0
SPON1	0.247	3.56E-09
ZNF285	0.247	0
ZFC3H1	0.247	0
SLC38A9	0.247	0
LGI2	0.247	0
PIGBOS1	0.247	0
CTHRC1	0.246	0
PKIA	0.246	0
LINC00663	0.246	1.30E-11
RAD51-AS1	0.246	4.16E-05
PIGM	0.246	0
ZNF689	0.246	0
SEMA3E	0.246	0
DENND1B	0.246	6.44E-12
GTF2E1	0.245	0
CCDC142	0.245	0
MYO5C	0.245	0
SFT2D3	0.244	2.22E-16
C2ORF72	0.244	0
GRIA4	0.244	0
SEMA3D	0.244	0
RPL4P6	0.244	0.038771931
BTN2A3P	0.243	0
BMPR1B	0.243	0
ANK3	0.243	0
TRMT10C	0.243	0
PSPH	0.243	0
ADGRV1	0.243	0
CRISPLD1	0.243	0
TMEM121	0.243	0
TRMT1L	0.242	0
TMEM19	0.242	0
AQP7P1	0.242	0.002564363
SLX4	0.241	0
EIF3J-DT	0.241	0
GRIA3	0.241	0.005029092
ACTR3B	0.241	0
CASP8	0.241	0.000116366
SLC25A24	0.240	5.22E-11
PIGV	0.240	0
TIMM21	0.240	0
ALOX15	0.240	0.01955787
SPRY3	0.240	0.02307234
SPRY3	0.240	0.02307234

SLC12A6	0.239	0
WBP4	0.239	0
LINC01560	0.238	6.92E-05
JMJD4	0.238	0
LIPT2	0.238	0.010831997
IFIT2	0.238	0.003497615
MTBP	0.238	0
IPP	0.237	0
NRCAM	0.237	0
FRMD4A	0.237	0
BRIP1	0.236	0
DENND4A	0.236	0
ZNF234	0.236	0
UST	0.236	0
THAP2	0.236	0
ANKRD46	0.236	0
MPZ	0.236	0
TIGD2	0.235	0
FAM181B	0.235	0
ZBED1	0.235	0
ZBED1	0.235	0
ETFBKMT	0.235	1.44E-10
NCAM2	0.234	0
JMJD7	0.234	0
KIF24	0.233	0
GABPB1-IT1	0.233	0
SPRY4	0.233	0
ORC6	0.232	0
RBL1	0.232	0
TST	0.232	0
OPHN1	0.231	0
GLIDR	0.231	0
SCAMP5	0.231	0
ITGA4	0.230	0
ZNF585B	0.230	0
MED18	0.229	0
ASTE1	0.229	0
WT1-AS	0.229	0.001533312
TEX15	0.229	0
CDC7	0.229	0
DMRT2	0.229	0
DSEL	0.229	0
NICN1	0.229	0
ERCC4	0.228	0
ZNF112	0.228	0

MMP16	0.228	0
CUTALP	0.228	0
C12ORF65	0.228	0
MECOM	0.228	0
ARRB1	0.228	2.07E-07
ACADM	0.228	0
YPEL1	0.227	0
ITGA2	0.227	0
ARMC7	0.227	0
CEBPZOS	0.227	0
HDX	0.226	0
HOMER1	0.226	0
MLYCD	0.226	0
FGL2	0.226	0.015560801
DICER1-AS1	0.225	2.09E-05
F8A1	0.225	0
TCEANC2	0.225	0
ZNF696	0.224	0
SLC4A4	0.224	0
ZNF213-AS1	0.224	1.05E-14
BRCC3	0.224	0
STAC2	0.224	0
TRNP1	0.224	0
COL25A1	0.224	0.021289602
CSTF2T	0.224	0
TNS2	0.223	0
SCAMP1-AS1	0.223	0
GPLD1	0.223	0.007787937
ZBTB11-AS1	0.223	4.29E-10
SUOX	0.223	0
RHBDL3	0.223	0
ACP2	0.223	0
MYOM1	0.223	2.65E-06
ARHGEF39	0.223	0
DISC1	0.222	0
RIMKLA	0.222	0
ITIH6	0.222	0
FAM198B	0.222	0
NLGN3	0.222	0
PCDH10	0.221	0
ZNF610	0.221	0.001408415
ZIC5	0.221	0
KDM4D	0.221	3.47E-07
ZNF137P	0.221	0.000157634
PDZD2	0.221	0

BICC1	0.220	0
TENM3	0.220	3.74E-09
WWTR1-AS1	0.220	0.010817035
OLIG2	0.220	0
ZNF180	0.219	0
CEMP1	0.219	2.63E-05
ZMYND8	0.219	0
DDX60	0.219	0.01364478
ZNF200	0.219	0
ZNF605	0.219	0
TWNK	0.218	0
LEPROT	0.218	0
ANKS1A	0.218	0
ZNF816	0.218	0
LPAR1	0.218	0
TMEM229B	0.218	0
WARS2-IT1	0.217	0.01764853
RWDD2B	0.217	0
ZNF439	0.216	0
MAN1A2	0.216	0
HAPLN4	0.216	0.00323098
IL10RB-DT	0.216	0
FAM86B3P	0.216	0.003063328
GJA1	0.216	0
EDNRB	0.216	0
RIOX1	0.216	0
ZNF100	0.216	0
APH1B	0.215	0
ZCCHC24	0.214	0
NLGN4X	0.214	0
DHRS4-AS1	0.214	0
PHOSPHO2	0.214	1.02E-07
SETMAR	0.214	0
ZNF561-AS1	0.213	0
MFSD3	0.213	0
ZNRD1ASP	0.213	0
CRYM	0.213	0
MTERF1	0.213	0
ZNF549	0.213	0
CERK	0.213	0
TEX9	0.213	0
TIGD7	0.213	0
PCDH15	0.212	0
GLB1L	0.212	0
CES2	0.212	0

YAE1D1	0.212	0
HDAC9	0.211	0
ZNF223	0.211	0
WDR5B	0.211	0
TIGD4	0.211	1.48E-11
ZNF554	0.210	1.26E-06
ZNF543	0.210	0
ZNF782	0.210	4.44E-16
ADGRA3	0.210	0
RNF144A-AS1	0.210	0
ZNF876P	0.210	0.000180249
ZNF710-AS1	0.210	0
OSGEPL1	0.210	0
ICK	0.209	0
PCMTD2	0.209	0
CHL1	0.209	0
FAM86EP	0.209	0
ATOH8	0.209	0
MTERF2	0.209	0
SLC16A9	0.209	0
POLN	0.209	7.71E-10
RAPGEF4	0.209	0
DNAJC3-DT	0.208	3.46E-10
ZSCAN32	0.208	0
WDR77	0.208	0
GINS1	0.208	0
CYP27C1	0.208	3.33E-16
PRELP	0.208	0
PDE5A	0.207	1.51E-11
NCDN	0.207	0
C3ORF70	0.207	0
ZNF45	0.207	0
CYP39A1	0.207	1.25E-05
EXTL1	0.207	0
ZNF19	0.207	7.58E-05
PLPP3	0.207	0
SAYSD1	0.207	0
INAVA	0.207	0
SELL	0.206	0.001117607
HOGA1	0.206	3.98E-08
PRSS12	0.206	1.13E-06
TMEM163	0.206	0.006703306
FAM169A	0.206	1.11E-16
ZSCAN29	0.206	0
F3	0.206	0

KAT2B	0.206	0
LINC00339	0.206	0
CENPS	0.206	0
TMEM67	0.206	0
LINC01291	0.206	2.55E-15
TTC32	0.206	2.00E-15
ZNF583	0.206	0
RNASEL	0.205	0
PCYOX1L	0.205	0
SLC25A45	0.205	0
NANOS1	0.205	1.04E-13
ZNF493	0.205	0
CPVL	0.205	0
POGLUT1	0.205	0
ZNF619	0.205	0
LINC00476	0.205	9.99E-16
ZNF624	0.204	5.55E-16
TMEM45A	0.204	0
INTS6-AS1	0.204	8.32E-13
CALHM2	0.204	2.95E-07
ZNF512	0.204	0
ATP6V1E2	0.204	0
C7ORF25	0.203	1.11E-16
ST3GAL2	0.203	0
PEX3	0.203	0
ZNF620	0.203	0
KBTBD8	0.203	0
SERF1A	0.203	2.84E-06
ZNF28	0.202	0
ZNF436	0.202	0
TMEM186	0.202	0
ZNF764	0.202	0
USP46-AS1	0.202	0.001938275
CYP4V2	0.201	0
HAS2	0.201	0
B4GALT6	0.201	0
TRMT12	0.201	0
ZNF132	0.201	0
MTFMT	0.201	0
C6ORF120	0.201	0
ABCB10	0.200	0
ADAT1	0.200	0
TMEM86A	0.200	0.00150452
RHOBTB2	0.200	0
CAAP1	0.200	0

RPARP-AS1	0.199	0.001190639
SFXN2	0.199	0
HIST1H3E	0.199	0
CYB5D2	0.199	0
AGFG2	0.199	0
CASP6	0.199	7.05E-10
ZBED5-AS1	0.199	0
SHC3	0.198	0
VASH1	0.198	0
RMI1	0.198	0
PRIMA1	0.198	0.021023393
THEM4	0.197	0
ZNF441	0.197	1.25E-14
FAM86B1	0.197	1.57E-13
ZNF682	0.197	2.33E-15
NMNAT1	0.197	0
ZSCAN5A	0.197	0
OSR1	0.197	0
C11ORF71	0.196	0
PWAR6	0.196	0
ANO5	0.196	0
TCF19	0.196	0
MLIP	0.195	0
RTL8B	0.195	0
CSPG5	0.195	0
RGS7BP	0.195	0
HOXD-AS2	0.194	1.62E-06
GABRB3	0.194	0.000696624
LINC00327	0.194	0
MORN1	0.193	1.46E-11
LINC01006	0.193	3.60E-06
HSPA1L	0.193	1.73E-06
RAB30-AS1	0.193	0
GNAS-AS1	0.192	3.19E-06
ZNF552	0.192	0
ELMO1	0.192	0
TUSC1	0.192	0
TIRAP	0.192	1.67E-09
ZC3H10	0.192	0
CCDC9B	0.192	0
KLRG1	0.191	1.36E-11
EGR2	0.191	0
SCYL3	0.191	0
RPRML	0.190	0
PLCXD2	0.190	1.59E-13

GRIK3	0.190	0
TOMM40L	0.189	0
TP73	0.189	2.13E-08
WT1	0.189	0
MMACHC	0.189	0
MIR503HG	0.189	7.03E-09
MRFAP1L1	0.189	0
ZDBF2	0.189	1.28E-13
ZNF648	0.189	0
RFXAP	0.189	0
BRD3OS	0.189	0
SHROOM2	0.188	0
PRR22	0.188	4.89E-10
HUNK	0.188	0
SLC30A6	0.188	0
UMPS	0.188	0
SPRY2	0.187	0
ADAM12	0.187	0
FAM122A	0.187	0
TFDP1	0.186	0
ZNF790	0.186	0
MPP2	0.186	0
TMEM203	0.186	0
MYT1	0.186	0
ZNF221	0.185	0
CSTF3	0.185	0
MPP6	0.185	0
ATP2B1-AS1	0.185	0
FLRT2	0.185	0
FERMT1	0.184	0
ZFP62	0.184	0
ZNF681	0.184	0
LPAR4	0.184	5.77E-10
E2F7	0.183	0
IFIT5	0.183	0
DTD2	0.183	0
AP1S3	0.183	0
HAGLR	0.183	0
ANGPTL4	0.182	1.76E-05
SLC35E3	0.182	0
AP5M1	0.182	0
SERPINI1	0.181	0
CNN2P3	0.181	1.46E-10
PEX5L	0.181	1.20E-09
RGR	0.181	1.78E-12

DHFR	0.181	0
LRRC4	0.181	1.23E-07
GPR37L1	0.180	0
LINC00963	0.180	0
ASB13	0.180	0
ZNF512B	0.179	0
SLC1A1	0.178	0
ST6GAL2	0.178	1.27E-14
LINC00310	0.178	3.71E-05
CLEC18B	0.178	0.018866423
C6ORF203	0.178	0
HIST2H3C	0.178	0.002012384
ZSWIM3	0.177	0
MGAT2	0.177	0
EPB41L4A	0.177	3.53E-09
TBC1D30	0.177	0
KBTBD7	0.177	0
ZIK1	0.177	0
THNSL1	0.177	0
RGCC	0.177	0
CYB5RL	0.176	0
RIPK1	0.176	0
CYP2R1	0.176	0
C2ORF68	0.176	0
TRMT61B	0.176	0
TMEM129	0.175	0
CHST14	0.175	0
AGGF1	0.175	0
STUM	0.175	4.07E-11
IQCH-AS1	0.175	0
ARL6	0.174	0
ZNF497	0.174	4.55E-14
SLC26A2	0.174	0
LINC01719	0.174	2.48E-06
FPGT	0.174	0
CTSO	0.173	0
TCTA	0.173	0
ARRDC4	0.173	0
FUT4	0.173	0
HERC6	0.173	5.58E-09
H1FX-AS1	0.172	6.17E-06
MSRB3	0.172	0
HCG18	0.172	0
CD82	0.171	0
ZFPM2	0.171	1.57E-10

RAB9B	0.171	3.79E-12
BOLA1	0.171	0
ZBED3-AS1	0.170	3.87E-14
TSSK6	0.170	8.09E-08
LINC00526	0.170	0
FIGNL1	0.170	0
ST7-AS1	0.169	0
ZNF655	0.169	0
ZNF268	0.169	0
GUCY1A2	0.169	0
ZNF501	0.169	0
PDE2A	0.169	7.09E-09
RGS17	0.169	1.03E-07
ZNF774	0.169	4.10E-11
ZNF804A	0.169	0
CDH20	0.168	0
KCTD21-AS1	0.168	1.15E-05
CERKL	0.168	0
OTUD6B-AS1	0.168	0
CORO7-PAM16	0.168	7.97E-13
SLC2A10	0.168	0
GHET1	0.168	0.000157948
HYLS1	0.168	1.67E-11
ZNF235	0.167	0
TMTC3	0.167	0
POLR3H	0.167	0
MAFG-DT	0.167	0
MEGF10	0.166	0
TMEM140	0.166	0
SOX21-AS1	0.165	0
FRRS1	0.165	7.39E-07
TRAF3IP1	0.165	0
TRIM45	0.165	0
C17ORF80	0.164	0
SHC4	0.164	0
RWDD2A	0.164	0
KLHDC8A	0.164	0
BBS10	0.164	0
PRKG1	0.163	0
ANKRD18EP	0.163	0
ALG14	0.163	0
ZNF319	0.163	0
GPR27	0.162	2.29E-09
LGR5	0.162	0
SEPT7-AS1	0.162	1.44E-09

DARS2	0.162	0
HMGN3-AS1	0.162	0.002937626
NLRX1	0.162	0
IGLV5-52	0.162	0.000484307
PIGW	0.162	0
MR1	0.162	0
ZNF780B	0.161	0
ACKR3	0.160	0
FAM208A	0.160	0
LIFR-AS1	0.160	0
KLHL14	0.160	0
BIVM	0.159	0
SUMF1	0.159	0
LINC00205	0.159	0
CPED1	0.159	5.24E-07
FHDC1	0.158	0
MRM1	0.158	0
TOB1-AS1	0.158	1.71E-09
ABCD1	0.158	0
MAP2K6	0.157	0
SLC19A3	0.157	0
FMO5	0.157	3.88E-10
ZNF107	0.156	0
IKZF2	0.156	2.49E-13
TUBD1	0.156	0
CARF	0.155	0
SNX22	0.155	0
TRIM2	0.155	0
ZNF781	0.155	3.23E-11
XK	0.155	1.82E-05
PAFAH2	0.155	0
SKIDA1	0.154	0
ZNF786	0.154	0
NR2F2	0.154	0.000233837
TIGD6	0.154	0
ZKSCAN7	0.153	0
MLH3	0.153	0
KRBA2	0.153	6.00E-15
LINC01089	0.153	0
AMMECR1	0.153	0
PAN3-AS1	0.152	2.63E-06
KDM8	0.152	0
GPR12	0.151	0
FANCL	0.151	0
ZNF79	0.151	0

DDX28	0.150	0
ZNF737	0.150	0
TMEM102	0.150	0.034825491
C2ORF16	0.149	0
BEST3	0.149	3.33E-16
FICD	0.149	0
PUS7L	0.149	0
TIGD5	0.148	0
SLC25A1P5	0.148	0.033142433
ZNF623	0.148	0
ADGRL2	0.148	1.64E-12
SOX5	0.148	0
FAM86C2P	0.148	0
DUSP19	0.148	0
ZNF599	0.147	0
NCK1-DT	0.147	1.08E-10
ZNF778	0.146	0
DCLRE1A	0.146	0
ARHGAP31	0.146	0
LPP-AS2	0.146	0.000616769
FGF14-AS2	0.145	2.64E-07
BBS12	0.145	0
TMCC1-AS1	0.145	0
ASB5	0.145	1.08E-05
PEX11A	0.145	3.35E-13
TNRC6C-AS1	0.145	0
TNR	0.145	0
LINC00467	0.145	0
WAC-AS1	0.145	0
TMEM169	0.145	0
TMEM80	0.144	0
EFCAB5	0.144	1.88E-12
EGLN3	0.144	0
GINS4	0.143	0
DISP1	0.143	0
LINC00641	0.143	0
CCDC18	0.143	0
CKMT2-AS1	0.142	0
ZNF587B	0.142	0
ZNF607	0.142	0
HOXB13	0.142	0
CHRNB2	0.142	9.55E-15
WDR31	0.142	0
POSTN	0.142	2.00E-05
TGFBR2	0.142	0

SWSAP1	0.141	1.70E-08
INKA2	0.141	0
DCC	0.141	0
CEP19	0.141	0
KIF26B	0.141	0
C17ORF100	0.141	0.000287678
CARD6	0.141	5.88E-15
ZNF606	0.140	0
BMP6	0.140	0
F8A3	0.140	2.94E-08
EFNB2	0.140	0
LYRM7	0.140	0
FAM69C	0.140	0
GUSBP1	0.140	0
OLIG1	0.140	0
ZNF253	0.139	0
TTC26	0.139	0
ERVK13-1	0.139	7.38E-13
ZNF780A	0.139	0
GSN-AS1	0.139	2.82E-05
RIPOR2	0.139	0
ZNF252P	0.138	0
CCDC121	0.138	0
TMEM255A	0.138	0
CYP26B1	0.138	0
RSPH9	0.138	6.02E-08
TMEM198B	0.137	0
TMEM26	0.137	0
ZNF611	0.136	0
TMPO-AS1	0.136	0
PPP2R2B	0.136	0
SH3TC2	0.136	7.06E-13
ZNF354C	0.136	0
PLPP6	0.135	0
CEP162	0.135	0
TPI1P2	0.135	6.25E-07
GHR	0.135	0
CADM2	0.134	0
FADD	0.134	0
MAGI2	0.133	0
OBSL1	0.133	0
HOMEZ	0.132	0
ZNF660	0.132	0
CPLANE2	0.131	0
EID2	0.131	0

SCN1A	0.131	0
SCUBE3	0.130	0
KRT8P12	0.130	0
SLC40A1	0.129	0
FAM217B	0.129	0
UNC80	0.129	0
LUZP2	0.128	0
ZKSCAN2	0.127	0
WDR92	0.127	0
DOK3	0.127	1.97E-09
FAM78A	0.127	0
SVIL	0.127	0
DCX	0.126	0
CYREN	0.126	0
PCDH18	0.126	0
PAQR8	0.125	0
ADAMTS12	0.125	0
GVQW3	0.125	0
LINC01301	0.124	2.26E-05
CCNE2	0.124	0
SATB2-AS1	0.123	8.83E-08
ZNF573	0.123	0
XRCC2	0.123	0
SULF2	0.123	1.11E-15
ZNF813	0.123	0
KITLG	0.122	7.00E-10
C22ORF46	0.122	0
GEN1	0.122	0
ZNF41	0.122	0
LINC00863	0.121	0
ETNPPL	0.121	2.59E-05
HIST2H4B	0.121	0
ZNF181	0.121	0
TSHR	0.120	0
SP2-AS1	0.119	5.50E-08
MASP2	0.119	0.037137376
LDLRAD4	0.118	0
ADGRD1	0.118	0
PDE3B	0.117	0
ZNF382	0.116	0
FAM173B	0.116	0
NOG	0.115	0
C2ORF81	0.115	0
ZNF225	0.115	0
RTN4IP1	0.115	0

COL2A1	0.115	0
SYT12	0.115	0.000851378
THBS1	0.114	0
C14ORF132	0.114	0
ZKSCAN3	0.113	0
DUXAP8	0.113	0
TMEM150C	0.113	0
KAT14	0.112	0
ZFP41	0.112	0
ZNF189	0.112	0
C21ORF58	0.112	0
NAT1	0.111	0
CHN2	0.111	0
CNTN5	0.111	1.37E-09
CFAP44	0.111	0
PYCR3	0.111	0
RNF170	0.110	0
ZNF436-AS1	0.110	0
ZNF629	0.110	0
VWA1	0.109	0
ZNF124	0.109	0
NBPF3	0.109	0
C12ORF60	0.108	0
ZNF239	0.107	0
FIBIN	0.107	0
ZBTB9	0.106	0
SEC14L5	0.106	0
ZNF837	0.106	4.44E-16
ABAT	0.104	0
WNT5A	0.104	6.00E-15
FBXO48	0.103	3.66E-11
FGD3	0.103	1.14E-10
KY	0.102	0
NDP	0.102	0
SENP8	0.102	0
CPT2	0.102	0
GXYLT1P4	0.102	1.12E-10
ROBO2	0.101	0
ITGA9	0.101	0
NKX3-1	0.101	7.11E-15
BDNF-AS	0.100	4.77E-09
ZNF572	0.099	0
SOX21	0.099	0
CLBA1	0.098	0
CHTF8	0.097	0

IPCEF1	0.096	0
EHHADH	0.096	0
CA2	0.096	3.02E-08
ARHGEF37	0.095	0
PPFIA4	0.095	1.94E-08
RGS8	0.095	7.58E-09
NUTM2D	0.095	0.018702328
SCN3A	0.095	0
FRAT1	0.094	0
ZNF546	0.094	0
CALCRL	0.092	0
AKAP7	0.092	0
TTC30A	0.092	0
GPR37	0.092	0
FAM86C1	0.092	0
INTS5	0.091	0
TTPAL	0.091	0
SMOC1	0.091	0
TTPA	0.091	1.27E-10
UBAC2-AS1	0.091	2.22E-16
ATP10B	0.091	0
ZNF347	0.090	0
GXYLT1P6	0.089	0
SAMD9	0.088	0
REP15	0.087	2.35E-14
RNF224	0.087	0.003963414
LNP1	0.087	0
GRIN1	0.087	0
F5	0.087	0
COL9A1	0.087	0
ZC3H4	0.086	0
ZNF236-DT	0.086	1.05E-05
LINC02473	0.086	0
NCOA5	0.086	0
PUDP	0.086	0
RBMS3-AS3	0.084	8.78E-07
PYGM	0.084	7.48E-13
JAKMIP1	0.083	8.22E-15
TTC30B	0.083	0
LINC00654	0.083	2.34E-08
LINC01410	0.082	4.06E-06
BRINP2	0.082	5.62E-06
ZNF37A	0.082	0
PPP1R12A-AS1	0.081	6.26E-12
EXOC3-AS1	0.081	0

SLC9A3	0.079	0
PPP1R10	0.079	0
OSTN	0.079	8.91E-11
PNMA8C	0.079	0
CCDC71	0.078	0
GALNT3	0.078	0
ZNF287	0.078	0
SLC26A4	0.075	0
DUX4L50	0.075	0
INHA	0.075	1.01E-11
CLEC18A	0.075	0
DPY19L2P2	0.075	0
POP1	0.074	0
ZNF879	0.074	0
GDPGP1	0.074	0
SLX1B	0.073	5.21E-08
ZNF75A	0.072	0
PPP1R3G	0.072	1.45E-09
DOLK	0.071	0
STEAP1	0.070	0.003637332
MBLAC2	0.070	0
ELAC1	0.069	0
SOWAHA	0.068	7.05E-11
LINC01521	0.067	0
PDGFD	0.067	0
ZNF658	0.066	0
MOCS3	0.065	0
TMEM147-AS1	0.065	0
PSKH1	0.065	0
PARS2	0.064	0
ZBED8	0.064	0
CYSRT1	0.064	1.05E-08
C1ORF74	0.064	0
LINC01963	0.063	0
ZNF658B	0.062	4.44E-11
SOX2-OT	0.062	0
FAM200A	0.060	0
TMEM177	0.059	0
LINC00235	0.059	1.08E-12
EBF3	0.058	0
CENPBD1	0.058	0
HPS6	0.057	0
ZNF37BP	0.056	0
DHFR2	0.056	0
KRCC1	0.056	0

HOXD8	0.053	2.22E-16
ZNF429	0.053	0
THAP7-AS1	0.053	4.62E-12
NTSR1	0.052	0
LINC01828	0.052	0
PRMT6	0.051	0
KCNK2	0.051	0
RHPN1-AS1	0.051	0
ZFP3	0.051	0
FLRT3	0.050	0
CCDC13-AS1	0.049	9.86E-09
CTBP1-DT	0.049	0
DDX11L2	0.049	1.25E-12
CXXC4	0.048	6.55E-11
FAM111B	0.047	0
PNMA8B	0.046	0
SAMMSON	0.045	0
MGP	0.045	0
PROM1	0.043	0
JCAD	0.042	0
CCDC39	0.042	7.23E-14
GPR17	0.042	0
B3GALT6	0.041	0
ZNF488	0.041	0
MIR210HG	0.041	1.62E-12
ZNF302	0.040	0
DNAH11	0.040	0
PSMG3-AS1	0.039	0
LINC00680	0.038	0
LINC00909	0.036	0
IPO5P1	0.036	0
BCDIN3D	0.035	0
LCMT2	0.035	0
TRIL	0.034	0
B3GNT10	0.034	0
ABHD15	0.030	0
EGR1	0.029	0
PDE7B	0.029	0
ATP6V0E2-AS1	0.025	0
PDE4C	0.025	0
APLN	0.024	0
HAPLN1	0.023	0
PCDH20	0.022	0
ESPN	0.020	1.55E-15
SLC16A3	0.020	0

DUSP6	0.019	0
MYLK4	0.019	0
MAP10	0.018	0
FAM86JP	0.018	0
STC1	0.016	0
PRSS35	0.013	0

Table S3. Changes in organic acids, acylcarnitines and amino acids upon SN treatment of GSC TS543 and mouse astrocytes. (* significant change)

	GSC TS543		Mouse astrocytes	
Organic acids	**Fold change (SN/DMSO)**	**p-value**	**Fold change (SN/DMSO)**	**p-value**
Citrate	*0.63	3.7E-03	0.73	2.4E-01
Lactate	*2.08	1.9E-02	0.60	8.5E-02
alpha-KG	*1.89	6.4E-03	NA	NA
Fumarate	1.11	2.2E-01	1.55	6.0E-02
Pyruvate	0.92	4.4E-01	1.00	9.9E-01
Succinate	1.07	6.4E-01	NA	NA

	GSC TS543		Mouse astrocytes	
Acylcarnitines	**Fold change (SN/DMSO)**	**p-value**	**Fold change (SN/DMSO)**	**p-value**
C2	*0.66	2.80E-02	0.88	5.10E-01
C3	*0.2	1.50E-03	0.37	5.30E-02
C5:1	*0.58	8.90E-03	NA	NA
C5	*0.13	2.80E-04	0.42	5.80E-02
C4-OH	0.87	5.90E-01	1.45	1.80E-01
C5-OH/C3-DC	*0.4	2.40E-03	*0.49	2.90E-02
C4-DC,C6-OH	0.66	1.40E-01	0.87	5.90E-01
C5-DC	1.24	1.80E-01	1.18	1.10E-01
C8:1-OH/C6:1-DC	0.84	3.80E-01	1.05	7.60E-01
C8-OH/C6-DC	0.78	2.30E-01	1.12	4.40E-01
C8-DC	*0.45	4.30E-02	*1.5	2.50E-02
C12:1	2.05	5.50E-02	NA	NA
C12	*2.16	4.20E-03	NA	NA
C12:1-OH	0.6	1.50E-01	1.36	1.20E-01
C12-OH/C10-DC	*0.39	8.90E-03	*2.28	2.10E-02
C14:1	1.49	1.50E-01	*2.08	2.10E-02
C14	*6.62	1.80E-03	*2.2	2.70E-03
C14:3-OH/C12:3-DC	2.89	5.20E-02	NA	NA
C14:1-OH	0.77	3.00E-01	2.06	7.20E-02
C14-OH/C12-DC	*0.34	1.90E-03	*3.11	8.60E-04
C16:2	0.81	3.30E-01	*3.03	3.00E-02
C16:1	*7.21	3.30E-02	*2.65	6.40E-03
C16	*12.73	2.80E-03	*2.39	4.20E-03
C16:2-OH	1.16	6.50E-01	NA	NA
C16:1-OH/C14:1-DC	1	9.90E-01	*2.97	1.40E-02
C16-OH	0.8	5.70E-02	*2.56	2.30E-03
C18:2	2.6	1.10E-01	*2.41	3.60E-02
C18:1	*20.16	3.00E-02	*2.13	2.30E-02
C18	*13.35	5.40E-03	NA	NA
C18:3-OH/C16:3-DC	0.93	7.20E-01	NA	NA
C18:2-OH/C16:2-DC	0.76	2.10E-01	*2.37	3.40E-02
C18:1-OH/C16:1-DC	*1.94	4.70E-02	*3.27	2.00E-02
C18-OH/C16-DC	0.95	3.30E-01	*2.14	1.90E-02
C20:3	0.66	1.80E-01	NA	NA

	GSC TS543		Mouse astrocytes	
Amino acids	**Fold change (SN/DMSO)**	**p value**	**Fold change (SN/DMSO)**	**p value**
Val	*1.55	7.2E-03	1.01	9.5E-01
Leu	*1.64	3.0E-03	1.01	9.6E-01
Ile	*1.74	1.1E-03	1.04	6.7E-01
Met	*1.31	1.1E-03	0.99	9.6E-01
His	*1.61	1.8E-03	0.98	8.5E-01
Phe	*1.50	7.2E-03	1.00	9.9E-01
Arg	*1.76	3.5E-03	0.82	1.7E-01
Glu	*1.20	9.6E-03	*1.21	1.0E-02
Trp	*1.51	2.1E-02	0.98	9.3E-01
Tyr	*1.53	6.0E-03	1.06	5.8E-01
Gly	*0.87	4.5E-03	1.10	1.7E-01
Ala	*0.61	2.0E-02	0.97	7.2E-01
Ser	0.96	6.6E-01	1.20	5.2E-02
Pro	1.01	9.1E-01	*1.62	2.0E-03
Cit	0.71	2.9E-01	1.06	6.3E-01
Asp	*0.33	1.1E-04	0.88	1.2E-01

Table S4. List of primers used in this study.

Genes	Forward/ Reverse	Primer Sequences (5'to 3')
HSP70	F	ATGTCGGTGGTGGGCATAGA
	R	CACAGCGACGTAGCAGCTCT
TBP	F	CGGTTTGCTGCGGTAATCAT
	R	TTTCTTGCTGCCAGTCTGGAC
LDLR	F	AAGTTCAAGTGTCACAGCGG
	R	CCGCACTCTTTGATGGGTTC
ACSS2	F	CGGGAATTCTGGGGAGACAT
	R	GCAGATGTTGGTAGTTGCTCC
HMGCS1	F	GGAACAGAGACAATCATCGACA
	R	GGAACAGAGACAATCATCGACA
HMGCR	F	AGTGACACTGACCATCTGCA
	R	AGGATGGCTATGCATCGTGT
MVK	F	AAGTGGACCTCAGCTTACCC
	R	TCTCCACTTGCTCTGAGGTG
MVD	F	CGATGAAGAGCTGGTTCTGC
	R	TCGGTGAAGTCCTTGCTGAT
DHCR7	F	CCCAACATTCCCAAAGCCAA
	R	CTCGCCAGTGAAAACCAGTC
DHCR24	F	CCGCTCTCGCTTATCTTCGA
	R	TCTTGCTACCCTGCTCCTTC
SQLE	F	TCATCACTTTGGCCAACAGG
	R	TATCCGAGAAGAGGGCGAAC
PDGFRA	F	TTT TTG TGA CGG TCT TGG AAG T
	R	TGT CTG AGT GTG GTT GTA ATA GC
SOX10	F	AGT ACC CGC ACC TGC ACA
	R	GAA GGG GCG CTT GTC ACT
NEU4	F	CCT TCA CGG ACA GTG CTC TT
	R	CTC CAC AAA GGC CAG CAG

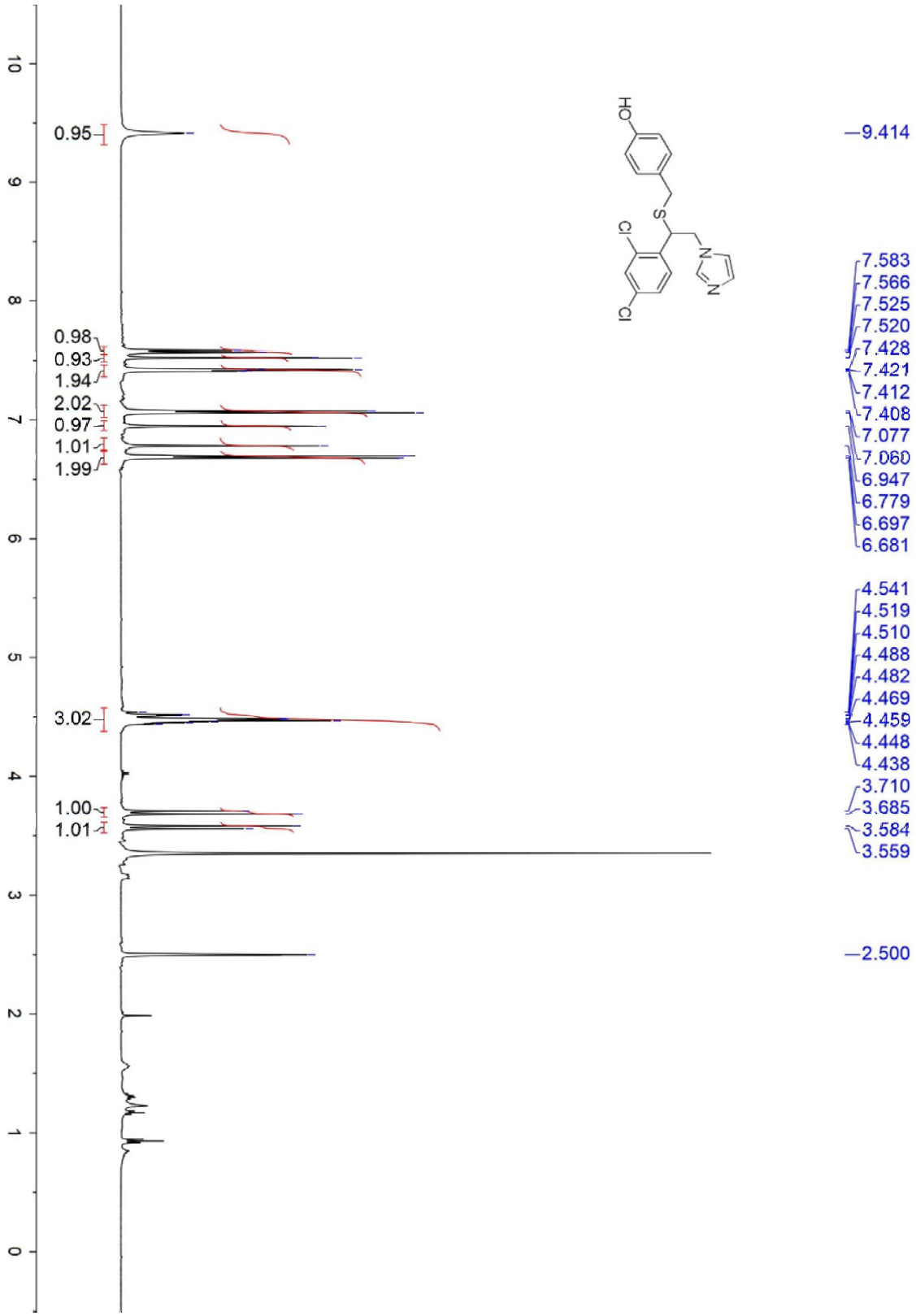

Data S1. ^{1}H NMR Spectrum of 7.

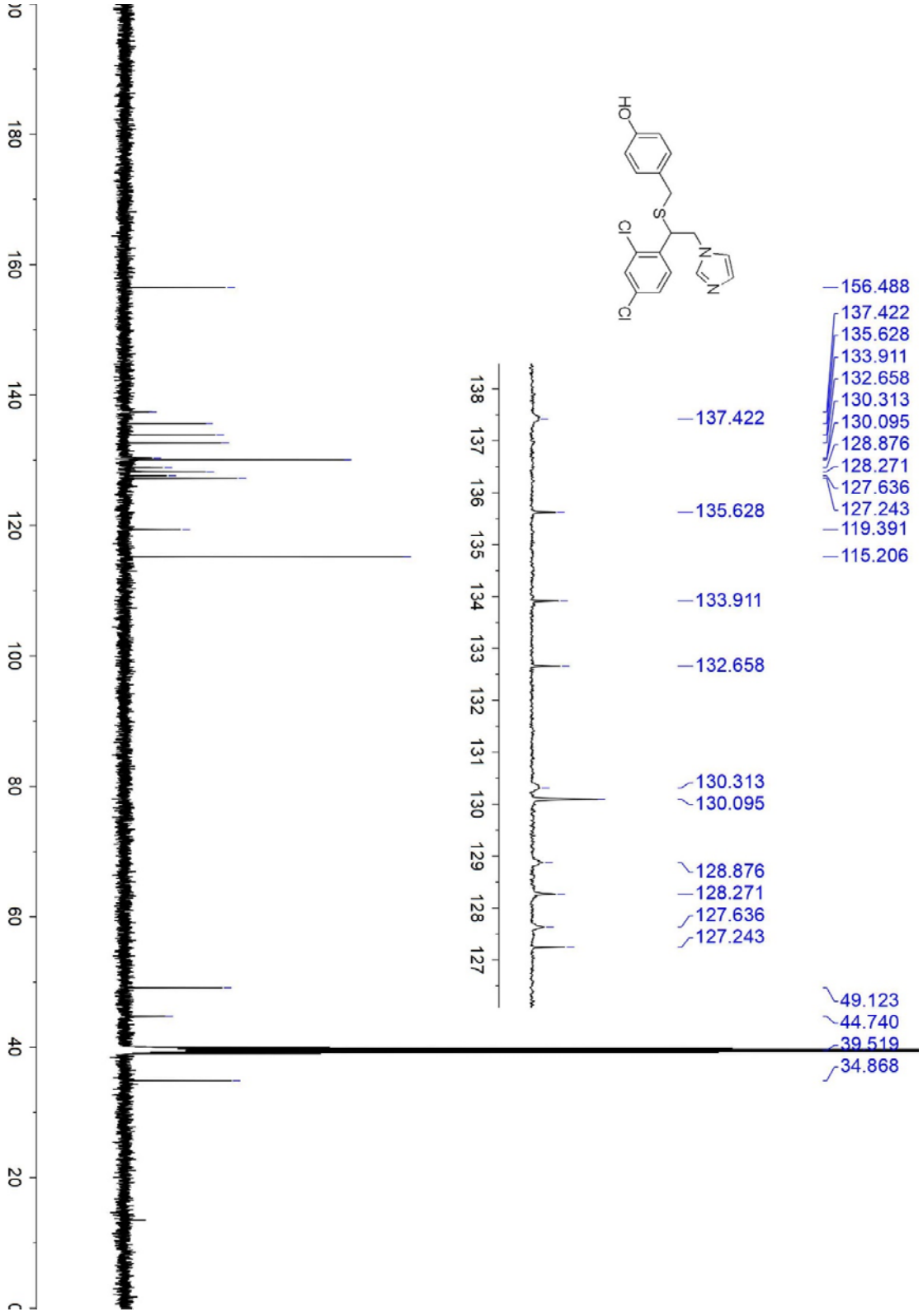

Data S2. ^{13}C NMR Spectrum of 7.

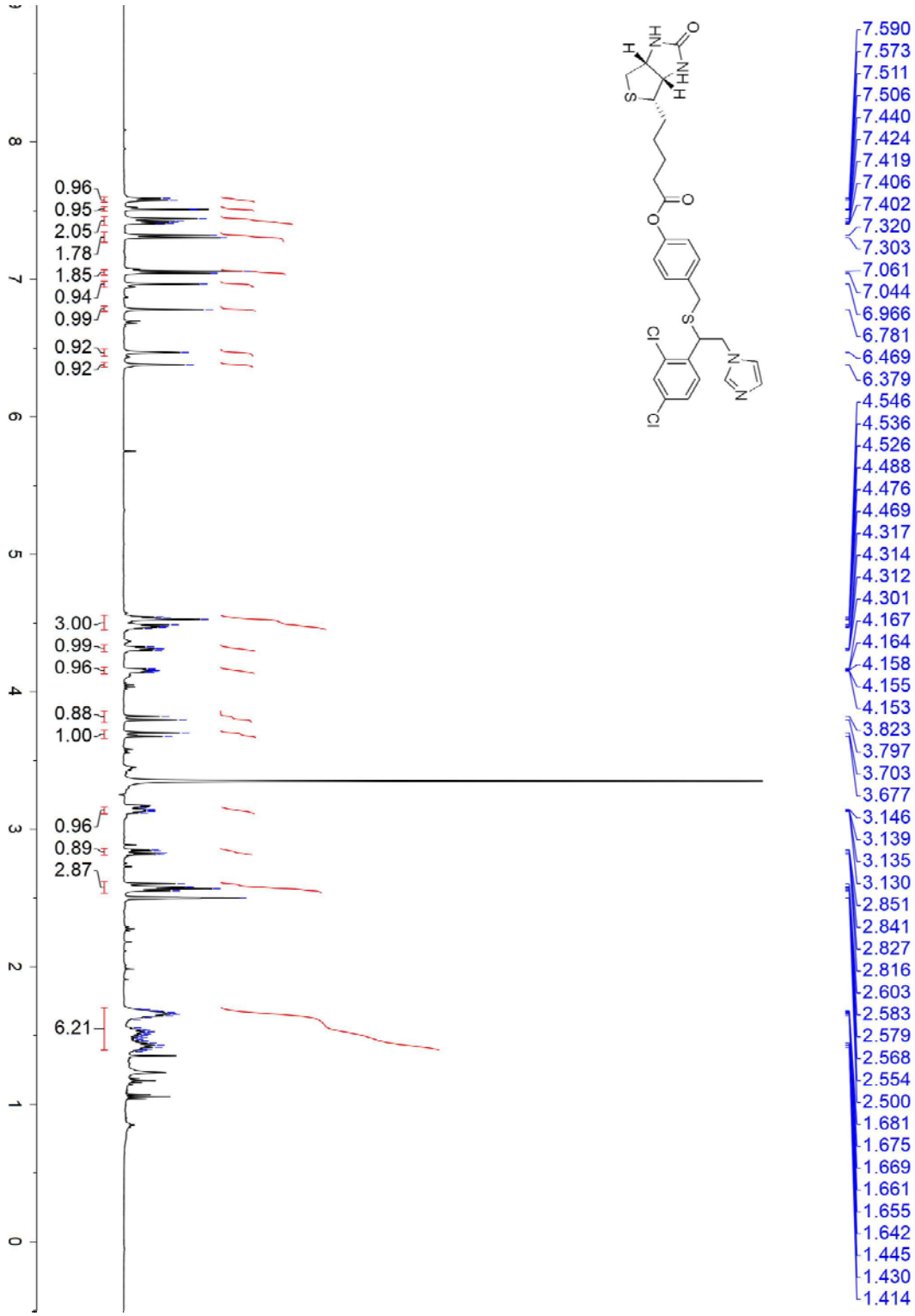

Data S3. ^{1}H NMR Spectrum of 8.

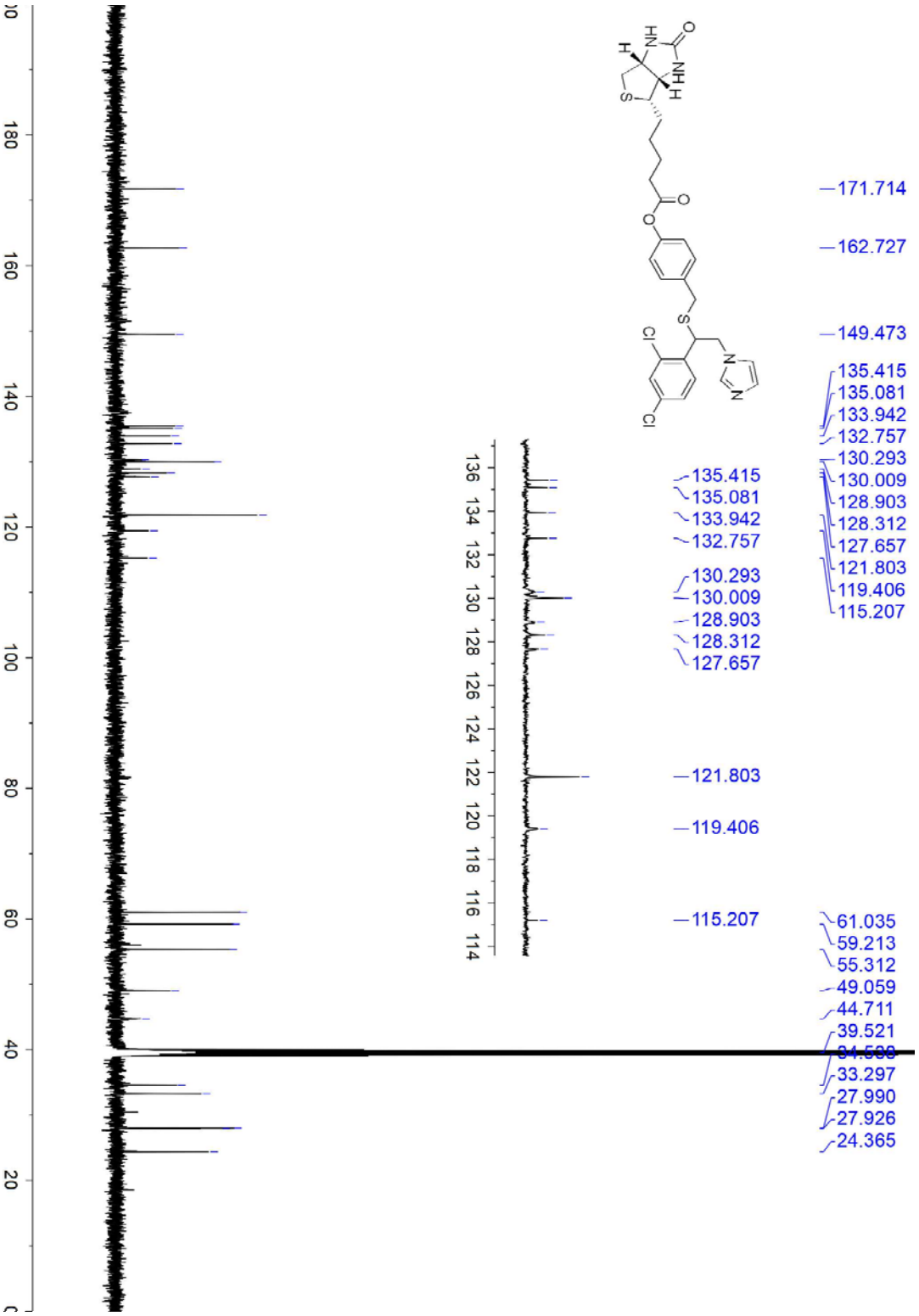

Data S4. ^{13}C NMR Spectrum of 8.

REFERENCES AND NOTES

1. B. L. Hu, Q. Wang, Y. A. Wang, S. Hua, C.-E. G. Sauvé, D. Ong, Z. D. Lan, Q. Chang, Y. W. Ho, M. M. Monasterio, X. Lu, Y. Zhong, J. Zhang, P. Deng, Z. Tan, G. Wang, W.-T. Liao, L. J. Corley, H. Yan, J. Zhang, Y. You, N. Liu, L. Cai, G. Finocchiaro, J. J. Phillips, M. S. Berger, D. J. Spring, J. Hu, E. P. Sulman, G. N. Fuller, L. Chin, R. G. W. Verhaak, R. A. De Pinho, Epigenetic activation of WNT5A drives glioblastoma stem cell differentiation and invasive growth. *Cell* **167**, 1281−1295.e18 (2016).

2. D. S. T. Ong, B. Hu, Y. W. Ho, C. E. G. Sauvé, C. A. Bristow, Q. Wang, A. S. Multani, P. Chen, L. Nezi, S. Jiang, C. E. Gorman, M. M. Monasterio, D. Koul, M. Marchesini, S. Colla, E. J. Jin, E. P. Sulman, D. J. Spring, W. K. A. Yung, R. G. W. Verhaak, L. Chin, Y. A. Wang, R. A. DePinho, PAF promotes stemness and radioresistance of glioma stem cells. *Proc. Natl. Acad. Sci. U.S.A.* **114**, E9086–E9095 (2017).

3. J. Chen, Y. Li, T.-S. Yu, R. M. McKay, D. K. Burns, S. G. Kernie, L. F. Parada, A restricted cell population propagates glioblastoma growth after chemotherapy. *Nature* **488**, 522−526 (2012).

4. S. D. Bao, Q. Wu, R. E. Mc Lendon, Y. Hao, Q. Shi, A. B. Hjelmeland, M. W. Dewhirst, D. D. Bigner, J. N. Rich, Glioma stem cells promote radioresistance by preferential activation of the DNA damage response. *Nature* **444**, 756–760 (2006).

5. J. Bi, S. Chowdhry, S. Wu, W. Zhang, K. Masui, P. S. Mischel, Altered cellular metabolism in gliomas—An emerging landscape of actionable co-dependency targets. *Nat. Rev. Cancer* **20**, 57–70 (2020).

6. A. Leon-Del-Rio, Biotin in metabolism, gene expression, and human disease. *J. Inherit. Metab. Dis.* **42**, 647–654 (2019).

7. A. Hernández-Vázquez, B. Wolf, K. Pindolia, D Ortega-Cuellar, R Hernández-González, A Heredia-Antúnez, I Ibarra-González, A Velázquez-Arellano, Biotinidase knockout mice show cellular energy deficit and altered carbon metabolism gene expression similar to that of nutritional biotin deprivation: Clues for the pathogenesis in the human inherited disorder. *Mol. Genet. Metab.* **110**, 248–254 (2013).

8. E. Ochoa-Ruiz, R. Díaz-Ruiz, A. . J. Hernández-Vázquez, I. Ibarra-González, A. Ortiz-Plata, D. Rembao, D. Ortega-Cuéllar, B. Viollet, S. Uribe-Carvajal, J. A. Corella, A. Velázquez-Arellano, Biotin deprivation impairs mitochondrial structure and function and has implications for inherited metabolic disorders. *Mol. Genet. Metab.* **116**, 204–214 (2015).

9. L. Tong, Structure and function of biotin-dependent carboxylases. *Cell. Mol. Life Sci.* **70**, 863–891 (2013).

10. J. Hymes, B. Wolf, Biotinidase and its roles in biotin metabolism. *Clin. Chim. Acta* **255**, 1–11 (1996).

11. N. Kothapalli, J. Zempleni, Biotinylation of histones depends on the cell cycle in NCI-H69 small cell lung cancer cells. *Faseb J.* **19**, A55 (2005).

12. Y. I. Hassan, J. Zempleni, Epigenetic regulation of chromatin structure and gene function by biotin. *J. Nutr.* **136**, 1763–1765 (2006).

13. M. A. Narang, R. Dumas, L. M. Ayer, R. A. Gravel, Reduced histone biotinylation in multiple carboxylase deficiency patients: A nuclear role for holocarboxylase synthetase. *Hum. Mol. Genet.* **13**, 15–23 (2004).

14. G. Russell-Jones, K. McTavish, J. McEwan, J. Rice, D. Nowotnik, Vitamin-mediated targeting as a potential mechanism to increase drug uptake by tumours. *J. Inorg. Biochem.* **98**, 1625–1633 (2004).

15. S. Chen, X. Zhao, J. Chen, J. Chen, L. Kuznetsova, S. S. Wong, I. Ojima, Mechanism-based tumor-targeting drug delivery system. Validation of efficient vitamin receptor-mediated endocytosis and drug release. *Bioconjug. Chem.* **21**, 979–987 (2010).

16. C. W. Brennan, R. G. W. Verhaak, A. McKenna, B. Campos, H. Noushmehr, S. R. Salama, S. Zheng, D. Chakravarty, J. Z. Sanborn, S. H. Berman, R. Beroukhim, B. Bernard, C. J. Wu, G. Genovese, I. Shmulevich, J. Barnholtz-Sloan, L. Zou, R. Vegesna, S. A. Shukla, G. Ciriello, W. K. Yung, W. Zhang, C. Sougnez, T. Mikkelsen, K. Aldape, D. D. Bigner, E. G. van Meir, M. Prados, A. Sloan, K. L. Black, J. Eschbacher, G. Finocchiaro, W. Friedman, D. W. Andrews, A. Guha, M. Iacocca, B. P. O'Neill, G. Foltz, J. Myers, D. J. Weisenberger, R. Penny, R. Kucherlapati, C. M. Perou, D. N. Hayes, R. Gibbs, M. Marra, G. B. Mills, E. Lander, P. Spellman, R. Wilson, C. Sander,

J. Weinstein, M. Meyerson, S. Gabriel, P. W. Laird, D. Haussler, G. Getz, L. Chin, C. Benz, J. Barnholtz-Sloan, W. Barrett, Q. Ostrom, Y. Wolinsky, K. L. Black, B. Bose, P. T. Boulos, M. Boulos, J. Brown, C. Czerinski, M. Eppley, M. Iacocca, T. Kempista, T. Kitko, Y. Koyfman, B. Rabeno, P. Rastogi, M. Sugarman, P. Swanson, K. Yalamanchii, I. P. Otey, Y. S. Liu, Y. Xiao, J. T. Auman, P. C. Chen, A. Hadjipanayis, E. Lee, S. Lee, P. J. Park, J. Seidman, L. Yang, R. Kucherlapati, S. Kalkanis, T. Mikkelsen, L. M. Poisson, A. Raghunathan, L. Scarpace, B. Bernard, R. Bressler, A. Eakin, L. Iype, R. B. Kreisberg, K. Leinonen, S. Reynolds, H. Rovira, V. Thorsson, I. Shmulevich, M. J. Annala, R. Penny, J. Paulauskis, E. Curley, M. Hatfield, D. Mallery, S. Morris, T. Shelton, C. Shelton, M. Sherman, P. Yena, L. Cuppini, F. DiMeco, M. Eoli, G. Finocchiaro, E. Maderna, B. Pollo, M. Saini, S. Balu, K. A. Hoadley, L. Li, C. R. Miller, Y. Shi, M. D. Topal, J. Wu, G. Dunn, C. Giannini, B. P. O'Neill, B. A. Aksoy, Y. Antipin, L. Borsu, S. H. Berman, C. W. Brennan, E. Cerami, D. Chakravarty, G. Ciriello, J. Gao, B. Gross, A. Jacobsen, M. Ladanyi, A. Lash, Y. Liang, B. Reva, C. Sander, N. Schultz, R. Shen, N. D. Socci, A. Viale, M. L. Ferguson, Q. R. Chen, J. A. Demchok, L. A. L. Dillon, K. R. M. Shaw, M. Sheth, R. Tarnuzzer, Z. Wang, L. Yang, T. Davidsen, M. S. Guyer, B. A. Ozenberger, H. J. Sofia, J. Bergsten, J. Eckman, J. Harr, J. Myers, C. Smith, K. Tucker, C. Winemiller, L. A. Zach, J. Y. Ljubimova, G. Eley, B. Ayala, M. A. Jensen, A. Kahn, T. D. Pihl, D. A. Pot, Y. Wan, J. Eschbacher, G. Foltz, N. Hansen, P. Hothi, B. Lin, N. Shah, J. G. Yoon, C. Lau, M. Berens, K. Ardlie, R. Beroukhim, S. L. Carter, A. D. Cherniack, M. Noble, J. Cho, K. Cibulskis, D. DiCara, S. Frazer, S. B. Gabriel, N. Gehlenborg, J. Gentry, D. Heiman, J. Kim, R. Jing, E. S. Lander, M. Lawrence, P. Lin, W. Mallard, M. Meyerson, R. C. Onofrio, G. Saksena, S. Schumacher, C. Sougnez, P. Stojanov, B. Tabak, D. Voet, H. Zhang, L. Zou, G. Getz, N. N. Dees, L. Ding, L. L. Fulton, R. S. Fulton, K. L. Kanchi, E. R. Mardis, R. K. Wilson, S. B. Baylin, D. W. Andrews, L. Harshyne, M. L. Cohen, K. Devine, A. E. Sloan, S. R. VandenBerg, M. S. Berger, M. Prados, D. Carlin, B. Craft, K. Ellrott, M. Goldman, T. Goldstein, M. Grifford, D. Haussler, S. Ma, S. Ng, S. R. Salama, J. Z. Sanborn, J. Stuart, T. Swatloski, P. Waltman, J. Zhu, R. Foss, B. Frentzen, W. Friedman, R. McTiernan, A. Yachnis, D. N. Hayes, C. M. Perou, S. Zheng, R. Vegesna, Y. Mao, R. Akbani, K. Aldape, O. Bogler, G. N. Fuller, W. Liu, Y. Liu, Y. Lu, G. Mills, A. Protopopov, X. Ren, Y. Sun, C. J. Wu, W. K. A. Yung, W. Zhang, J. Zhang, K. Chen, J. N. Weinstein, L. Chin, R. G. W. Verhaak, H. Noushmehr, D. J. Weisenberger, M. S. Bootwalla, P. H. Lai, T. J. Triche Jr, D. J. van den Berg, P. W. Laird, D. H. Gutmann, N. L. Lehman,

E. G. VanMeir, D. Brat, J. J. Olson, G. M. Mastrogianakis, N. S. Devi, Z. Zhang, D. Bigner, E. Lipp, R. McLendon, The somatic genomic landscape of glioblastoma. *Cell* **155**, 462–477 (2013).

17. R. G. W. Verhaak, K. A. Hoadley, E. Purdom, V. Wang, Y. Qi, M. D. Wilkerson, C. R. Miller, L. Ding, T. Golub, J. P. Mesirov, G. Alexe, M. Lawrence, M. O'Kelly, P. Tamayo, B. A. Weir, S. Gabriel, W. Winckler, S. Gupta, L. Jakkula, H. S. Feiler, J. Graeme Hodgson, C. D. James, J. N. Sarkaria, C. Brennan, A. Kahn, P. T. Spellman, R. K. Wilson, T. P. Speed, J. W. Gray, M. Meyerson, G. Getz, C. M. Perou, D. N. Hayes, Integrated genomic analysis identifies clinically relevant subtypes of glioblastoma characterized by abnormalities in PDGFRA, IDH1, EGFR, and NF1. *Cancer Cell* **17**, 98–110 (2010).

18. S. Mazzoleni, L. S. Politi, M. Pala, M. Cominelli, A. Franzin, L. Sergi Sergi, A. Falini, M. de Palma, A. Bulfone, P. L. Poliani, R. Galli, Epidermal growth factor receptor expression identifies functionally and molecularly distinct tumor-initiating cells in human glioblastoma multiforme and is required for gliomagenesis. *Cancer Res.* **70**, 7500–7513 (2010).

19. J. Lamb, E. D. Crawford, D. Peck, J. W. Modell, I. C. Blat, M. J. Wrobel, J. Lerner, J. P. Brunet, A. Subramanian, K. N. Ross, M. Reich, H. Hieronymus, G. Wei, S. A. Armstrong, S. J. Haggarty, P. A. Clemons, R. Wei, S. A. Carr, E. S. Lander, T. R. Golub, The connectivity map: Using gene-expression signatures to connect small molecules, genes, and disease. *Science* **313**, 1929–1935 (2006).

20. R. A. Fromtling, Overview of medically important antifungal azole derivatives. *Clin. Microbiol. Rev.* **1**, 187–217 (1988).

21. G. I. Lepesheva, L. Friggeri, M. R. Waterman, CYP51 as drug targets for fungi and protozoan parasites: Past, present and future. *Parasitology* **145**, 1820–1836 (2018).

22. F. Ahmad, Q. Sun, D. Patel, J. M. Stommel, Cholesterol metabolism: A potential therapeutic target in glioblastoma. *Cancer* **11**, 146 (2019).

23. G. R. Villa, J. J. Hulce, C. Zanca, J. Bi, S. Ikegami, G. L. Cahill, Y. Gu, K. M. Lum, K. Masui, H. Yang, X. Rong, C. Hong, K. M. Turner, F. Liu, G. C. Hon, D. Jenkins, M. Martini, A. M. Armando, O. Quehenberger, T. F. Cloughesy, F. B. Furnari, W. K. Cavenee, P. Tontonoz, T. C. Gahman, A. K.

Shiau, B. F. Cravatt, P. S. Mischel, An LXR-cholesterol axis creates a metabolic co-dependency for brain cancers. *Cancer Cell* **30**, 683–693 (2016).

24. B. J. Burri, L. Sweetman, W. L. Nyhan, Heterogeneity of holocarboxylase synthetase in patients with biotin-responsive multiple carboxylase deficiency. *Am. J. Hum. Genet.* **37**, 326–337 (1985).

25. A. Hernández-Vázquez, E. Ochoa-Ruiz, I. Ibarra-González, D. Ortega-Cuellar, A. Salvador-Adriano, A. Velázquez-Arellano, Temporal development of genetic and metabolic effects of biotin deprivation. A search for the optimum time to study a vitamin deficiency. *Mol. Genet. Metab.* **107**, 345–351 (2012).

26. D. M. Mock, Biotin: From nutrition to therapeutics. *J. Nutr.* **147**, 1487–1492 (2017).

27. C.-W. Kim, C. Addy, J. Kusunoki, N. N. Anderson, S. Deja, X. Fu, S. C. Burgess, C. Li, M. Ruddy, M. Chakravarthy, S. Previs, S. Milstein, K. Fitzgerald, D. E. Kelley, J. D. Horton, Acetyl CoA carboxylase inhibition reduces hepatic steatosis but elevates plasma triglycerides in mice and humans: A bedside to bench investigation. *Cell Metab.* **26**, 394−406.e6 (2017).

28. Y. Shi, S. K. Lim, Q. Liang, S. V. Iyer, H.-Y. Wang, Z. Wang, X. Xie, D. Sun, Y.-J. Chen, V. Tabar, P. Gutin, N. Williams, J. K. De Brabander, L. F. Parada, Gboxin is an oxidative phosphorylation inhibitor that targets glioblastoma. *Nature* **567**, 341−346 (2019).

29. B. Dasgupta, R. R. Chhipa, Evolving lessons on the complex role of AMPK in normal physiology and cancer. *Trends Pharmacol. Sci.* **37**, 192–206 (2016).

30. F. Tang, Z. Yang, Y. Tan, Y. Li, Super-enhancer function and its application in cancer targeted therapy. *npj Precis. Oncol.* **4**, 2 (2020).

31. S. Darmanis, S. A. Sloan, D. Croote, M. Mignardi, S. Chernikova, P. Samghababi, Y. Zhang, N. Neff, M. Kowarsky, C. Caneda, G. Li, S. D. Chang, I. D. Connolly, Y. Li, B. A. Barres, M. H. Gephart, S. R. Quake, Single-cell RNA-Seq analysis of infiltrating neoplastic cells at the migrating front of human glioblastoma. *Cell Rep.* **21**, 1399–1410 (2017).

32. S. F. Suchy, B. Wolf, Effect of biotin deficiency and supplementation on lipid metabolsim in rats: Cholesterol and lipoproteins. *Am. J. Clin. Nutr.* **43**, 831–838 (1986).

33. I. Marin-Valencia, C. Yang, T. Mashimo, S. Cho, H. Baek, X.-L. Yang, K. N. Rajagopalan, M. Maddie, V. Vemireddy, Z. Zhao, L. Cai, L. Good, B. P. Tu, K. J. Hatanpaa, B. E. Mickey, J. M. Matés, J. M. Pascual, E. A. Maher, C. R. Malloy, R. J. DeBerardinis, R. M. Bachoo, Analysis of tumor metabolism reveals mitochondrial glucose oxidation in genetically diverse human glioblastomas in the mouse brain in vivo. *Cell Metab.* **15**, 827–837 (2012).

34. J. E. C. Jones, W. P. Esler, R. Patel, A. Lanba, N. B. Vera, J. A. Pfefferkorn, C. Vernochet, Inhibition of acetyl-CoA carboxylase 1 (ACC1) and 2 (ACC2) reduces proliferation and de novo lipogenesis of EGFRvIII human glioblastoma cells. *PLOS ONE* **12**, e0169566 (2017).

35. F. Röhrig, A. Schulze, The multifaceted roles of fatty acid synthesis in cancer. *Nat. Rev. Cancer* **16**, 732–749 (2016).

36. M. Murakami, Y. Ushio, Y. Mihara, J.-I. Kuratsu, S. Horiuchi, Y. Morino, Cholesterol uptake by human glioma cells via receptor-mediated endocytosis of low-density lipoprotein. *J. Neurosurg.* **73**, 760–767 (1990).

37. E. M. Smith, J. T. Hoi, J. C. Eissenberg, J. D. Shoemaker, W. S. Neckameyer, A. M. Ilvarsonn, L. G. Harshman, V. L. Schlegel, J. Zempleni, Feeding *Drosophila* a biotin-deficient diet for multiple generations increases stress resistance and lifespan and alters gene expression and histone Biotinylation patterns. *J. Nutr.* **137**, 2006–2012 (2007).

38. S. Nagaraja, N. A. Vitanza, P. J. Woo, K. R. Taylor, F. Liu, L. Zhang, M. Li, W. Meng, A. Ponnuswami, W. Sun, J. Ma, E. Hulleman, T. Swigut, J. Wysocka, Y. Tang, M. Monje, Transcriptional dependencies in diffuse intrinsic pontine glioma. *Cancer Cell* **31**, 635−652.e6 (2017).

39. R. C. Gimple, R. L. Kidwell, L. J. Y. Kim, T. Sun, A. D. Gromovsky, Q. Wu, M. Wolf, D. Lv, S. Bhargava, L. Jiang, B. C. Prager, X. Wang, Q. Ye, Z. Zhu, G. Zhang, Z. Dong, L. Zhao, D. Lee, J. Bi, A. E. Sloan, P. S. Mischel, J. M. Brown, H. Cang, T. Huan, S. C. Mack, Q. Xie, J. N. Rich, Glioma stem cell-specific superenhancer promotes polyunsaturated fatty-acid synthesis to support EGFR signaling. *Cancer Discov.* **9**, 1248–1267 (2019).

40. C. Dravis, B. T. Spike, J. C. Harrell, C. Johns, C. L. Trejo, E. M. Southard-Smith, C. M. Perou, G. M. Wahl, Sox10 regulates stem/progenitor and mesenchymal cell states in mammary epithelial cells. *Cell Rep.* **12**, 2035–2048 (2015).

41. I. Silvestri, F. Testa, R. Zappasodi, C. W. Cairo, Y. Zhang, B. Lupo, R. Galli, M. Di Nicola, B. Venerando, C. Tringali, Sialidase NEU4 is involved in glioblastoma stem cell survival. *Cell Death Dis.* **5**, e1381 (2014).

42. W. Sukjoi, S. Siritutsoontorn, P. Chansongkrow, S. Waiwitlikhit, S. W. Polyak, M. Warnnissorn, V. Charoensawan, C. Thuwajit, S. Jitrapakdee, Overexpression of holocarboxylase synthetase predicts lymph node metastasis and unfavorable prognosis in breast cancer. *Anticancer Res.* **40**, 4557–4565 (2020).

43. L. Chen, P. Jenjaroenpun, A. M. C. Pillai, A. V. Ivshina, G. S. Ow, M. Efthimios, T. Zhiqun, T. Z. Tan, S.-C. Lee, K. Rogers, J. M. Ward, S. Mori, D. J. Adams, N. A. Jenkins, N. G. Copeland, K. H.-K. Ban, V. A. Kuznetsov, J. P. Thiery, Transposon insertional mutagenesis in mice identifies human breast cancer susceptibility genes and signatures for stratification. *Proc. Natl. Acad. Sci. U.S.A.* **114**, E2215–E2224 (2017).

44. O. V. Grinchuk, S. P. Yenamandra, R. Iyer, M. Singh, H. K. Lee, K. H. Lim, P. K.-H. Chow, V. A. Kuznetsov, Tumor-adjacent tissue co-expression profile analysis reveals pro-oncogenic ribosomal gene signature for prognosis of resectable hepatocellular carcinoma. *Mol. Oncol.* **12**, 89–113 (2018).

45. S. C. Mack, I. Singh, X. Wang, R. Hirsch, Q. Wu, R. Villagomez, J. A. Bernatchez, Z. Zhu, R. C. Gimple, L. J. Y. Kim, A. Morton, S. Lai, Z. Qiu, B. C. Prager, K. C. Bertrand, C. Mah, W. Zhou, C. Lee, G. H. Barnett, M. A. Vogelbaum, A. E. Sloan, L. Chavez, S. Bao, P. C. Scacheri, J. L. Siqueira-Neto, C. Y. Lin, J. N. Rich, Chromatin landscapes reveal developmentally encoded transcriptional states that define human glioblastoma. *J. Exp. Med.* **216**, 1071–1090 (2019).

46. R. L. Bowman, Q. Wang, A. Carro, R. G. W. Verhaak, M. Squatrito, GlioVis data portal for visualization and analysis of brain tumor expression datasets. *Neuro Oncol.* **19**, 139–141 (2017).

47. Z. Gu, R. Eils, M. Schlesner, Complex heatmaps reveal patterns and correlations in multidimensional genomic data. *Bioinformatics* **32**, 2847–2849 (2016).

48. A. Šali, T. L. Blundell, Comparative protein modelling by satisfaction of spatial restraints. *J. Mol. Biol.* **234**, 779–815 (1993).

49. S. Kannan, M. R. Pradhan, G. Tiwari, W.-C. Tan, B. Chowbay, E. H. Tan, D. S.-W. Tan, C. Verma, Hydration effects on the efficacy of the epidermal growth factor receptor kinase inhibitor afatinib. *Sci. Rep.* **7**, 1540 (2017).

50. J. Lescar, I. Meyer, K. Akshita, K. Srinivasaraghavan, C. Verma, M. Palous, D. Mazier, A. Datry, A. Fekkar, *Aspergillus fumigatus* harbouring the sole Y121F mutation shows decreased susceptibility to voriconazole but maintained susceptibility to itraconazole and posaconazole. *J. Antimicrob. Chemother.* **69**, 3244–3247 (2014).

51. T. Darden, D. York, L. Pedersen, Particle mesh Ewald: An $N\cdot\log(N)$ method for Ewald sums in large systems. *J. Chem. Phys.* **98**, 10089–10092 (1993).

52. S. Miyamoto, P. A. Kollman, Settle: An analytical version of the SHAKE and RATTLE algorithm for rigid water models. *J. Comput. Chem.* **13**, 952–962 (1992).

53. B. Li, C. N. Dewey, RSEM: Accurate transcript quantification from RNA-Seq data with or without a reference genome. *BMC Bioinformatics* **12**, 323 (2011).

54. D. M. Muoio, R. C. Noland, J.-P. Kovalik, S. E. Seiler, M. N. Davies, K. L. DeBalsi, O. R. Ilkayeva, R. D. Stevens, I. Kheterpal, J. Zhang, J. D. Covington, S. Bajpeyi, E. Ravussin, W. Kraus, T. R. Koves, R. L. Mynatt, Muscle-specific deletion of carnitine acetyltransferase compromises glucose tolerance and metabolic flexibility. *Cell Metab.* **15**, 764–777 (2012).

55. C. B. Newgard, J. An, J. R. Bain, M. J. Muehlbauer, R. D. Stevens, L. F. Lien, A. M. Haqq, S. H. Shah, M. Arlotto, C. A. Slentz, J. Rochon, D. Gallup, O. Ilkayeva, B. R. Wenner, W. S. Yancy Jr., H. Eisenson, G. Musante, R. S. Surwit, D. S. Millington, M. D. Butler, L. P. Svetkey, A branched-chain amino acid-related metabolic signature that differentiates obese and lean humans and contributes to insulin resistance. *Cell Metab.* **9**, 311–326 (2009).

56. S. K. Bowman, M. D. Simon, A. M. Deaton, M. Tolstorukov, M. L. Borowsky, R. E. Kingston, Multiplexed Illumina sequencing libraries from picogram quantities of DNA. *BMC Genomics* **14**, 466 (2013).

57. S. Madhavan, J.-C. Zenklusen, Y. Kotliarov, H. Sahni, H. A. Fine, K. Buetow, Rembrandt: Helping personalized medicine become a reality through integrative translational research. *Mol. Cancer Res.* **7**, 157–167 (2009).

58. L. A. M. Gravendeel, M. C. M. Kouwenhoven, O. Gevaert, J. J. de Rooi, A. P. Stubbs, J. E. Duijm, A. Daemen, F. E. Bleeker, L. B. C. Bralten, N. K. Kloosterhof, B. De Moor, P. H. C. Eilers, P. J. van der Spek, J. M. Kros, P. A. E. Sillevis Smitt, M. J. van den Bent, P. J. French, Intrinsic gene expression profiles of gliomas are a better predictor of survival than histology. *Cancer Res.* **69**, 9065–9072 (2009).

59. Y. Wang, T. Qian, G. You, X. Peng, C. Chen, Y. You, K. Yao, C. Wu, J. Ma, Z. Sha, S. Wang, T. Jiang, Localizing seizure-susceptible brain regions associated with low-grade gliomas using voxel-based lesion-symptom mapping. *Neuro Oncol.* **17**, 282–288 (2015).

60. Roadmap Epigenomics Consortium, Integrative analysis of 111 reference human epigenomes. *Nature* **518**, 317–330 (2015).

61. A. Butler, P. Hoffman, P. Smibert, E. Papalexi, R. Satija, Integrating single-cell transcriptomic data across different conditions, technologies, and species. *Nat. Biotechnol.* **36**, 411−420 (2018).

62. M. S. Y. Tan, E. Sandanaraj, Y. K. Chong, S. W. Lim, L. W. H. Koh, W. H. Ng, N. S. Tan, P. Tan, B. T. Ang, C. Tang, A STAT3-based gene signature stratifies glioma patients for targeted therapy. *Nat. Commun.* **10**, 3601 (2019).